REMARKS

I. Status of the claims

An after-final Amendment and Response, filed on July 17, 2006, sought to amend independent claims 3 and 7. In light of the Advisory Action dated July 31, 2006, Applicants understand that the amendments have been entered for purposes of the present reply. Accordingly, claims 3-11 are pending, with claims 3 and 7 being independent. Claims 1-2 and 12-21 are cancelled. Claims 3-11 stand rejected.

The pending claims are supported by the originally filed claims and the specification at, *inter alia*, page 3, line 9 to page 4, line 5, page 14, line 14 to page 15, line 20; page 24, line 23 to page 25, line 6; the Examples on pages 41 to 49; and Tables 1 and 4. Having generally identified textual support for the claimed invention, Applicants present the following chart that identifies precisely what passages of the specification describe the subject matter as claimed in each independent claim.

Independent Claim	Claimed Subject Matter	Support in the Specification
3	An isolated polynucleotide encoding a polypeptide comprising an amino acid sequence having at least 95% sequence identity to the amino acid sequence of SEQ ID NO:2,	original claims 1-5, page 56; Table 1, page 50; Table 4, page 53; page 3, ll. 9-24.
	wherein the polypeptide is associated with cell proliferation.	page 3, ll. 9-24; page 14, ll. 14-34; page 24, l. 23- page 25, l. 6; page 41, l. 27-page 49, l. 9
7	An isolated polynucleotide comprising a polynucleotide sequence having at least 95% sequence identity to the polynucleotide sequence of SEQ ID NO:7,	original claims 7-8, page 56; Table 1, page 50; Table 4, page 53; page 3, l. 31- page 4, l. 5;
	wherein the polynucleotide encodes a polypeptide associated with cell proliferation	page 3, ll. 9-24; page 14, l. 14- page 15, l. 20; page 24, l. 23- page 25, l. 6; page 41, l. 27-page 49, l. 9.

II. Summary of the pending rejections

Three issues remain:

1. Whether claims 3-11 are supported by a specific, substantial and credible asserted utility under 35 U.S.C. § 101.

2. Whether claims 3-11 are enabled, under 35 U.S.C. § 112, first paragraph. The Examiner asserts that, because claims 3-11 do not meet the utility requirement under 35 U.S.C. § 101, then one of ordinary skill would not know how to make or use the invention. Therefore, a finding of utility in the first issue will render moot this issue.

3. Whether claims 3-11 find adequate written description in the specification under 35 U.S.C. § 112, first paragraph. The Examiner has accepted that the recitation of "at least 95%" is supported by the specification, but asserts that the claims recite a utility to which Applicants are not entitled. Therefore, a finding of utility in the first issue will also render moot this issue.

III. Utility under 35 U.S.C. § 101

1. Brief statement of the issue

The Office asserts that claims 3-11 are not supported by either a specific, substantial and credible asserted utility, or a well established utility, and therefore has rejected claims 3-11 under 35 U.S.C. § 101. Applicants have argued throughout prosecution that the specification provides a specific, substantial and credible utility.

Applicants incorporate by reference herein all prior submissions to the Examiner regarding this matter, and continue to assert that these prior submissions are sufficient to demonstrate that the specification meets the requirements of U.S.C. § 101. Nevertheless, Applicants provide additional evidence to show that: (a) the present specification provides a specific, substantial and credible utility for MACP-2; (b) MACP-2 is homologous to a compound with a well established utility; (c) additional post-filing references provide objective evidence of the asserted utility; and (d) the specification meets various factors recently elaborated by the Federal Circuit in *In re Fisher*, 421 F.3d 1365 (Fed. Cir. 2005).

2. The Applicable Legal Standard

To meet the utility requirement of 35 U.S.C. § 101, the applicant need only show that the claimed invention is "practically useful," *Anderson v. Natta*, 480 F.2d 1392, 1397, 178 USPQ 458 (CCPA 1973), and confers a "specific benefit" on the public. *Brenner v. Manson*, 383 U.S. 519, 534-35, 148 USPQ 689 (1966). As acknowledged by the Federal Circuit, the utility threshold is not high:

> An invention is "useful" under section 101 if it is capable of providing some identifiable benefit. See *Brenner v. Manson*, 383 U.S. 519, 534 [148 USPQ 689] (1966); *Brooktree Corp. v. Advanced Micro Devices, Inc.*, 977 F.2d 1555, 1571 [24 USPQ2d 1401] (Fed. Cir. 1992) ("to violate Section 101 the claimed device must be totally incapable of achieving a useful result"); *Fuller v. Berger*, 120 F. 274, 275 (7th Cir. 1903) (test for utility is whether invention "is incapable of serving any beneficial end").

Juicy Whip Inc. v. Orange Bang Inc., 51 USPQ2d 1700 (Fed. Cir. 1999). While an asserted utility must be described with specificity, the patent applicant need not demonstrate utility to a certainty. In *Stiftung v. Renishaw PLC*, 945 F.2d 1173, 1180, 20 USPQ2d 1094 (Fed. Cir. 1991), the United States Court of Appeals for the Federal Circuit explained:

> An invention need not be the best or only way to accomplish a certain result, and it need only be useful to some extent and in certain applications: "[T]he fact that an invention has only limited utility and is only operable in certain applications is not grounds for finding lack of utility." *Envirotech Corp. v. Al George, Inc.*, 730 F.2d 753, 762, 221 USPQ 473, 480 (Fed. Cir. 1984).

The specificity requirement is not, therefore, an onerous one. If the asserted utility is described so that a person of ordinary skill in the art would understand how to use the claimed invention, it is sufficiently specific. See *Standard Oil Co. v. Montedison, S.p.a.*, 212 U.S.P.Q. 327, 343 (3d Cir. 1981). The specificity requirement is met unless the asserted utility amounts to a "nebulous expression" such as "biological activity" or "biological properties" that does not convey meaningful information about the utility of what is being claimed. *Cross* v. *Iizuka*, 753 F.2d 1040, 1048 (Fed. Cir. 1985).

In addition to conferring a specific benefit on the public, the benefit must also be "substantial." *Brenner*, 383 U.S. at 534. A "substantial" utility is a practical, "real-world" utility. *Nelson v. Bowler*, 626 F.2d 853, 856, 206 USPQ 881 (CCPA 1980).

If persons of ordinary skill in the art would understand that there is a "well-established" utility for the claimed invention, the threshold is met automatically and the applicant need not make any showing to demonstrate utility. Manual of Patent Examining Procedure at § 706.03(a). Only if there is no "well-established" utility for the claimed invention must the applicant demonstrate the practical benefits of the invention. *Id.*

Once the patent applicant identifies a specific utility, the claimed invention is presumed to possess it. *In re Cortright*, 165 F.3d 1353, 1357, 49 USPQ2d 1464 (Fed. Cir. 1999); *In re Brana*, 51 F.3d 1560, 1566; 34 USPQ2d 1436 (Fed. Cir. 1995). In that case, the Patent Examiner bears the burden of demonstrating that a person of ordinary skill in the art would reasonably doubt that the asserted utility could be achieved by the claimed invention.

Id. To do so, the Patent Examiner must provide evidence or sound scientific reasoning. See *In re Langer*, 503 F.2d 1380, 1391-92, 183 USPQ 288 (CCPA 1974). If and only if the Patent Examiner makes such a showing, the burden shifts to the applicant to provide rebuttal evidence that would convince the person of ordinary skill that there is sufficient proof of utility. *Brana*, 51 F.3d at 1566. The applicant need only prove a "substantial likelihood" of utility; certainty is not required. *Brenner*, 383 U.S. at 532.

The USPTO has published Utility Guidelines that reflect the Office's interpretation of the law. The MPEP and Guidelines "are not binding on this court, but may be given judicial notice to the extent they do not conflict with the statute." *Enzo Biochem v. Gen-Probe*, 323 F.3d 956, 964 (Fed.Cir.2002) (citing *Molins PLC v. Textron, Inc.*, 48 F.3d 1172, 1180 n. 10 (Fed.Cir.1995)). The Federal Circuit has recently indicated that it agrees with the standards outlined in the guidelines: "[t]he PTO's standards for assessing whether a claimed invention has a specific and substantial utility comport with this court's interpretation of the utility requirement of § 101." *In re Fisher* 421 F.3d 1365, 1372 (Fed. Cir. 2005).

In examining the utility requirement as it applies to EST, the Federal circuit upheld the Examiner's finding that Fisher's disclosure of an EST was not supported by a specific and substantial utility and therefore rejected under both 35 U.S.C. §§ 101 and 112, first paragraph. *Id.* The court noted that each EST did not encode a complete gene, that it did not correspond to a protein with a known function, was not used as a molecular marker or to analyze gene expression, and can only be used as an intermediate for further research. Fisher had not identified a function for the EST. The court stated:

> Thus, while Fisher's claimed ESTs may add a noteworthy contribution to biotechnology research, our precedent dictates that the '634 application does not meet the utility requirement of § 101 because Fisher does not identify the function for the underlying protein-encoding genes. Absent such identification, we hold that the claimed ESTs have not been researched and understood to the point of providing an immediate, well-defined, real world benefit to the public meriting the grant of a patent.

Id. at 1376.

3. The specification asserts a specific and substantial utility

The pending claims are directed to a protein (MACP-2) and the gene encoding it, and recites that MACP-2 is associated with cell proliferation. The assertion that MACP-2 is associated with cell proliferation is found not only in the original claims, but throughout the specification. Indeed, the acronym "MACP" derives from "molecules associated with cell proliferation," the application is titled "molecules associated with cell proliferation," and all polypeptides and polynucleotides in the specification are associated with cell proliferation. The specification at page 14, ll. 14-16 recites:

> The invention is based on the discovery of new molecules associated with cell proliferation (MACP), the polynucleotides encoding MACP, and the used of these compositions for the diagnosis, treatment, or prevention of cell proliferative and immune disorders.

Proliferative disorders include cancer, including cancers of the brain, breast, cervix, gastrointestinal tract, ovary, lung, prostate and uterus. *See* specification at, *e.g.*, page 25, ll. 2-6. Accordingly, the asserted utility is *specific.* The specification also provides methods for using the MACP-2 protein and nucleic acid sequence for the diagnosis, treatment or prevention of cell proliferation. For example, page 34, l. 1 to page 38, l. 11, describes how the invention may be used for diagnostic purposes, such as "to detect and quantitate gene expression in biopsied tissues in which expression of MACP may be correlated with disease." Specification at page 34, ll. 24-25. As the asserted utility is relevant to the diagnosis, treatment or prevention of cell proliferation and cancer, it is clearly *substantial.* The present issue therefore depends on whether one of ordinary skill in the art would believe that the asserted utility is *credible* or is *well known.*

4. The specification demonstrates that the asserted utility is *credible*

Those of ordinary skill in the art would find credible the asserted utility, based on the abundant evidence provided by the specification showing that MACP-2 is associated with cell proliferation.

(a) The expression profile of MACP-2 demonstrates the association with proliferative disease

Table 1 of the specification illustrates that the clone of MACP-2 was isolated from a cDNA library (PROSNOT15) derived from a prostate cancer tumor. *See* Table 4, page 53, for a description of the library. MACP-2 was found to be expressed in libraries from diseased breast, lung, prostate and brain. *See* Table 1, page 50; page 41, line 26 to page 42, line 17. Furthermore, the nucleotide sequence encoding MACP-2 (SEQ ID NO:7) was found in 71.4% of cDNA libraries that were proliferative in nature (*see* Table 3). These data support the assertion that MACP-2 is associated with cell proliferative disease.

(b) Homology of MACP-2 to tenascin is prima facie evidence of the association of MACP-2 with proliferative disease, and is further supported by the expression data

The specification states that MACP-2 is homologous to a 190 kDa precursor to the protein tenascin. *See* Table 2, page 51. The specification also states that tenascin is involved in cell proliferation. *See* page 1, line 32-page 2, line 8. It was well known by those of ordinary skill in the art at the time of filing of the application that tenascin was linked to cancer. For example, Vollmer *et al.*, "Expression of tenascin during carcinogenesis and involution of hormone-dependent tissues," *Biochem Cell Biol.*, 72: 505-514 (1994), reports that "a high expression [of tenascin] was found in embryonic development and during carcinogenesis of almost all organs," and that tenascin is associated with tumors of the endometrium, breast and prostate. *Id* at page 505. Tenascin is also important in glioma and neural development. *See e.g.* Bourdon and Ruoslahti, "Tenascin mediates cell attachment through an RGD-dependent receptor," *J. Cell Biol.*, 108: 1149-1155, 1149 (1989).

Alone, the homology to tenascin provides prima facie evidence that MACP-2 is associated with proliferative disease. That the sequence homology is replicated in a similar *expression* profile provides more than sufficient evidence for the association of MACP-2 with proliferative disease. Tenascin is associated with proliferative diseases in the brain, breast and prostate. The specification teaches that MACP-2 is homologous to a tenascin precursor, and is over-expressed in diseases of the brain, breast and prostate, just like tenascin.

(c) The combined evidence is overwhelming proof of the credibility of the asserted utility

The expression profile of MACP-2 and the similarities with tenascin are each sufficient alone to demonstrate that the asserted utility for MACP-2 is credible. In combination, therefore, the person of ordinary skill in the art would readily conclude that MACP-2 is associated with cell proliferation.

5. The specification provides support based on a *well known* utility

The USPTO utility guidelines indicate that a *well known* utility can provide independent support for the utility of an invention. (Revised Interim Utility Guidelines Training Materials. Available at www.uspto.gov/web/menu/utility.pdf, last accessed November 8, 2006). In view of the well established utility of tenascin, the similarities in sequence and expression profile demonstrates to those of ordinary skill that MACP-2 has a *well established utility.*

Indeed, the present situation is analogous to Example 10 on page 53, in the USPTO utility guidelines (Revised Interim Utility Guidelines Training Materials. Available at www.uspto.gov/web/menu/utility.pdf, last accessed November 8, 2006). Example 10 in the USPTO utility guidelines indicates that the identification of a sequence with homology to a ligase, and claimed as a ligase, is supported by a "well established utility" as a ligase. Accordingly, for this additional reason, the specification provides sufficient support for the utility of MACP-2 under 35 U.S.C. § 101.

6. The post-filing art confirms Applicants asserted utility

Applicants may provide post filing evidence that the specification asserted a specific, substantial and credible utility at the time of filing. There is in fact no restriction on the kinds of evidence a Patent Examiner may consider in determining whether a "real-world" utility exists. "Real-world" evidence, such as evidence showing actual use or commercial success of the invention, can demonstrate conclusive proof of utility. *Raytheon v. Roper*, 220 USPQ2d 592 (Fed. Cir. 1983); *Nestle v. Eugene*, 55 F.2d 854, 856, 12 USPQ 335 (6th Cir. 1932). Indeed, proof that the invention is made, used or sold by any person or entity other than the

patentee is conclusive proof of utility. *United States Steel Corp.* v. *Phillips Petroleum Co.*, 865 F.2d 1247, 1252, 9 USPQ2d 1461 (Fed. Cir. 1989). The USPTO utility guidelines also recognize that post-filing evidence may be used to demonstrate utility. *See e.g.* page 61.

Abundant post-filing evidence demonstrates that MACP-2, now known as WIF-1, is associated with proliferative disease, including cancer. The role of WIF-1 in cancer differs, however, between different types of cancer and different stages of disease. Applicants provide herewith post-filing evidence of increased MACP-2/WIF-1 expression associated with proliferative disease, particularly cancer.

WIF-1 was expressed in tissues samples from 5/6 human ovarian endometriod adenocarcinomas, but was not expressed in normal ovarian tissue. Therefore, WIF-1 is associated with cancer and is a diagnostic marker for ovarian cancer. Steg *et al.*, "Multiple gene expression analysis in paraffin embedded tissues by TaqMan low-density array," *J. Molecular Diagnostics*, 8: 76-83 (2006)). Similar work in mice had also demonstrated that WIF-1 was over-expressed in ovarian granulosa cell tumors and in solid pretumoral lesions in the ovaries of mice, compared with normal ovarian tissue. Boerboom *et al.*, "Dominant-stable β-catenin expression causes cell fate alterations and Wnt signaling antagonist expression in a murine granulosa cell tumor model," *Cancer Res.*, 66: 1964-1973 (2006), *see* abstract, page 1964; pages 1966.

WIF-1 over expression has also been observed in other cancer types. Cebrat *et al.*, "Wnt inhibitory factor-1: a candidate for a new player in tumorigenesis of intestinal epithelial cells," *Cancer Lett.*, 206: 107-113 (2004), demonstrated that WIF-1 was over expressed in intestinal adenoma's compared to normal epithelial cells in APC mice, and was also over expressed in cell lines derived from murine and human mammary gland adenocarcinoma and human colon adenocarcinoma. *Id.* at page 107, 111. Using *lux* reporter construct, Reguart *et al.*, "Cloning and characterization of the promoter of human Wnt inhibitory factor-1," *Biochem Biophys Res Comm.*, 323:229-234 (2004), demonstrated increased transcription in human cell lines derived from colon and non-small-cell lung cancers, but not from mesothelioma. Such results, demonstrating the association between increased WIF-1 expression and proliferative disease in humans and mice, support a utility asserted in the

specification. Therefore, these results establish that the present specification, at the time of filing, complied with 35 U.S.C. § 101.

7. Under the Federal Circuit's reasoning in *Fisher*, Applicants meet the utility requirement

In the recent Federal Circuit case *In re Fisher*, 421 F.3d 1365 (Fed. Cir. 2005), the court found that a specification that disclosed only ESTs failed to meet the utility requirements under 35 U.S.C. § 101. In its reasoning, the court noted that Fisher had *not* identified a function for any EST, that *no* EST encoded a complete gene, that *no* EST corresponded to a protein with a known function, and that further research was *not* performed to determine if the EST was a disease marker or to analyze gene expression. These multiple failings were important to the reasoning of the court, which found that the EST of Fisher was only useful as an intermediate for further research. The multiple failings are Fisher are not found in Applicants' disclosure.

Applicants' disclosure is in marked contrast to that of Fisher. Unlike Fisher, Applicants *have* isolated a complete gene, *have* identified a function for the gene, *have* found that the cloned gene was homologous to a protein with known function, and *have* performed further analysis to demonstrate that the gene was a useful marker for proliferative disease. Thus, all the things that Fisher is criticized for failing to do, Applicants *have already done* as of the filing date of the application.

8. Conclusion

Applicants have shown that the claimed invention is supported by a specific and substantial utility. In view of the expression data and homology to a protein associated with cell proliferation, the asserted specific and substantial utility is both *credible* and also, that it is *well known.* Furthermore, post-filing references provide objective evidence that support the utility disclosed and claimed in the specification. Finally, the present specification has none of the defects that were, cumulatively, crucial in *Fisher, Id.* For all of these reasons, both individually, and together, the present specification meets the utility requirement under

35 U.S.C. § 101. Applicants therefore respectfully request that the Examiner reconsider and withdraw the outstanding rejection under 35 U.S.C. § 101.

IV. Enablement under 35 U.S.C. § 112, first paragraph

The rejection of claims 3-11 under 35 U.S.C. § 112, first paragraph, for lack of enablement depends entirely on the Examiner's assertion that these claims fail to meet 35 U.S.C. § 101. *See* Advisory Action of July 31, 2006. For the reasons outlined above, Applicants have shown that the claimed invention is supported by a specific, substantial and credible utility. As claims 3-11 meet the utility requirement under 35 U.S.C. § 101, they also meet the enablement requirement of 35 U.S.C. § 112, first paragraph. Applicants therefore respectfully request that the Examiner reconsider and withdraw the outstanding rejection under 35 U.S.C. § 112, first paragraph, enablement.

V. Written description under 35 U.S.C. § 112, first paragraph

The final issue is whether there is sufficient written description under 35 U.S.C. § 112, first paragraph, to support the claimed invention. The Examiner has accepted that the recitation of "at least 95%" is supported by the specification, but asserts that the claims recite a utility "to which Applicants are not entitled." *See* Advisory Action of July 31, 2006. As the sole issue raised by the Examiner was an asserted lack of utility, it follows that Applicants demonstration that the claims *do* meet the requirements under 35 U.S.C. § 101 means that the claims *also* meet the written description requirement under 35 U.S.C. § 112, first paragraph. Applicants therefore respectfully request that the Examiner reconsider and withdraw the outstanding rejection under 35 U.S.C. § 112, first paragraph, enablement.

CONCLUSION

Pending claims 3-11 have been rejected under the utility requirement of 35 U.S.C. § 101 and the enablement and written description requirements of 35 U.S.C. § 112, first paragraph. The sole basis of these rejections is that the Examiner does not consider *credible* Applicants' asserted utility. Applicants have demonstrated that the specification provides a specific and substantial utility; that on the basis of the specification alone, this utility is credible and well known; that the asserted utility is supported by the post-filing art; and meets

recently enunciated factors described by the Federal Circuit. Since Applicants have overcome the Examiner's utility rejection, the remaining rejections are also overcome. Applicants courteously request the Examiner reconsider and withdraw all grounds for rejection of the claims. If it is believed that personal communication will expedite this matter, the Examiner is invited to contact the undersigned.

Respectfully submitted,

Date February 6, 2007 By /Elliott/

FOLEY & LARDNER LLP
Customer Number: 22428
Telephone: (202) 295-4726
Facsimile: (202) 672-5399

Simon J. Elliott, Ph.D.
Agent for Applicants
Registration No. 54,083

EVIDENCE APPENDIX

Applicants append copies of the following documents in support of the foregoing remarks:

1. Vollmer *et al.*, "Expression of tenascin during carcinogenesis and involution of hormone-dependent tissues," *Biochem Cell Biol.*, 72: 505-514 (1994), PubMed abstract only.

2. Bourdon and Ruoslahti, "Tenascin mediates cell attachment through an RGD-dependent receptor," *J. Cell Biol.*, 108: 1149-1155 (1989).

3. Steg *et al.*, "Multiple gene expression analysis in paraffin embedded tissues by TaqMan low-density array," *J. Molecular Diagnostics*, 8: 76-83 (2006).

4. Boerboom *et al.*, "Dominant-stable β-catenin expression causes cell fate alterations and Wnt signaling antagonist expression in a murine granulosa cell tumor model," *Cancer Res.*, 66: 1964-1973 (2006).

5. Cebrat *et al.*, "Wnt inhibitory factor-1: a candidate for a new player in tumorigenesis of intestinal epithelial cells," *Cancer Lett.*, 206: 107-113 (2004).

6. Reguart *et al.*, "Cloning and characterization of the promoter of human Wnt inhibitory factor-1." *Biochem Biophys Res Comm.*, 323: 229-234 (2004).

1: Biochem Cell Biol. 1994 Nov-Dec;72(11-12):505-14.

Links

Expression of tenascin during carcinogenesis and involution of hormone-dependent tissues.

Vollmer G.

Institut fur Biochemische Endokrinologie, Medizinische Universitat, Lubeck, Germany.

Cytotactin/tenascin/hexabrachion, now referred to as tenascin-C (TN-C), is a hexameric glycoprotein of the extracellular matrix of mesenchymal tissue constituents. A high expression was found in embryonic development and during carcinogenesis of almost all organs. TN-C expression by the mesenchyme thereby appears to be induced by paracrine-acting, epithelial-derived (growth) factors. In normal adult organs there is little, if any, TN-C expression. In the human endometrium for instance, tenascin expression is low in the normal proliferative endometrium and undetectable in the normal secretory endometrium. In this paper, the appearance and expression of TN-C in hormone-dependent tissues, regressing hormone-dependent tissues, and tumors of the endometrium, breast and prostate is reviewed. Further, the regulation of TN-C expression is summarized and possible functions of TN-C during regression and carcinogenesis of hormone-dependent tissues are discussed.

PMID: 7544587 [PubMed - indexed for MEDLINE]

Related Links

Stromal expression of tenascin is inversely correlated to epithelial differentiation of hormone dependent tissues. [J Steroid Biochem Mol Biol. 1994]

Localization of tenascin in uterine sarcomas and partially transformed endometrial stroma cells. [Pathobiology. 1993]

Induction of tenascin in cancer cells by interactions with embryonic mesenchyme mediated by a diffusible factor. [J Cell Sci. 1993]

Mammary epithelial cell differentiation in vitro is regulated by an interplay of EGF action and tenascin-C downregulation. [J Cell Sci. 1995]

Epithelial cells are an important source of tenascin in normal and malignant human breast tissue. [Breast Cancer Res Treat. 1994]

See all Related Articles...

Display AbstractPlus Show 20 Sort by Send to

Write to the Help Desk
NCBI | NLM | NIH
Department of Health & Human Services
Privacy Statement | Freedom of Information Act | Disclaimer

Nov 6 2006 15:24:20

Tenascin Mediates Cell Attachment through an RGD-dependent Receptor

Mario A. Bourdon and Erkki Ruoslahti

La Jolla Cancer Research Foundation, Cancer Research Center, La Jolla, California 92037

Abstract. Tenascin is an extracellular matrix glycoprotein expressed in association with mesenchymal–epithelial interactions during development and in the neovasculature and stroma of undifferentiated tumors. This selective expression of tenascin indicates a specific role in cell matrix interactions. We now show that tenascin can support the adhesion of a variety of cell types, including various human tumor cells, normal fibroblasts, and endothelial cells, all of which can attach to a substrate coated with tenascin. Detailed studies on the mechanism of the tenascin-promoted cell attachment were carried out with the human glioma cell line U251MG. The attachment of these cells and others to tenascin were inhibited specifically by peptides containing the RGD cell attachment signal. Affinity chromatography procedures similar to those that have been used to isolate other adhesion receptors yielded a heterodimeric cell surface protein which bound to a tenascin affinity matrix in an RGD-dependent fashion. One of the subunits of this putative tenascin receptor comigrates with the β subunit of the fibronectin receptor in SDS-PAGE and cross reacts with antibodies prepared against the fibronectin receptor in immunoblotting. These results identify the tenascin receptor as a member of the fibronectin receptor family within the integrin superfamily of receptors. The cell attachment response on tenascin is distinctly different from that seen on fibronectin, suggesting that cell adhesion and motility may be modulated at those sites where tenascin is expressed in the extracellular matrix.

THE extracellular matrix is a complex assembly of molecules that interact with one another as well as with cells to effect a wide range of cellular and tissue functions. The extracellular matrix molecules include fibronectin, laminin, interstitial and basement membrane collagens, and proteoglycans. A number of these molecules have been shown to have important functional properties including the promotion of cell adhesion and spreading, cell motility, directed cell migration, cellular differentiation, and proliferation (Cardarelli and Pierschbacher, 1986; Couchman et al., 1982; Edgar et al., 1984; Ekblom, 1984; Gospodarowicz et al., 1980; Greenberg and Hay, 1986; Lacovara et al., 1984; Manthorpe et al., 1983; Rovasio et al., 1983; Ruoslahti and Pierschbacher, 1987). More recently, it has been found that a number of extracellular matrix components interact with cells through specific cell surface receptors (Giancotti et al., 1985; Horwitz et al., 1985; Pytela et al., 1985*a*,*b*; Pytela et al., 1986; Takada et al., 1989; Tamkun et al., 1986; Tomaselli et al., 1987). These receptors belong to an integrin superfamily of proteins and many of them recognize the tripeptide sequence Arg-Gly-Asp (RGD) in their extracellular ligands (Hynes, 1987; Pierschbacher and Ruoslahti, 1984*a*; Ruoslahti and Pierschbacher, 1987). While a number of extracellular matrix molecules have been well-characterized, new molecules are likely to be found that play specific roles in cell matrix interactions.

One such novel extracellular matrix molecule is the glial-mesenchymal extracellular matrix glycoprotein tenascin (Bourdon et al., 1983; Chiquet-Ehrismann et al., 1986). This glycoprotein has been described as GMEM (Bourdon et al., 1983) cytotactin (Grumet et al., 1985), hexabrachion protein (Erickson and Taylor, 1987), and myotendinous antigen (Chiquet and Fambrough, 1984). Human tenascin is a 250-kD glycoprotein that is secreted as a high molecular mass (>10^6 kD) disulfide-bonded oligomer (Bourdon et al., 1983; Bourdon et al., 1985). In rotary shadowing images tenascin appears as a hexameric structure (Erickson and Taylor, 1987; Vaughn et al., 1987). This structurally unusual matrix molecule is further distinguished by its highly selective oncodevelopmental expression.

Tenascin is expressed in a variety of solid tumors, but is largely absent in normal adult tissues (Bourdon et al., 1983; Mackie et al., 1987; McComb et al., 1987). In human gliomas, it is expressed around the tumor neovasculature, and in fibrosarcomas within the stroma. Developmentally, tenascin is selectively expressed in condensing mesenchyme during the initial stages of organogenesis of mammary gland, toothbud, and kidney (Aufderheide et al., 1987; Chiquet-Ehrismann et al., 1986). In each of these organs, epithelial–mesenchymal interactions are of key importance in normal organ development. Temporally restricted expression of tenascin is also seen in the developing nervous system (Gru-

met et al., 1985; Crossin et al., 1986). The selective oncodevelopmental expression of tenascin within the extracellular matrix makes it likely that this molecule plays a specific role in cell–matrix interactions and that such interactions are mediated by cell surface receptors.

In this study, we show that tenascin has RGD-dependent cell adhesion activity and describe an integrin-type cell surface receptor that binds to tenascin with the same RGD-dependent specificity as the cells.

Materials and Methods

Cell Culture

Tumor cell lines and normal fibroblasts were cultured in DME supplemented with 10% FBS, glutamine, penicillin, and streptomycin. Cultures were maintained at 37°C in 7% CO_2. Human umbilical vein endothelial cells were cultured in DME, supplemented with 20% FBS, heparin, and endothelial cell growth factors (Collaborative Research, Lexington, MA). Adherent cell lines were passaged by treatment with 100 μg/ml trypsin/0.02% EDTA in PBS.

Cell Attachment Assay

Cells for the cell attachment assay were detached using 0.02% EDTA in PBS, pH 7.4, washed in DME containing 2 mg/ml BSA and plated at 2×10^4 cells per well in 96-well flat bottom microtitration plates (Titertek; Flow Laboratories, McLean, VA). Wells were previously coated overnight with dilutions of cell attachment proteins in PBS. Plates were washed and then incubated for 30 min with a solution containing the DMEM-BSA medium to block nonspecific binding sites before their use in cell attachment assays. Peptides added to the cell attachment assays were dissolved in DME. The peptides were not cytotoxic at the concentration used as determined by trypan blue exclusion by cells in the assays. Assays were carried out at 37°C in a CO_2 incubator for 90 min. Nonadherent cells were removed by washing with PBS and adherent cells fixed with 3% paraformaldehyde and stained with 0.5% toluidine blue. Adherent cells were either counted directly or their numbers determined by lysing cells with 1% SDS and measuring dye absorbance at 600 nm in a Multiscan plate reader (Flow Laboratories).

Purification of Tenascin

Tenascin was purified from the spent culture media of U251MG human glioma cells by affinity chromatography on an 81C6 antitenascin monoclonal antibody (Bourdon et al., 1983) coupled to Sepharose 4B. The spent culture media was first concentrated by tangential flow filtration over PLMK300 filters (Millipore Corp., Bedford, MA). A Sepharose 4B column was used to remove debris and aggregated protein before application of the sample to the monoclonal antibody affinity column. Nonbound proteins were washed from the antibody–Sepharose column with 0.5 M NaCl, 1 M urea, 10 mM sodium phosphate, pH 7.4, and tenascin eluted with 0.5 M NaCl, 4 M urea, 10 mM sodium phosphate, pH 7.4. Protein elution was monitored at 280 nm. Purity of the tenascin preparations was monitored by SDS-PAGE analysis on 7% acrylamide gels followed by Coomassie Blue or silver staining, by HPLC chromatography on a TSK-400 column (7.5 × 60 mm), and by ELISA. Fibronectin and vitronectin were purified from human plasma as described (Hayman et al., 1983; Engvall and Ruoslahti, 1977). Rotary shadowing of purified tenascin was performed using standard procedures (Engvall et al., 1986), and the shadowed molecules were imaged on a Hitachi H-60 scanning-transmission electron microscope.

Isolation of Cell Surface Receptors

The receptor isolation was carried out essentially as described (Pytela et al., 1985*a*,*b*). Pools of 10^8 cells were surface labeled with ^{125}I and lysed in 50 mM octylglucoside, 1 mm $CaCl_2$, 1 mM $MgCl_2$, 0.15 NaCl, 1 mm PMSF, 10 mM Tris, pH 7.2. Cell extracts were passed over tenascin–Sepharose, GRGDSPK–Sepharose, or fibronectin 120-kD fragment–Sepharose columns, the affinity columns were washed with 25 mM octylthioglucoside, 1 mM $CaCl_2$, 1 mM $MgCl_2$ alone, or with 1 mg/ml GRGESP peptide, and the receptors were eluted with 1 mg/ml GRGDSP peptide. Fractions were analyzed by SDS-PAGE and autoradiography on XAR5 x-ray film with an enhancer screen.

Immunoblot and Immunoprecipitation Analyses

Receptors isolated as described above from unlabeled cells were concentrated by precipitation in acetone and separated by SDS-PAGE on 7.5% acrylamide gel. The separated proteins were then electroblotted onto a nitrocellulose membrane. Blotted protein bands were visualized by staining the membrane with ponceau S stain and destained in PBS. The blots were incubated in PBS containing 1% BSA for 1–2 h to block nonspecific protein binding sites and subsequently incubated with primary antibodies in PBS–1% BSA overnight at 4°C. After the incubation, the blots were washed and incubated with either HRP-conjugated goat anti-mouse IgG or goat anti-rabbit IgG antibodies (Bio-Rad Laboratories, Richmond, CA) in PBS–1% BSA for 1 h. Bound antibodies were visualized by addition of diaminobenzidine tetrahydrochloride in PBS 0.01% H_2O_2 solution to washed blots.

Immunoprecipitation was performed by incubating ^{125}I-labeled samples with antireceptor antisera overnight at 4°C, followed by recovery of the bound label with protein A–Sepharose. Bound material was analyzed by SDS-PAGE followed by fluorography as described above.

Antibodies

Monoclonal antibody 81C6 is an antitenascin antibody previously described (Bourdon et al., 1983). Polyclonal antisera against tenascin were prepared by immunization of rabbits with purified human tenascin. The antisera were absorbed with fibronectin–Sepharose and bovine plasma protein–Sepharose, and their IgG fraction was isolated on protein A–Sepharose.

Polyclonal rabbit antibodies to vitronectin receptor were affinity purified on vitronectin receptor–Sepharose (Suzuki et al., 1987). Polyclonal rabbit antibodies to fibronectin receptor β subunit were affinity purified as described (Argraves et al., 1987).

Synthetic Peptides

The peptide GRGDSP derived from the fibronectin cell attachment site and control peptide GRGESP were synthesized on a peptide synthesizer (Applied Biosystems Inc., Foster City, CA) using solid phase chemistry. Peptides were purified by ion exchange HPLC and lyophilized. Peptides were resuspended in appropriate buffered solutions for cell attachment assays or elution of tenascin receptors.

Results

Isolation and Characterization of Tenascin

Human tenascin was isolated from spent culture media of U251MG human glioma cells by 81C6 monoclonal antibody affinity chromatography. The purified tenascin migrated as a single prominent band at ~250 kD in SDS-PAGE under reducing conditions (Fig. 1 *A*). Unreduced tenascin behaved as a high molecular mass (>10^6 kD) disulfide bonded oligomer both in SDS-PAGE and HPLC TSK 400 sizing chromatography (not shown). In electron microscopic images obtained after rotary shadowing, tenascin appeared as a hexameric oligomer (Fig. 1 *B*). Polyclonal antiserum to chicken tenascin (Chiquet and Fambrough, 1984) immunoprecipitated the same 250-kD tenascin polypeptide from U251MG spent culture medium as the 81C6 antibody (not shown). These results identify the isolated protein as highly purified tenascin.

Cell Attachment Activity of Tenascin

Cell attachment to tenascin was examined in an in vitro cell attachment assay. Cells adhering to tenascin included a variety of tumor cell lines of glial (U251MG, Rugli), epithelial (A431), endodermal (PFHR-9), and mesenchymal (MG63, HT1080) origin as well as fibroblasts, and human umbilical

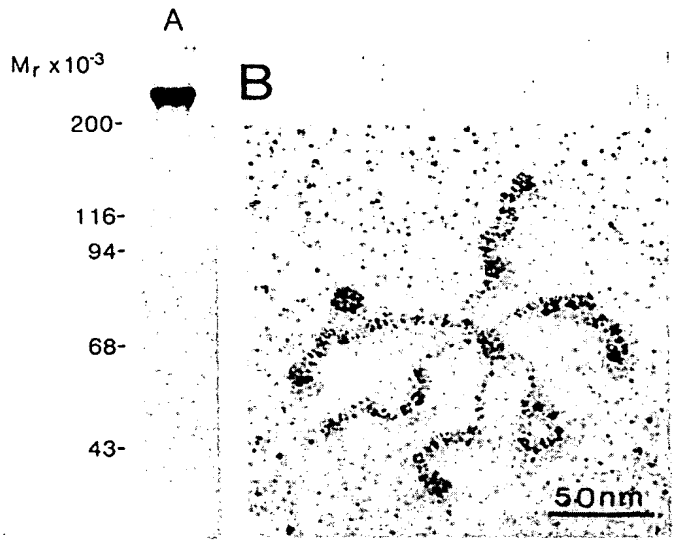

Figure 1. Analysis of purified human tenascin by SDS-PAGE and electron microscopy. (*A*) Tenascin (20 μg) isolated from the spent culture media of U251MG cells by affinity chromatography on monoclonal antibody 81C6–Sepharose was characterized by SDS-PAGE on a 7% acrylamide gel under reducing conditions. Protein was stained with Coomassie Blue. (*B*) A rotary shadowed image of one tenascin molecule is shown.

vein endothelial cells. Human M21 melanoma cells, F9 mouse embryonic carcinoma cells and cells of lymphoid origin (EL4, WR.1, thymocytes), and monocytic U937 cells adhered poorly or not at all to tenascin. Results for the attachment of U251MG cells to tenascin are shown in Figs. 2 and 3.

The morphology of cells adhering to tenascin was distinctly different from the morphology of cells adhering to fibronectin or vitronectin. The U251MG cells generally assumed a more polar, elongated morphology on tenascin with larger numbers of cellular extensions and less extensive spreading than they did on fibronectin (Fig. 2) or on vitronectin (not shown). Cells remained attached to tenascin-coated wells for periods of up to at least 24 h. Cells cultured for 24 h on fibronectin or vitronectin appeared indistinguishable from cells adhering to tenascin. Despite the reduced cell spreading observed for cells adhering to tenascin, the level of cell attachment to tenascin was found to be similar to the level of attachment to fibronectin. As shown for the U251MG cells in Fig. 3, the cell attachment titration curves for tenascin and fibronectin closely paralleled one another with maximum cell attachment (75–85% of cells added) on either tenascin or fibronectin occurring at a coating concentration of 3 μg/ml protein and higher. The similarity of the attachment efficiencies of the two proteins indicated that the attachment of cells to tenascin was not due to contamination of tenascin by fibronectin. This was further supported by the finding that there was no detectable fibronectin in tenascin samples as tested by ELISA. Moreover, antitenascin antibodies blocked cell attachment to tenascin but not to fibronectin (Fig. 4), whereas antifibronectin antibodies inhibited cell attachment to fibronectin, but not to tenascin. Neither type of antibody inhibited the attachment of cells to vitronectin.

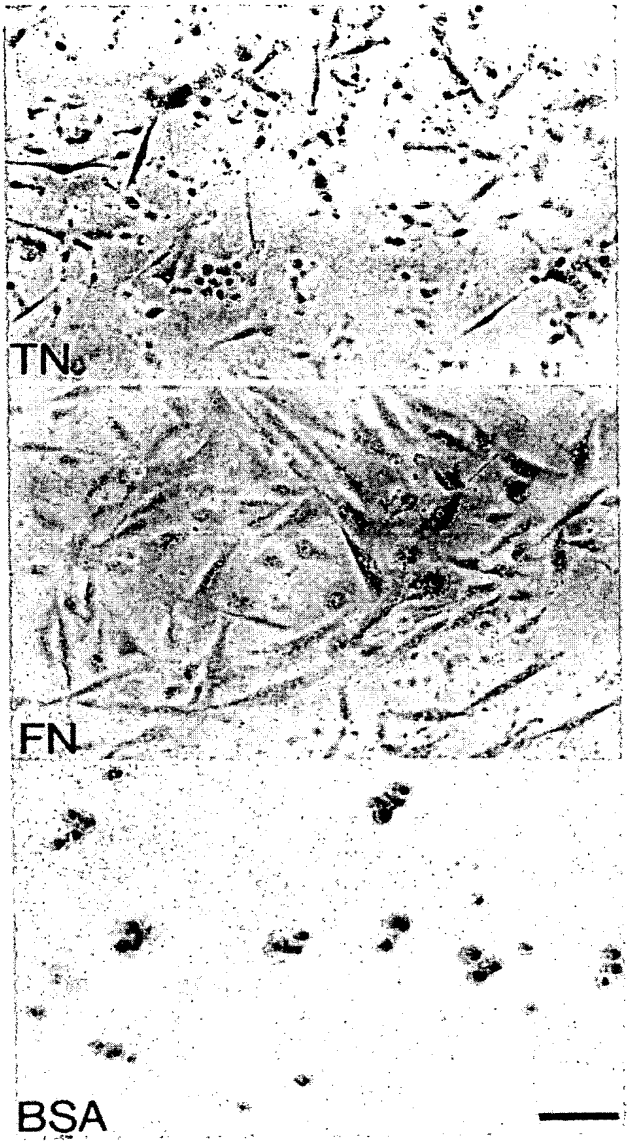

Figure 2. Cell attachment to purified tenascin. The attachment of U251MG cells to tenascin (*TN*), fibronectin (*FN*), and bovine serum albumin (*BSA*) are shown. Microtiter wells were coated with 5 μg/ml protein in PBS. Cells were seeded into the coated wells at a density of 2 × 10^4 cells/200 μl in DME–BSA and incubated at 37°C for 90 min. Bar, 100 μm.

Inhibition of Cell Attachment to Tenascin by RGD Peptides

The peptide GRGDSP inhibited the cell attachment of the U251MG cells to tenascin in a dose-dependent manner (Fig. 5), while the control peptide GRGESP (Pierschbacher and Ruoslahti, 1984*b*) had no effect, even at high concentrations (10 mg/ml, not shown).

Inhibition of cell attachment to tenascin by the GRGDSP peptide occurred at concentrations of 30 and 150 times lower than were needed for comparable inhibition of cell attachment on vitronectin or fibronectin (Fig. 5). The concentra-

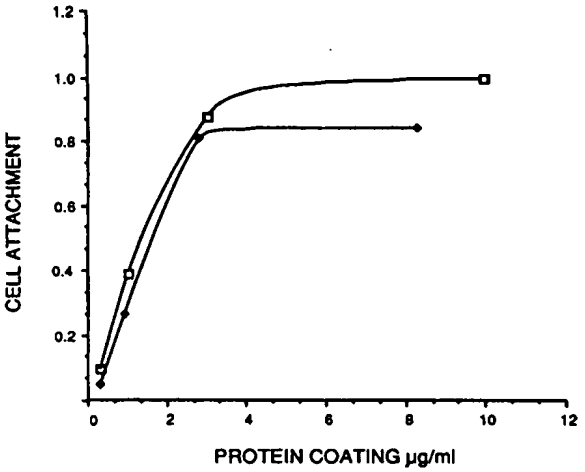

Figure 3. Comparison of cell attachment activity of tenascin and fibronectin. The attachment of U251MG cells to microtiter wells coated with tenascin (♦) or fibronectin (□) at various concentrations was assayed. Cells at 2 × 10^4/200 μl in DME–BSA were seeded into the wells and allowed to adhere. The cell attachment activity is plotted relative to maximum cell attachment to fibronectin.

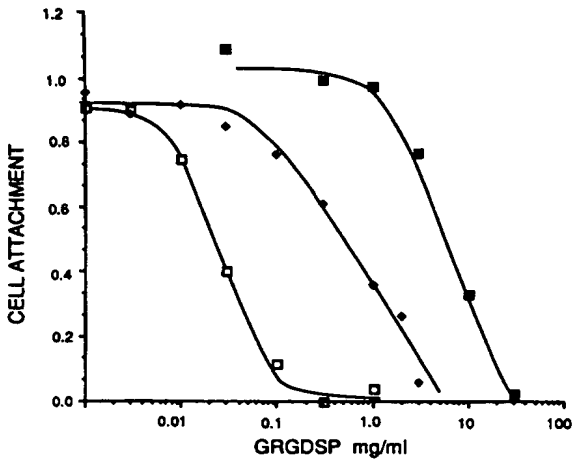

Figure 5. Effect of GRGDSP peptide on tenascin-mediated cell attachment. Cell attachment to tenascin (□), vitronectin (♦), and fibronectin (■), in the presence of various concentrations of GRGDSP peptide is shown. Wells were coated with 3 μg/ml adhesion protein and 2 × 10^4 cells added in serum-free media containing increasing amounts of GRGDSP peptide.

tion of GRGDSP resulting in a 50% inhibition of cell attachment to tenascin was 25 μg/ml, whereas 500 μg/ml and 4.5 mg/ml, respectively, were necessary to produce the same degree of inhibition on vitronectin and fibronectin.

RGD-dependent Tenascin Receptor

A receptor for tenascin was isolated from octylglucoside extracts of surface-labeled cells by affinity chromatography on a tenascin–Sepharose column. After the column was washed with octylthioglucoside, it was eluted with peptides, first GRGESP and then GRGDSP. As has been found to be the case with other RGD-directed receptors (Pytela et al., 1985*a*,*b*), the GRGESP peptide at 1 mg/ml eluted from the tenascin column a small proportion of protein, but the bulk of the bound protein eluted with the GRGDSP peptide. SDS-PAGE revealed specifically eluted 145- and 125-kD polypeptides (Fig. 6 *A*). The eluted material also contained a minor band at ~200 kD, the identity of which was not studied further because it was not observed in all receptor preparations. Upon reduction of disulfide bonds, the GRGDSP-eluted material gave only a one major band at 130 kD, presumably because the main polypeptides comigrate after reduction (Fig. 6 *B*).

The decrease of the size of the larger (α) subunit on reduction indicated the α subunit may be composed of a heavy and light chain as is seen for the fibronectin receptor α subunit. However, the light chain of the tenascin receptor α subunit could not be readily identified in the reduced receptor preparations, perhaps due to a paucity of radiolabeling sites in this particular chain. The polypeptide composition is similar to that of the integrin-type adhesion receptors (Hynes, 1987; Ruoslahti and Pierschbacher, 1987). In particular the tenascin receptor β subunit had the same chain mobility as the fibronectin receptor β subunit, suggesting that the tenascin receptor was a member of the fibronectin receptor subfamily of integrins. This assumption was confirmed by immunological analysis as shown below.

The tenascin receptor was compared with the vitronectin receptor and fibronectin receptor isolated from U251MG cell extracts. The previously characterized vitronectin receptor (Pytela et al., 1985*b*) was obtained when the U251MG cell extract was fractionated on a GRGDSP–Sepharose affinity matrix (not shown). The tenascin receptor did not bind detectably to a GRGDSPK–Sepharose column. Moreover, the tenascin receptor could be isolated on tenascin–Sepharose even after the U251MG extract was first passed over GRGDSPK–Sepharose. Similar experiments with the cell-binding 120-kD fragment of fibronectin (Pytela et al., 1985*a*) showed that the U251MG cells also have a distinct fibronectin receptor (Fig. 7) and that no detectable tenascin receptor bound to this affinity matrix.

Receptor immunoprecipitation and immunoblotting were used to confirm the heterodimer composition of the receptor

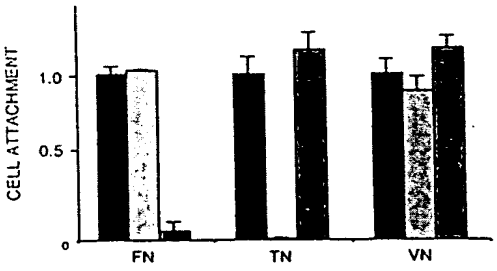

Figure 4. Inhibition of tenascin-mediated cell attachment by anti-tenascin antibodies. Cell attachment to fibronectin (*FN*), tenascin (*TN*), and vitronectin (*VN*) was assayed in the presence or absence of polyclonal antifibronectin antibodies and polyclonal antitenascin antibodies. Wells were coated with 5 μg/ml of adhesion protein. Antibody concentrations per well were 20 μg/ml antifibronectin antibody or 200 μg/ml antitenascin antibody. Values represent relative cell attachment ± SD. Controls represent maximum cell attachment on each adhesion protein in the absence of added antibody. ■, control; ▨, anti-TN; ▩, anti-FN.

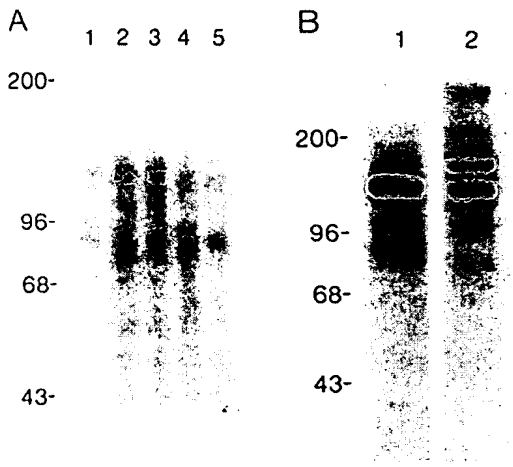

Figure 6. Affinity isolation of tenascin receptor. Tenascin receptor was isolated on tenascin–Sepharose from ^{125}I cell surface labeled U251MG cells, solubilized in 50 mM octylglucoside, 1 mM $CaCl_2$, 1 mM $MgCl_2$. (*A*) Tenascin receptor was eluted from a 1-ml tenascin–Sepharose column with 1 mg/ml GRGDSP peptide in octylthioglucoside, 1 mM $CaCl_2$, 1 mM $MgCl_2$ (lanes *2–5*). The column was first washed with 1 mg/ml GRGESP peptide in octylthioglucoside as above (lane *1*, final wash fraction). Fraction volumes were 0.5 ml. Samples of each fraction were subjected to electrophoresis on a 7% SDS-acrylamide gel under reducing conditions and autoradiographed. (*B*) Comparison of ^{125}I-labeled tenascin receptor subjected to electrophoresis on a 7.5% SDS-acrylamide gel under reducing (*1*) and nonreducing (*2*) conditions. Molecular mass markers in kilodaltons are shown.

and to identify the β subunit of the tenascin receptor. The tenascin receptor α and β subunits were both immunoprecipitated with antifibronectin receptor β subunit polyclonal antibodies, suggesting an immunologic identity between the β subunits of these receptors (Fig. 7, *left*). Receptor immunoblots with an antifibronectin receptor β subunit monoclonal antibody confirmed the immunological similarity between the tenascin receptor and fibronectin receptor β subunits (Fig. 7). Based on these results it appears that the two receptors share the same β subunit. The α subunit of the tenascin receptor was not reactive with an antibody against the fibronectin receptor α subunit and neither subunit of the tenascin receptor bound anti-vitronectin receptor antibodies.

Discussion

In this paper we have shown by using cell attachment assays that tenascin can interact with cells in an RGD-dependent manner and have isolated and partially characterized a receptor that binds to tenascin with a similar specificity as the cells.

Cell attachment assays showed that human tenascin insolubilized on plastic interacts with a number of tumor and normal cell types supporting their attachment. Perhaps as significant was the finding that at least several cell lines and lymphoid cells did not attach or attached poorly to tenascin. This may indicate that these cells either lack cell receptors or the receptor interaction is not detectable by cell attachment.

Titration curves comparing the attachment of cells to tenascin and fibronectin in a serum-free medium showed that similar numbers of cells attached to the two proteins. Inhibition of cell attachment to tenascin by tenascin-specific antibodies but not by antifibronectin antibodies, indicated a specific interaction of tenascin with the cells. Among the cell lines tested, the U251MG glioma cells attached to tenascin particularly well, and these cells were chosen for detailed studies on the cell–tenascin interaction.

Tenascin appears to be a member of the RGD family of cell attachment proteins (Ruoslahti and Pierschbacher, 1987), as demonstrated by the specific, dose-dependent inhibition of cell attachment to tenascin by RGD peptides. These results imply the presence of an RGD sequence within the tenascin polypeptide and, indeed at least chicken cytotactin (tenascin) does contain this sequence (Jones et al., 1988).

Previous work on the cellular interactions of tenascin has indicated that tenascin lacks cell attachment-promoting activity (Erickson and Taylor, 1987) or that it can interact with cells promoting attachment, but is an inhibitor of fibronectin-mediated cell attachment (Chiquet-Ehrismann et al., 1988). These results are not necessarily in conflict with ours for the following reasons.

Our results show that the cell attachment-promoting activity to tenascin is distinct from that of fibronectin and vitronectin in that little cell spreading is seen on tenascin. The cell attachment-inhibiting activity observed by others could be an indication that the cell–tenascin interaction, which initially manifests itself as cell attachment, is primarily a signal for another type of response, such as migration or differentiation. In this regard, the cell attachment-promoting activity of tenascin might be considered a manifestation of an interaction between the cell and tenascin rather than an indication of the physiological result of the interaction. In fact, it is an exciting possibility that while some extracellular matrix molecules give to cells signals leading to attachment and spreading others may signal migration or even detachment. In addition to tenascin, such a role has been proposed for thrombospondin (Lahav, 1988), which may also interact with cells in an RGD-dependent manner (Lawler and Hynes, 1986).

We find that the cell–tenascin interaction can be inhibited with an RGD peptide, and others have found that soluble tenascin inhibits the attachment of cells to an RGD peptide substrate (Chiquet-Ehrismann et al., 1988). However, these investigators also found that the soluble RGD peptide was not capable of inhibiting the attachment of the same cells to tenascin. The reasons for this difference are not known, but it may be that cells can also bind to tenascin through a non-RGD–dependent mechanism. Fibronectin and laminin are each known to have more than one integrin-type receptor (Gehlsen et al., 1988; Hemler et al., 1987; Horwitz et al., 1985; Ignatius and Reichardt, 1988; Johansson et al., 1987; Pytela et al., 1985*a*, 1986; Takada et al., 1988; Wiersma et al., 1988), and other types of molecules, such as proteoglycans, can also mediate cell attachment to fibronectin (LeBaron et al., 1988; Saunders and Bernfield, 1988). If more than one receptor exists for tenascin, differences in the source of tenascin, the methods used in its isolation, the cell type employed in the assays and the details of the assay methodology may favor one receptor over others, explaining the divergent observations by different laboratories. From our results it ap-

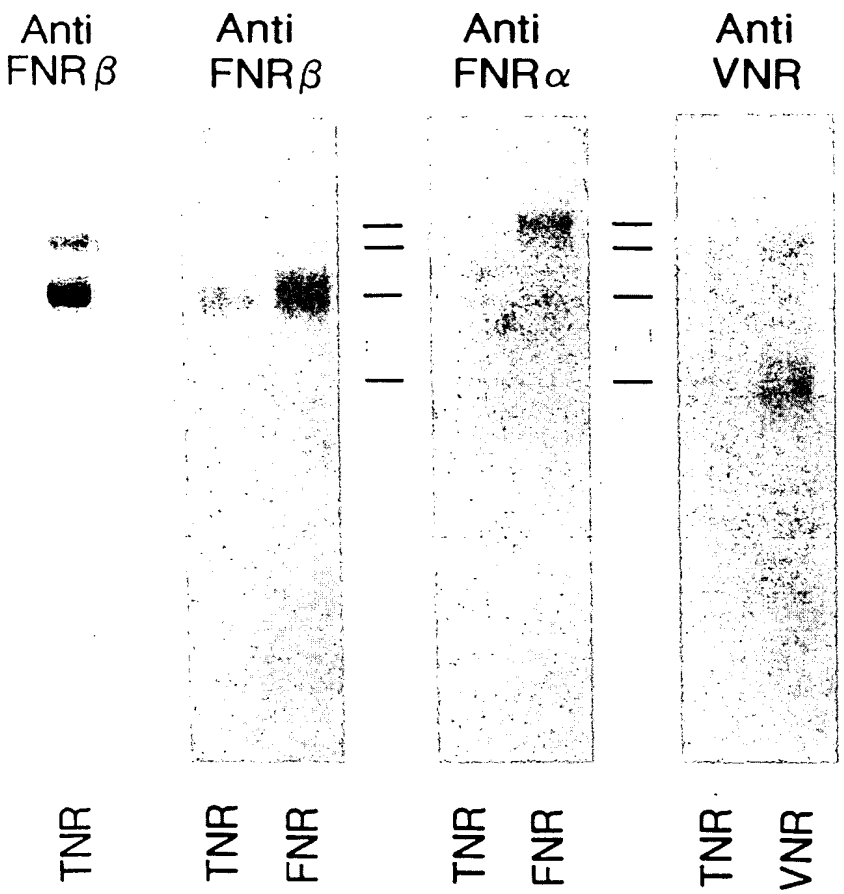

Figure 7. Immunoprecipitation and immunoblotting analysis of tenascin, fibronectin and vitronectin receptors. Immunoprecipitation (*far left*): Affinity-purified tenascin receptor (*TNR*) was immunoprecipitated with polyclonal antibodies to the fibronectin receptor β subunit and analyzed by SDS-PAGE on a 7.5% acrylamide gel under nonreducing conditions. Immunoblots: Affinity-purified tenascin receptor (*TNR*), fibronectin receptor (*FNR*), and a vitronectin receptor (*VNR*) all from the U251MG cells were subjected to electrophoresis as above and electroblotted onto nitrocellulose membranes for immunoblotting. The antibodies used were an antifibronectin receptor β subunit monoclonal antibody 442 (*Anti-FNRβ*; Cheresh, D., J. O. Gailit, and E. Ruoslahti, unpublished results), a rabbit antibody prepared against the cytoplasmic peptide of the fibronectin receptor α subunit (*Anti-FNRα*; Argraves, W. S., and E. Ruoslahti, unpublished results), and polyclonal antivitronectin receptor antibodies (*Anti-VNR*). Approximately equal amounts of receptor protein were blotted as estimated by Ponceau-S staining before immunoblotting. Relative positions of α and β subunits are indicated.

pears that one mechanism whereby cells can interact with tenascin is through an RGD-dependent integrin-type receptor.

The tenascin receptor we have isolated has a β subunit that is similar and possibly identical to the fibronectin receptor β subunit. This β subunit is shared by at least six different integrins that together comprise the fibronectin receptor or VLA family within the integrin superfamily (Hynes, 1987; Ruoslahti and Pierschbacher, 1987; Hemler et al., 1987; Takada et al., 1988). Like the other integrins, the tenascin receptor appears to be a heterodimer of the β subunit and an α subunit, because the two subunits coprecipitated upon immunoprecipitation with antibodies reactive with the β subunit. The α subunit of the tenascin receptor is clearly distinct from the fibronectin receptor α subunit, but whether it might be identical to one of the many other known integrin α subunits will have to be determined in future studies. It will also be important to determine whether tenascin is the only ligand for the receptor we have identified. The affinity chromatography results presented here suggest that it does not bind to fibronectin and that it has a specificity different from that of the vitronectin receptor. However, the lack of sufficient quantities of the receptor has so far precluded more detailed specificity studies by assays such as the liposome assay used with other receptors (Pytela et al., 1985*a*,*b*).

A functional difference between tenascin and fibronectin or vitronectin is suggested by the differences in cell morphology seen as cells attach to these proteins. Since tenascin is selectively expressed in developing organs and in tumors (Aufderheide et al., 1987; Bourdon et al., 1983; Chiquet-Ehrismann et al., 1986; Grumet et al., 1985), the interaction of cells with tenascin may have a special significance in cell differentiation, proliferation, and migration. Our identification of the first receptor for tenascin will facilitate studies on the involvement of tenascin in these phenomena. The sensitivity of this receptor to inhibition by RGD peptides indicates that these peptides can be used to probe its functional role without substantially affecting the functions of other integrins.

We thank Drs. Scott Argraves, James Gailit, and David Cheresh for receptor antibodies, and Dr. Douglas Fambrough for antisera to chick tenascin. This work was supported by grants CA45586 (to M. A. Bourdon), CA42507, CA28896 (E. Ruoslahti), and Cancer Center Support Grant CA 30199 from the National Cancer Institute.

Received for publication 18 June 1988 and in revised form 8 November 1988.

References

Argraves, W. S., S. Suzuki, H. Arai, K. Thompson, M. D. Pierschbacher, and E. Ruoslahti. 1987. Amino acid sequence of the human fibronectin receptor. *J. Cell Biol.* 105:1183–1190.

Aufderheide, E., R. Chiquet-Ehrismann, and P. Ekblom. 1987. Epithelial–mesenchymal interactions in the developing kidney lead to expression

of tenascin in the mesenchyme. *J. Cell Biol.* 105:599–608.
Bourdon, M. A., C. J. Wikstrand, H. Furthmayr, T. J. Matthews, and D. D. Bigner. 1983. A human glioma-mesenchymal extracellular matrix antigen defined by monoclonal antibody. *Cancer Res.* 43:2796–2806.
Bourdon, M. A., T. J. Matthews, S. V. Pizzo, and D. D. Bigner. 1985. Immunochemical and biochemical characterization of a glioma associated extracellular matrix glycoprotein. *J. Cell. Biochem.* 28:183–195.
Cardarelli, P. M., and M. D. Pierschbacher. 1986. T-lymphocyte differentiation and the extracellular matrix: identification of a thymocyte subset that attaches specifically to fibronectin. *Proc. Natl. Acad. Sci. USA.* 83:2647–2651.
Chiquet, M., and D. M. Fambrough. 1984. Chick myotendinous antigen II. A novel extracellular glycoprotein complex consisting of large disulfide-linked subunits. *J. Cell Biol.* 98:1937–1946.
Chiquet-Ehrismann, R., E. J. Mackie, C. A. Pearson, and T. Sakakura. 1986. Tenascin: an extracellular matrix protein involved in tissue interactions during fetal development and oncogenesis. *Cell.* 47:131–139.
Chiquet-Ehrismann, R., P. Kalla, C. Pearson, K. Beck, and M. Chiquet. 1988. Tenascin interferes with fibronectin action. *Cell.* 53:383–390.
Couchman, J. R., D. A. Rees, M. R. Green, and C. G. Smith. 1982. Fibronectin has a dual role in locomotion and anchorage of primary chick fibroblasts and can promote entry into the division cycle. *J. Cell Biol.* 93:402–410.
Crossin, K. L., S. Hoffman, M. Grumet, J.-P. Thiery, and G. M. Edelman. 1986. Site-restricted expression of cytotactin during development of the chicken embryo. *J. Cell Biol.* 102:1917–1930.
Edgar, D., R. Timpl, and H. Thoenen. 1984. The heparin-binding domain of laminin is responsible for its effects on neurite outgrowth and neuronal survival. *EMBO (Eur. Mol. Biol. Organ.) J.* 3:1463–1468.
Ekblom, P. 1984. Basement membrane proteins and growth factors in kidney differentiation. *In* The Role of Extracellular Matrix in Development. R. L. Trelstad, editor. Alan R. Liss Inc., New York. 173–206.
Engvall, E., and E. Ruoslahti. 1977. Binding of soluble form of fibroblast surface protein, fibronectin, to collagen. *Int. J. Cancer.* 20:1–5.
Engvall, E., H. Hessle, and G. Klier. 1986. Molecular assembly secretion and matrix deposition of type VI collagen. *J. Cell Biol.* 102:703–710.
Erickson, H. P., and H. C. Taylor. 1987. Hexabrachion proteins in embryonic chicken tissues and human tumors. *J. Cell Biol.* 105:1387–1394.
Gehlsen, K. R., L. Dillner, E. Engvall, and E. Ruoslahti. 1988. The human laminin receptor is a member of the integrin family of cell adhesion receptors. *Science (Wash. DC).* 241:1228–1229.
Giancotti, F. G., C. G. Tarone, K. Knudsen, C. Damsky, and P. M. Comoglio. 1985. Cleavage of a 135 kd cell surface glycoprotein correlates with loss of fibroblast adhesion to fibronectin. *Exp. Cell Res.* 156:182–190.
Gospodarowicz, D., D. Delgado, and I. Vlodavsky. 1980. Permissive effect of the extracellular matrix on cell proliferation in vitro. *Proc. Natl. Acad. Sci. USA.* 77:4094–4098.
Greenberg, G., and E. D. Hay. 1986. Cytodifferentiation and tissue phenotype change during transformation of embryonic lens epithelium to mesenchyme-like cells in vitro. *Dev. Biol.* 115:363–379.
Grumet, M., S. Hoffman, K. L. Crossin, and G. M. Edelman. 1985. Cytotactin, an extracellular matrix protein of neural and non-neural tissues that mediates glia-neuron interaction. *Proc. Natl. Acad. Sci. USA.* 82:8075–8079.
Hayman, E. G., M. D. Pierschbacher, Y. Ohgren, and E. Ruoslahti. 1983. Serum spreading factor (vitronectin) is present at the cell surface and in tissues. *Proc. Natl. Acad. Sci. USA.* 80:4003–4007.
Hemler, M. E., C. Huang, and L. Schwarz. 1987. The VLA protein family. Characterization of five distinct cell surface heterodimers each with a common 130k molecular weight β subunit. *J. Biol. Chem.* 262:3300–3309.
Horwitz, A., K. Duggan, R. Greggs, C. Deckey, and C. Buck. 1985. The cell substrate attachment (CSAT) antigen has properties of a receptor for laminin and fibronectin. *J. Cell Biol.* 101:2134–2144.
Hynes, R. O. 1987. Integrins: a family of cell surface receptors. *Cell.* 48: 549–554.
Ignatius, M. J., and L. F. Reichardt. 1988. Identification and characterization of a neuronal laminin receptor: an integrin heterodimer that binds laminin in a divalent cation-dependent manner. *Neuron.* 1:713.
Johansson, S., E. Forsberg, and B. Lundgren. 1987. Comparison of fibronectin receptors from rat hepatocytes and fibroblasts. *J. Biol. Chem.* 262:7819–7824.
Jones, F. S., M. P. Burgoon, S. Hoffman, K. L. Grossin, B. A. Cunningham, and G. M. Edelman. 1988. A cDNA clone for cytotactin contains a sequence similar to epidermal growth factor-like repeats and segments of fibronectin and fibrinogen. *Proc. Natl. Acad. Sci. USA.* 85:2186–2190.
Lacovara, J., E. B. Cramer, and J. P. Quigley. 1984. Fibronectin enhancement of directed migration of B16 melanoma cells. *Cancer Res.* 44:1657–1663.
Lahav, J. 1988. Thrombospondin inhibits adhesion of endothelial cells. *Exp. Cell Res.* 177:199–204.
Lawler, J., and R. O. Hynes. 1986. The structure of human thrombospondin, an adhesive glycoprotein with multiple calcium-binding sites and homologies with several different proteins. *J. Cell Biol.* 103:1635–1648.
LeBaron, R., J. Esko, A. Woods, S. Johansson, and M. Hook. 1988. Adhesion of glycosaminoglycan-deficient Chinese hamster ovary cell mutants to fibronectin substrata. *J. Cell Biol.* 106:945–952.
Mackie, E. J., R. Chiquet-Ehrismann, C. A. Pearson, Y. Inaguma, K. Taya, Y. Kawarada, and T. Sakakura. 1987. Tenascin is a stromal marker for epithelial malignancy in the mammary gland. *Proc. Natl. Acad. Sci. USA.* 84:4621–4625.
Manthorpe, M., E. Engvall, E. Ruoslahti, F. M. Longo, G. E. Davis, and S. Varon. 1983. Laminin promotes neuritic regeneration from cultured peripheral and central neurons. *J. Cell Biol.* 97:1882–1890.
McComb, R. D., J. M. Moul, and D. D. Bigner. 1987. Distribution of type VI collagen in human gliomas: comparison with fibronectin and glioma-mesenchymal matrix glycoprotein. *J. Neuropathol. & Exp. Neurol.* 46: 623–633.
Pierschbacher, M. D., and E. Ruoslahti. 1984*a*. Cell attachment activity at fibronectin can be duplicated by small synthetic fragments of the molecule. *Nature (Lond.).* 309:30–33.
Pierschbacher, M. D., and E. Ruoslahti. 1984*b*. Variants of the cell recognition site of fibronectin that retain attachment-promoting activity. PNAS 81: 5985–5988.
Pytela, R., M. D. Pierschbacher, and E. Ruoslahti. 1985*a*. Identification and isolation of a 140 kd cell surface glycoprotein with properties expected of a fibronectin receptor. *Cell.* 40:191–198.
Pytela, R., M. D. Pierschbacher, and E. Ruoslahti. 1985*b*. A 125/115 kd cell surface receptor specific for vitronectin interacts with the arginine-glycine-aspartic acid adhesion sequence derived from fibronectin. *Proc. Natl. Acad. Sci. USA.* 82:5766–5770.
Pytela, R., M. D. Pierschbacher, M. H. Ginsberg, E. F. Plow, and E. Ruoslahti. 1986. Platelet membrane glycoprotein IIb/IIIa is a member of a family of arg-gly-asp-specific adhesion receptors. *Science (Wash. DC).* 231:1559–1562.
Rovasio, R. A., A. Delouvee, K. M. Yamada, R. Timpl, and J.-P. Thiery. 1983. Neural crest cell migration: requirements for exogenous fibronectin and high cell density. *J. Cell Biol.* 96:462–473.
Ruoslahti, E., and M. D. Pierschbacher. 1987. New perspectives in cell adhesion: RGD and integrins. *Science (Wash. DC)* 238:491–497.
Saunders, S., and M. Bernfield. 1988. Cell surface proteoglycan binds mouse mammary epithelial cells to fibronectin and behaves as an interstitial matrix receptor. *J. Cell Biol.* 106:423–430.
Suzuki, S., W. S. Argraves, H. Arai, L. R. Languino, M. D. Pierschbacher, and E. Ruoslahti. 1987. Amino acid sequence of the vitronectin receptor α subunit and comparative expression of adhesion receptor mRNAs. *J. Biol. Chem.* 262:14080–14085.
Takada, Y., E. A. Wayner, W. G. Carter, and M. E. Hemler. 1988. Extracellular matrix receptors, ECMRII and ECMRI, for collagen and fibronectin correspond to VLA-2 and VLA-3 in the VLA family of heterodimers. *J. Cell. Biochem.* 37:385–393.
Tamkun, J. W., D. W. DeSimone, D. Fonda, R. S. Patel, C. Buck, A. F. Horwitz, and R. O. Hynes. 1986. Structure of integrin, a glycoprotein involved in the transmembrane linkage between fibronectin and actin. *Cell.* 46:271–282.
Tomaselli, K. J., C. H. Damsky, and L. F. Reichardt. 1987. Interactions of a neuronal cell line (PC12) with laminin, collagen IV, and fibronectin: identification of integrin-related glycoproteins involved in attachment and process outgrowth. *J. Cell Biol.* 105:2347–2358.
Vaughn, L., S. Huber, M. Chiquet, and K. H. Winterhalter. 1987. A major, six-armed glycoprotein from embryonic cartilage. *EMBO (Eur. Mol. Biol. Organ.) J.* 6:349–353.
Wiersma, E., G. Froman, S. Johansson, and T. Wadstrom. 1988. Carbohydrate specific binding of fibronectin to vibrio cholerae cells. *FEMS (Fed. Eur. Microbiol. Soc.) Microbiol. Lett.* 44:365–369.

Journal of Molecular Diagnostics, Vol. 8, No. 1, February 2006

DOI: 10.2353/jmoldx.2006.040402

Multiple Gene Expression Analyses in Paraffin-Embedded Tissues by TaqMan Low-Density Array

Application to Hedgehog and Wnt Pathway Analysis in Ovarian Endometrioid Adenocarcinoma

Adam Steg,* Wenquan Wang,† Carmelo Blanquicett,* Jessica M. Grunda,* Isam A. Eltoum,‡ Kangsheng Wang,* Donald J. Buchsbaum,§ Selwyn M. Vickers,¶ Suzanne Russo,§ Robert B. Diasio,* Andra R. Frost,‡ Al F. LoBuglio,‖ William E. Grizzle,‡ and Martin R. Johnson*

From the Departments of Pharmacology and Toxicology, Division of Clinical Pharmacology, Biostatistics,† Pathology,‡ Radiation Oncology,§ Surgery,¶ and the Comprehensive Cancer Center,‖ University of Alabama at Birmingham, Birmingham, Alabama*

Recent studies have shown the hedgehog and Wnt families of signaling proteins to be associated with tumor initiation, growth, and survival. However, these pathways remain unexplored in ovarian endometrioid adenocarcinoma (OEA). Here, we describe a novel TaqMan low-density array to examine the expression of 26 and 20 genes in the hedgehog and Wnt pathways, respectively, in six matched snap-frozen and formalin-fixed, paraffin-embedded (FPE) OEA specimens. Expression values were normalized to uninvolved ovarian epithelium. Gene expression in matched frozen and FPE tissues demonstrated significant concordance ($r = 0.92$, $P < 0.0001$). However, comparison of amplified and unamplified RNA from frozen OEA tissues revealed an altered molecular profile in amplified RNA. Amplification of RNA from FPE tissues was not successful. The expression of *Desert hedgehog* (*DHH*), *Indian hedgehog* (*IHH*), *Hedgehog interacting protein* (*HHIP*), *Wnt10B*, *Wnt9B*, and *Wnt inhibitory factor* (*WIF1*) were tumor-specific with no detectable expression in normal ovarian epithelium. In addition, several genes were significantly ($P < 0.025$) down-regulated in OEA, including *cyclin E2*, *Porcupine*, c-*Myc*, and *Axin 2* (4.8-, 3.6-, 2.9-, and 1.9-fold, respectively). TaqMan low-density array provides an effective multivariate technique for examining gene expression in RNA isolated from either snap-frozen or archival FPE tissues and can identify tumor-specific genes, possibly leading to novel treatments. *(J Mol Diagn 2006, 8:76–83; DOI: 10.2353/jmoldx.2006.040402)*

Ovarian cancer is distinguished by particularly aggressive local invasiveness potential and in the United States, remains the fourth highest cause of cancer death in women.[1,2] Epithelial ovarian cancer is the major ovarian malignancy consisting of four histological subtypes including serous, mucinous, endometrioid, and clear cell with ovarian endometrioid adenocarcinoma (OEA) being the second most common.[3] Unfortunately, ~80% of patients diagnosed with advanced OEA die within 5 years.[4] In addition, the limited knowledge of the molecular mechanisms involved in the development and clinical progression of OEA have hampered attempts to develop novel rationally designed treatment paradigms.

Activation of the hedgehog signaling pathway, normally involved in embryogenesis, can lead to tumor formation and is necessary for tumor survival in several types of cancer (including medulloblastoma, basal cell carcinoma, small-cell lung cancer, and breast cancer).[5–10] Recent studies have also implicated hedgehog signaling as an early mediator of tumorigenesis in cancers of the digestive tract, particularly pancreatic adenocarcinoma.[11,12] Collectively, these studies suggest that abrogation of the hedgehog pathway may provide a novel, targeted therapeutic approach. Interestingly, the hedgehog pathway has not been examined in OEA. The Wnt pathway, also involved in embryogenesis, has been found to possess similarities to the hedgehog pathway with respect to posttranslational modification, secretion, signaling mechanisms, and tumorigenesis.[13,14] Recent studies have shown that increased expression of components in the Wnt pathway have been implicated in ovarian

Supported by the National Institutes of Health (grants CA101955-01 and CA086359-06).

Accepted for publication August 5, 2005.

Address reprint requests to Martin R. Johnson, Ph.D., Department of Clinical Pharmacology, 1824 6th Ave. South, Wallace Tumor Institute, Room 620, University of Alabama at Birmingham, Birmingham, AL 34294-3300. E-mail: martin.johnson@ccc.uab.edu.

tumorigenesis, although the exact molecular mechanisms remain to be elucidated.[15,16]

Despite recent advances in gene quantitation technology, there is limited analysis of large clusters of genes, such as the hedgehog and Wnt families, in ovarian carcinomas in part because of the limited availability of fresh frozen tissue. Conversely, formalin-fixed, paraffin-embedded (FPE) tissues, derived from institutional archives, offer a more readily available alternative to frozen tissue in most cancer treatment/research facilities. Several studies have shown that real-time quantitative (RTQ) polymerase chain reaction (PCR) can be used to quantify gene expression from RNA isolated from FPE tissue.[17–22] However, these studies have been limited by RTQ's ability to quantify only one gene at a time in a single RNA sample. In addition, validation of gene expression profiles obtained from frozen versus FPE tissue has been problematic due to the difficulty in obtaining matched frozen and paraffin-embedded samples. The capabilities of RTQ have recently been expanded with the development of TaqMan low-density arrays (TLDAs) (Applied Biosystems, Foster City, CA), which are able to determine the expression of multiple, user-defined gene clusters simultaneously.

In the current study, we examine whether TLDA could be used for the analysis of archival, paraffin-embedded tissues by correlating the expression of 26 and 20 genes in the hedgehog and Wnt pathways, respectively, in six matched snap-frozen and FPE OEA specimens. In addition, expression profiles of amplified versus unamplified RNA were compared to determine whether the small amounts of RNA available from needle biopsies or laser capture-microdissected samples could be increased and quantified while conserving the expression profile. These analyses represent the first multivariate examination of the hedgehog and Wnt pathways in OEA.

Materials and Methods

Tissue Collection and Processing

Six ovarian endometrioid tumors were obtained from the Department of Pathology at the University of Alabama at Birmingham using an institutional review board-approved protocol. The samples were collected in the operating room and sectioned into three pieces. The central piece was immediately snap-frozen in liquid nitrogen and stored at −80°C before RNA isolation. The other two end pieces were immediately fixed in neutral-buffered formalin for 6 to 18 hours before paraffin embedding. Paraffin-embedded tissues were cut into 20-μm sections and stored at room temperature before RNA isolation. Normal ovarian surface epithelium (OSE) that harbored no neoplasms was scraped from the ovaries of two unrelated patients and immediately snap-frozen in liquid nitrogen and stored at −80°C before RNA isolation.

RNA Extraction

Total RNA was isolated from frozen tissues using Trizol reagent (Invitrogen, Carlsbad, CA) as per the manufacturer's instructions. RNA was then DNase treated and purified using the RNeasy mini kit (Qiagen, Hilden, Germany) as per the manufacturer's instructions. RNA was eluted in 30 μl of RNase-free water and stored at −80°C.

Paraffin tissue sections were deparaffinized by incubation with 800 μl of xylene and 400 μl of 100% ethanol. The samples were then centrifuged and the supernatant was removed. Tissue pellets were washed with 1 ml of 100% ethanol and dried for 10 minutes at 55°C. The RNA isolation that followed was performed using the Roche High Pure RNA paraffin kit (Roche Diagnostics, Mannheim, Germany) as per the manufacturer's instructions. RNA was eluted in 30 μl of RNase-free water and stored at −80°C.

Housekeeping Gene Variability

Assessment of housekeeping gene variability between normal and neoplastic ovarian tissues was performed as previously described.[23] Briefly, the RNA concentrations of both the OEA and OSE samples were determined spectrophotometrically by A_{260} measurement and adjusted to 20 ng/μl to ensure that differences in housekeeping gene expression were not because of variability in RNA concentrations. Because of the low amounts of tissue obtained from the two scraped OSE specimens, their RNA was combined to obtain a sufficient concentration for further analysis. The concentration of each sample was confirmed by densitometry and RNA integrity (degradation) was verified by electrophoresis and ethidium bromide staining on a 1% agarose gel. Primers and probe for the *ribosomal protein, large, P0* (*RPLP0*) (NM_001002) gene were obtained from Applied Biosystems (Foster City, CA) and used according to the manufacturer's instructions. The concentration of all RNA samples (OSE and OEA) was then determined using *RPLP0* and linear regression analysis of a standard curve derived from known concentrations of normal ovary total RNA (Ambion, Austin, TX) as previously described by our laboratory.[23,24]

RNA Amplification

A fixed amount of 20 ng of total RNA isolated from either frozen or paraffin-embedded OEA was amplified using the Ovation Nanosample RNA amplification system (NuGEN Technologies, Inc., San Carlos, CA), Full Spectrum Global amplification kit (System Biosciences, Mountain View, CA), MessageAmp aRNA kit (Ambion) and RiboAmp RNA amplification kit (Arcturus, Mountain View, CA) as per the manufacturers' instructions. The yield obtained from each amplification procedure was assessed by the RPLP0 housekeeping gene.

Reverse Transcription

Before cDNA synthesis, all RNA samples, amplified and unamplified, were diluted to 4 ng/μl using RNase-free

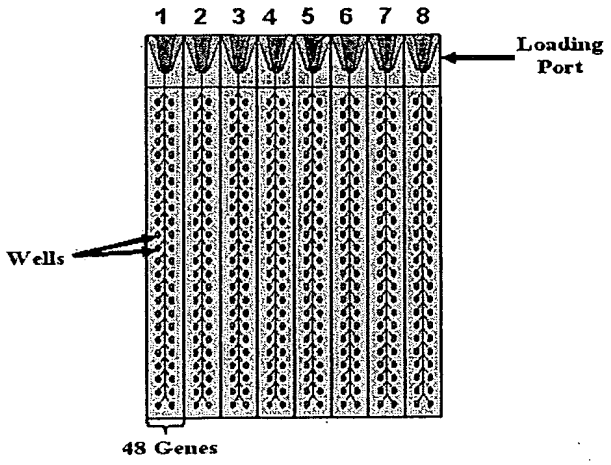

Figure 1. TLDA design using a 48-gene template.

water containing 12.5 ng/μl of total yeast RNA (Ambion) as a carrier. cDNA was prepared using the High Capacity cDNA archive kit (Applied Biosystems) as per the manufacturer's instructions. The resulting cDNA samples were used immediately for TLDA analysis.

PCR Amplification Efficiency

For RNA isolated from frozen and FPE tissues, a standard curve was prepared using 20, 10, 5, 2.5, and 1.25 ng RNA. RTQ was performed for the *RPLP0* housekeeping gene. The slope to each standard curve was then calculated and the efficiency of PCR amplification was determined using the equation $e = 10^{(-1/\text{slope})}$. In a PCR reaction that is 100% efficient, the amount of amplicon doubles at each cycle such that an e of 2 represents 100% PCR amplification efficiency.

TLDA

TLDA Design

For each card of the low-density array, there are eight separate loading ports that feed into 48 separate wells for a total of 384 wells per card (Figure 1). Each 2-μl well contains specific, user-defined primers and probes, capable of detecting a single gene. In this study, the TLDA card was configured into eight identical 48-gene sets (Figure 1). Genes were chosen based on literature reviews of the hedgehog, Wnt, and cell cycle molecular pathways and their involvement in tumorigenesis.[5,6,13,14,25] Each set of 48 genes (Table 1) also contains two housekeeping genes, *RPLP0* and 18S (a mandatory control designed into each card by the manufacturer). In this study, however, *RPLP0* was used exclusively as the housekeeping gene.

TLDA Preparation

Each cDNA sample (100 μl) was added to an equal volume of 2× TaqMan Universal PCR Master Mix (Applied Biosystems). After gentle mixing and centrifugation, the mixture was then transferred into a loading port on a TLDA card (Applied Biosystems). Each of the six matched OEA samples were run in quadruplicate with one matching pair (frozen and FPE) on each card. Amplified RNA samples were also run in quadruplicate on separate cards. To distinguish tumor-specific activation of the hedgehog and Wnt pathways, RNA from two combined snap-frozen OSE samples were also analyzed. The array was centrifuged twice for 1 minute each at 1200 rpm (306 × g) to distribute the samples from the loading port into each well. The card was then sealed and PCR amplification was performed using an Applied Biosystems Prism 7900HT sequence detection system. Thermal cycler conditions were as follows: 2 minutes at 50°C, 10 minutes at 94.5°C, 30 seconds at 97°C, 1 minute at 59.7°C for 40 cycles.

TLDA Analysis

Expression values were calculated using the comparative C_T method as previously described (User Bulletin No. 2, Applied Biosystems). Briefly, this technique uses the formula $2^{-\Delta\Delta CT}$ to calculate the expression of target genes normalized to a calibrator. The threshold cycle (C_T) indicates the cycle number at which the amount of amplified target reaches a fixed threshold. C_T values range from 0 to 40 (the latter representing the default upper limit PCR cycle number that defines failure to detect a signal). ΔC_T values [$\Delta C_T = C_T$ (target gene) − C_T (*RPLP0*)] were calculated for the combined frozen OSE sample and subsequently used as the calibrator, for which all gene expression values were assigned a relative value of 1.00, to determine comparative gene expression such that $\Delta\Delta C_T = \Delta C_T$ (OEA sample) − ΔC_T (OSE sample). A range for each expression value was calculated based on the SD (s) of the $\Delta\Delta C_T$ value where $2^{-(\Delta\Delta CT + s)}$ is the lower limit and $2^{-(\Delta\Delta CT - s)}$ is the upper limit.

Validation of TLDA

Primers and probes for *Desert Hedgehog* (*DHH*) (NM_021044), *Indian Hedgehog* (*IHH*) (NM_002181), *Sonic Hedgehog* (*SHH*) (NM_000193), *Patched* (*PTCH*) (NM_000264), *Patched 2* (*PTCH2*) (NM_003738), *Smoothened* (*SMO*) (NM_005631), *Glioma-associated oncogene homolog 1* (*GLI*) (NM_005269), and *Glioma-associated oncogene homolog 3* (*GLI3*) (NM_000168) were obtained from Applied Biosystems and used according to the manufacturer's instructions. RTQ was then performed for these eight genes on the six matched frozen and FPE OEA samples as well as the combined OSE sample using an ABI Prism 7900HT sequence detection system. Gene expression was calculated using the comparative C_T method.

Statistical Analysis

All statistical analyses were conducted with SAS Ver. 9.1 (SAS Institute, Cary, NC). Because of the small sample size, a more stringent $P < 0.025$ was used to establish statistically significant differences rather than 0.05, which

Table 1. Hedgehog and Wnt Gene Expression in Ovarian Endometrioid Adenocarcinoma

Gene	Average frozen*	*P* value†	Ratio‡	Average paraffin*	*P* value†	Ratio‡
Desert hedgehog (DHH)	X		6/6	X		3/6
Hedgehog interacting protein (HHIP)	X		2/6	X		2/6
Indian hedgehog (IHH)	X		4/6	X		3/6
Wnt inhibitory factor 1 (WIF1)	X		5/6	X		4/6
Wingless-type MMTV integration site family, member 10B (WNT1)	X		5/6	X		4/6
Wingless-type MMTV integration site family, member 9B (WNT9B)	X		1/6	X		1/6
Porcupine (PPN)	0.28 ± 0.11	<0.0001	6/6	0.48 ± 0.39	0.021	6/6
Cyclin E2 (CCNE2)	0.21 ± 0.20	<0.0001	6/6	0.38 ± 0.45	0.020	6/6
c-Myc oncogene (MYC)	0.35 ± 0.39	0.010	6/6	0.12 ± 0.08	0.000	6/6
Axin 2 (AXIN2)	0.54 ± 0.29	0.011	6/6	0.54 ± 0.23	0.005	6/6
GLI pathogenesis-related 1 (GLIPR1)	0.46 ± 0.29	0.006	6/6	2.16 ± 2.53	0.312	6/6
HER-2/Neu (ERBB2)	1.39 ± 2.03	0.654	6/6	0.36 ± 0.51	0.027	6/6
Patched (PTCH)	0.83 ± 0.63	0.536	6/6	1.64 ± 0.55	0.035	6/6
Epidermal growth factor receptor (EGFR)	1.09 ± 0.86	0.802	6/6	2.90 ± 2.07	0.074	6/6
Wingless-type MMTV integration site family, member 7A (WNT7A)	7.01 ± 11.00	0.238	4/6	16.49 ± 18.06	0.090	4/6
Smoothened (SMO)	1.61 ± 1.44	0.345	6/6	2.96 ± 2.29	0.091	6/6
Frizzled homolog (FRZD1)	5.56 ± 10.29	0.328	6/6	9.34 ± 10.46	0.108	6/6
Patched 2 (PTCH2)	0.66 ± 0.56	0.194	6/6	5.60 ± 5.80	0.110	6/6
Glioma-associated oncogene (GLI)	3.84 ± 6.20	0.312	6/6	12.99 ± 15.39	0.114	5/6
Kringle-containing transmembrane protein 1 (KREMEN1)	1.22 ± 1.29	0.692	6/6	0.68 ± 0.43	0.126	6/6
Platelet-derived growth factor receptor-α (PDGFRA)	10.49 ± 7.80	0.031	6/6	12.79 ± 15.84	0.128	6/6
Glioma-associated oncogene 3 (GLI3)	1.22 ± 1.09	0.645	6/6	6.16 ± 7.06	0.134	6/6
Glioma-associated oncogene 2 (GLI2)	3.17 ± 4.47	0.289	6/6	5.41 ± 6.47	0.156	6/6
Low-density lipoprotein receptor-related protein 6 (LRP6)	1.85 ± 1.57	0.241	6/6	4.35 ± 4.99	0.161	6/6
Cyclin B1 (CCNB1)	0.46 ± 0.42	0.026	6/6	0.61 ± 0.58	0.163	6/6
p21, Cip1 (CDKNA1)	1.08 ± 1.30	0.881	6/6	2.93 ± 2.97	0.172	6/6
Frizzled related protein (FRZB)	1.60 ± 2.37	0.563	6/6	2.38 ± 2.16	0.178	6/6
K-ras oncogene 2 (KRAS2)	1.00 ± 0.85	0.992	6/6	0.75 ± 0.41	0.185	6/6
Receptor-like tyrosine kinase (RYK)	1.05 ± 0.93	0.896	6/6	2.39 ± 2.37	0.209	6/6
Cyclin D1 (CCND1)	0.67 ± 0.53	0.182	6/6	1.71 ± 1.24	0.218	6/6
Sonic hedgehog (SHH)	0.88 ± 1.41	0.840	3/6	5.26 ± 7.76	0.237	3/6
Cyclin D3 (CCND3)	2.97 ± 3.33	0.208	6/6	4.23 ± 6.18	0.257	6/6
Wingless-type MMTV integration site family, member 8A (WNT8A)	0.83 ± 1.95	0.837	2/6	0.45 ± 1.10	0.278	1/6
Suppressor of fused (SUFU)	0.54 ± 0.45	0.052	6/6	1.56 ± 1.13	0.279	6/6
Cyclin D2 (CCND2)	1.10 ± 1.29	0.860	6/6	2.51 ± 3.21	0.302	6/6
Low-density lipoprotein receptor-related protein 5 (LRP5)	0.61 ± 0.32	0.029	6/6	1.34 ± 0.84	0.368	6/6
E2F1 transcription factor (E2F1)	1.01 ± 0.73	0.987	6/6	2.14 ± 3.16	0.416	6/6
Retinoblastoma 1 (RB1)	1.20 ± 0.68	0.511	6/6	1.24 ± 0.87	0.537	6/6
Wingless-type MMTV integration site family, member 1 (WNT1)	0.25 ± 0.60	0.028	1/6	2.66 ± 6.51	0.560	1/6
Wingless-type MMTV integration site family, member 7B (WNT7B)	0.60 ± 0.92	0.338	5/6	0.68 ± 1.44	0.610	4/6
Axin 1 (AXIN1)	0.73 ± 0.54	0.278	6/6	1.18 ± 0.82	0.621	6/6
Cyclin E1 (CCNE1)	0.92 ± 0.87	0.836	6/6	1.10 ± 1.56	0.881	6/6
Insulin promotor factor 1 (IPF1)	NE		0/6	NE		0/6
Wingless-type MMTV integration site family, member 16 (WNT16)	NE		0/6	NE		0/6
Wingless-type MMTV integration site family, member 8B (WNT8B)	NE		0/6	NE		0/6
Wingless-type MMTV integration site family, member 9A (WNT9A)	NE		0/6	NE		0/6

*Values are expressed as the mean of six samples ± SD. Genes designated by X did not express in normal ovarian epithelium. Genes designated by NE (no expression) did not express in either normal or OEA.
†$P < 0.025$ was considered statistically significant.
‡Ratio indicates OEA samples expressing gene/total samples examined.

is typically used. To check the reproducibility of TLDA, the coefficient of variance (CV) was calculated for each gene in each sample. The C_T values of all 48 genes examined in both snap-frozen and FPE tissue were measured four times (four replicates) for each of the six matched OEA samples. The average and range of CVs for the four replicates of each gene were calculated for ΔC_T values, which were used instead of C_T values so that

different amounts of RNA added to each of the four replicates would not be reflected in the average CV.

To examine the correlation between matched frozen and FPE tissue, average ΔC_T values for the four replicates of each gene were calculated in each of the six matched OEA samples. A two-dimensional plot was then created depicting ΔC_T values from the six frozen samples as the explanatory variable (x) and ΔC_T values from the six paraffin-embedded samples as the dependent variable (y). Linear regression analysis and Pearson correlation was then performed to determine the agreement in gene expression between frozen and FPE tissue. A similar comparison of amplified and unamplifed RNA was performed, however C_T values were used instead of ΔC_T values to illustrate the significant number of genes that could not be detected after amplification.

To distinguish significant differences between expression levels in OEA relative to normal tissue, a one-sample, two-sided t-test was applied to compare the average expression level of the six samples to the normalized ovarian epithelium (which was assigned an expression level of 1.00 for each of the genes examined). The significance level for this test is 0.025.

Results

Quantitation of Housekeeping Gene Expression in Human Tissues Using RTQ

Comparative analysis demonstrated no significant ($P < 0.01$) difference in *RPLP0* expression between normal (OSE) and neoplastic (OEA) tissues.

Reliability of TLDA

For either frozen or FPE samples, the average coefficient of variance (CV) for all four replicates, using ΔC_T values, is ~5%, with a SD of 5%, over the 48 genes examined. In calculating the average CV, genes with a C_T value of 40, the default upper limit PCR cycle number that defines no signal, as well as *RPLP0* and 18S, were excluded. Those genes that failed to express ($C_T = 40$) are designated as NE in Table 1 and include *insulin promoter factor 1* (*IPF1*), *Wnt16*, *Wnt8B*, and *Wnt9A*.

PCR Amplification Efficiency

Analysis of the standard curves for *RPLP0* amplification in both frozen and FPE OEA RNA yielded slopes of −3.00 and −3.11, respectively. The PCR amplification efficiency was calculated as 108% for frozen tissue and 105% for FPE tissue.

Correlation of Gene Expression in Matched Frozen and FPE Tissue

To determine whether archival FPE tissue is suitable for use with TLDA, we examined the correlation of 48 genes in frozen versus FPE OEA. As shown in Figure 2, a two-dimensional plot depicting average ΔC_T values from the six frozen (x) and matching six FPE samples (y) demonstrates a significant ($P < 0.0001$) linear correlation ($r^2 = 0.85$) with a Pearson correlation coefficient (r) of 0.92.

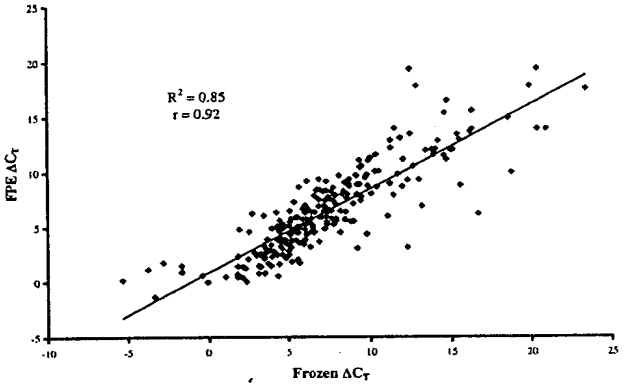

Figure 2. Correlative plot of mean ΔC_T values obtained by TLDA analysis of 48 genes in six frozen (x) compared to six matching paraffin-embedded OEA samples (y). Regression analysis demonstrated a coefficient of determination (r^2) of 0.85 and a Pearson correlation coefficient (r) of 0.92 ($P < 0.0001$).

Correlation of Gene Expression in Amplified and Unamplified RNA

To examine whether commercially available kits could be used to amplify small amounts of RNA without altering the expression profile, we examined the correlation of 48 genes in matched amplified versus unamplified frozen and FPE OEA samples. Total RNA from frozen OEA successfully amplified using the Ovation, MessageAmp RiboAmp, and Full Spectrum amplification protocols and resulted in increases of 448-, 110-, 2757-, and 333-fold, respectively. Repeated attempts to amplify total RNA isolated from FPE tissue were unsuccessful using the four protocols examined.

The conservation of gene expression in matched amplified versus unamplified (template) RNA from frozen OEA samples was examined using TLDA. As shown in Figure 3A, a two-dimensional plot depicting average C_T values from the amplified (x) and unamplified (y) frozen OEA sample using the Ovation amplification system demonstrates a weak correlation with $r = 0.55$ ($P < 0.0001$). Twenty-four of a total forty-two genes (57%) that expressed in unamplified RNA were undetectable after amplification (as shown by the boxed data points). Similar results were obtained for RNA amplified using the MessageAmp and RiboAmp kits (data not shown). Figure 3B depicts a comparison of the same frozen OEA sample using the Full Spectrum amplification system and demonstrates a stronger correlation with $r = 0.75$ ($P < 0.0001$) and only 12 of 42 genes (29%) becoming undetectable after amplification. Although C_T values were plotted instead of ΔC_T values to emphasize undetectable genes in amplified RNA (boxed), identical r^2 and r values were obtained when ΔC_T values were used (data not shown).

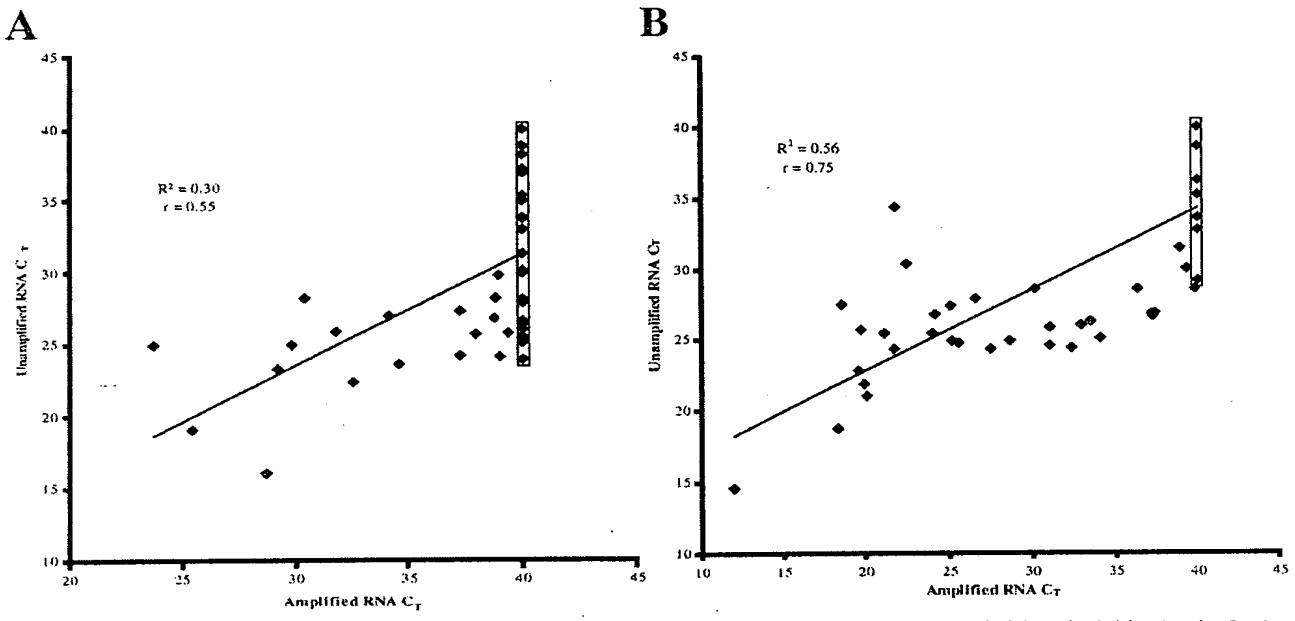

Figure 3. Correlative plot of C_T values obtained by TLDA analysis of 48 genes in amplified (x) compared to unamplified (template) (y) using the Ovation Nanosample RNA amplification system with a coefficient of determination (r^2) of 0.30 and a Pearson correlation coefficient (r) of 0.53 ($P < 0.0001$) (**A**); and the Full Spectrum Global RNA amplification kit with a coefficient of determination (r^2) of 0.56 and a Pearson correlation coefficient (r) of 0.75 ($P < 0.0001$) (**B**).

Expression of Hedgehog and Wnt Genes in OEA

The expression of 46 independent genes in the hedgehog and Wnt pathways across six pairs of matched frozen and FPE OEA samples are summarized in Table 1. For both the frozen and FPE categories, each gene expression value represents an average of the six samples ± SD. Thus, the standard deviations in Table 1 reflect the range in expression over the six samples examined. Gene expression and statistical analysis show that 11 genes from frozen and 10 genes from FPE (Table 1, bolded) were differentially expressed in OEA compared to OSE (91% agreement).

Three members of the hedgehog pathway (*DHH*, *IHH*, *HHIP*) and three members of the Wnt pathway (*Wnt9B*, *Wnt10B*, *WIF1*) were found to be tumor-specific in both frozen and FPE tissues. The average expression, SD and *P* value for each of these genes could not be calculated because none of them express in the OSE calibrator. These six genes are designated as X in Table 1. Several other hedgehog- and Wnt-related genes were significantly lower in OEA (both frozen and FPE) compared to normal ovarian epithelium including *cyclin E2* (*CCNE2*), *Porcupine* (*PPN*), *c-Myc* (*MYC*), and *Axin 2* (*AXIN2*). The proapoptotic *Gli-pathogenesis-related protein* (*GLIPR1*) was significantly lower in frozen but not FPE OEA compared to normal ovarian epithelium. The difference in expression of the remaining 19 and 12 genes in the hedgehog and Wnt pathways, respectively, were not found to be significantly different due to their range in expression over the samples examined (Table 1). *Insulin promoter factor 1* (*IPF1*), *Wnt16*, *Wnt8B*, and *Wnt9A* did not express in either OSE or OEA (designated as NE in Table 1).

Validation of TLDA

To validate the gene expression results obtained with TLDA, 8 genes (*DHH*, *IHH*, *SHH*, *PTCH*, *PTCH2*, *SMO*, *GLI*, *GLI3*) of the original 46 were individually analyzed in both frozen and FPE samples using TaqMan RTQ. A similar gene expression correlation ($r = 0.91$, $P < 0.01$) (Figure 4) between matched frozen and FPE tissues was obtained. When compared separately, gene expression values for these eight genes were not significantly differ-

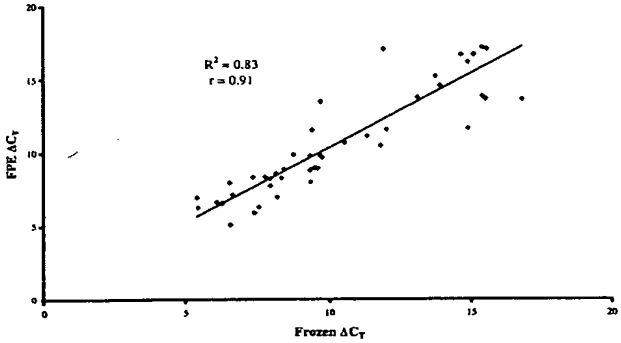

Figure 4. Correlative plot of ΔC_T values obtained by RTQ analysis of eight genes (DHH, IHH, SHH, PTCH, PTCH2, SMO, GLI, GLI3) in six frozen (x) compared to six matching paraffin-embedded OEA samples (y). Regression analysis demonstrated a coefficient of determination (r^2) of 0.83 and a Pearson correlation coefficient (r) of 0.91 ($P < 0.0001$).

ent from the values obtained with TLDA in either frozen or FPE OEA (data not shown).

Discussion

Initial studies examined the reliability and amplification efficiency of the TLDA method and demonstrated an intra-assay CV of ~5% with almost equal PCR amplification efficiency in RNA isolated from matched frozen and FPE tissues (108% and 105%, respectively). Pearson correlation (r) between the six matched fresh frozen and FPE OEA tissues for all tested genes was 92% (Figure 2). This agreement was further validated when similar gene expression correlation (r = 0.91, Figure 4) between the matched OEA samples was obtained by individually analyzing 8 genes of the original 46 using RTQ. This multivariate analysis is unique in that both snap-frozen and matched archival FPE specimens, routinely processed through the University of Alabama at Birmingham's Department of Pathology, were examined simultaneously. Although encouraging, future studies involving the analysis of expression profiles in FPE tissues should consider the variability in the stability of any particular gene being examined and must be independently validated.

Based on these promising preliminary data, we examined whether RNA amplification could be used in combination with TLDA. RNA amplification is a method whereby nanogram amounts of total RNA (usually obtained from needle biopsies or laser-capture microdissected clinical samples) undergo a multistep process for linear amplification of the mRNA fraction. Pearson correlation (r) between matched amplified versus unamplified RNA isolated from frozen OEA varied among the four amplification protocols tested from a low of 53% to a high of 75% (Figure 3). The three amplification protocols (Ovation, MessageAmp, RiboAmp) using polydT oligomer priming (which requires the 3′ poly-A tail in template mRNA to bind with a modified oligo-dT primer) gave the poorest correlations of 53% (Figure 3A), 44%, and 55% (data not shown), respectively. The Full Spectrum amplification protocol, which utilizes a random hexamer (N_6) priming method that does not require an intact 3′ poly-A tail, demonstrated the best correlation of 75% between amplified and unamplified RNA (Figure 3B). Unfortunately, RNA isolated from FPE samples failed to amplify using any of the four procedures and correlative studies could not be conducted. Collectively, these data suggest random hexamer priming may have an advantage over oligo-dT priming when comparing expression profiles in snap-frozen tissues but that sheared or degraded RNA (such as that obtained from FPE tissues) cannot be amplified using these protocols.

To identify potential tumor-specific therapeutic targets, we used TLDA to quantify the expression of 26 and 20 genes in the hedgehog and Wnt pathways, respectively, in six matched frozen and FPE OEA specimens (Table 1). These pathways, normally involved in embryogenesis, have both been implicated in cancer initiation and are similar in terms of posttranslational modification, secretion, and some signaling mechanisms and may have evolved from a common pathway.[13] Recent studies have shown activation of the hedgehog signaling pathway in adult tissues can initiate and sustain tumor growth; however, this pathway has never been examined in OEA.[5–10] Inhibition of the hedgehog pathway by small molecule inhibitors such as cyclopamine has been shown to be effective in decreasing tumor growth and is a promising new therapeutic strategy.[26,27] Similarly, Wnt signaling is involved in normal follicular development and ovarian function.[28] Because OSE is believed to be the origin of ovarian adenocarcinomas and Wnts have been implicated in oncogenic transformation of epithelial cells, it is thought that aberrant expression of this pathway could lead to ovarian carcinogenesis.[16] Quantitation of hedgehog- and Wnt-associated genes in OEA revealed several tumor-specific genes including the two hedgehog ligands, *DHH* and *IHH*, and hedgehog pathway regulator, *HHIP*, as well as the two Wnt ligands, *Wnt10B* and *Wnt9B*, and Wnt pathway regulator, *WIF1* (Table 1). Interestingly, these genes did not consistently express in all of the OEA samples. Other genes directly involved in the hedgehog and Wnt pathways including *Smoothened* (*SMO*), *Glioma-associated oncogene* (*GLI*), *GLI2*, *GLI3*, and *Wnt7A*, *Frizzled homolog* (*FRZD1*), *low-density lipoprotein receptor-related protein 6* (*LRP6*), and *Frizzled related protein* (*FRZB*) were all overexpressed in both frozen and FPE OEA in comparison to normal OSE, but did not reach statistical significance. Similar gene expression results were obtained when eight differentially expressed genes (*DHH*, *IHH*, *SHH*, *PTCH*, *PTCH2*, *GLI*, *GLI3*, *SMO*) were examined individually using RTQ in both frozen and FPE samples (data not shown). In relation to statistically significant and tumor-specific genes, the differing genetic profiles among the OEA samples suggest variable activity of the hedgehog and Wnt pathways in this cancer. Thus, future studies involving individual analysis of a larger population of both normal and cancer patients to distinguish tumor-specific differences from interindividual variation are warranted. These studies could then offer the potential of identifying patients with advanced OEA who would benefit from anti-hedgehog or anti-Wnt therapy such as cyclopamine and nonsteroidal anti-inflammatory drugs, respectively.[27,29,30]

The TLDA methodology presented in this study represents a robust and reproducible technique for quantifying gene expression in tens to hundreds of independent genes concurrently in RNA samples isolated from either frozen or FPE tissues. This approach represents a significant advance in multivariate gene analysis that is less time and labor intensive than individually analyzing single genes by RTQ. The correlation of gene expression profiles between matched frozen and FPE tissues offers the exciting possibility that archival, paraffin-embedded tissues (a more abundant alternative to frozen tissue available from most cooperative groups) may be examined to identify specific therapeutic targets and/or prognostic indicators. The importance of these multivariate analyses have been emphasized by recent studies that have shown that examination of genes acting collectively in a specific pathway, such as the hedgehog or Wnt pathway, offers more information about clinical outcome than ex-

amination of individual genes.[31–34] In the current study, TLDA analysis was used to quantify the expression of hedgehog and Wnt-related genes in OEA and determined that elements of both these pathways are expressed in a subset of the patient samples examined. These analyses could potentially be used to identify patients with advanced OEA who would benefit from specifically targeted anti-hedgehog and/or anti-Wnt therapy.

References

1. Greenlee RT, Murray T, Bolden S, Wingo PA: Cancer statistics, 2000. CA Cancer J Clin 2000, 50:7–33
2. Engel J, Eckel R, Schubert-Fritschle G, Kerr J, Kuhn W, Diebold J, Kimmig R, Rehbock J, Holzel D: Moderate progress for ovarian cancer in the last 20 years: prolongation of survival, but no improvement in the cure rate. Eur J Cancer 2002, 38:2435–2445
3. Goodman MT, Correa CN, Tung KH, Roffers SD, Cheng Wu X, Young Jr JL, Wilkens LR, Carney ME, Howe HL: Stage at diagnosis of ovarian cancer in the United States, 1992–1997. Cancer 2003, 97:2648–2659
4. McGuire WP, Hoskins WJ, Brady MF, Kucera PR, Partridge EE, Look KY, Clarke-Pearson DL, Davidson M: Cyclophosphamide and cisplatin versus paclitaxel and cisplatin: a phase III randomized trial in patients with suboptimal stage III/IV ovarian cancer (from the Gynecologic Oncology Group). Semin Oncol 1996, 23:40–47
5. Wicking C, Smyth I, Bale A: The hedgehog signalling pathway in tumorigenesis and development. Oncogene 1999, 18:7844–7851
6. Pasca di Magliano M, Hebrok M: Hedgehog signalling in cancer formation and maintenance. Nat Rev Cancer 2003, 3:903–911
7. Berman DM, Karhadkar SS, Hallahan AR, Pritchard JI, Eberhart CG, Watkins DN, Chen JK, Cooper MK, Taipale J, Olson JM, Beachy PA: Medulloblastoma growth inhibition by hedgehog pathway blockade. Science 2002, 297:1559–1561
8. Gailani MR, Stahle-Backdahl M, Leffell DJ, Glynn M, Zaphiropoulos PG, Pressman C, Unden AB, Dean M, Brash DE, Bale AE, Toftgard R: The role of the human homologue of Drosophila patched in sporadic basal cell carcinomas. Nat Genet 1996, 14:78–81
9. Watkins DN, Berman DM, Burkholder SG, Wang B, Beachy PA, Baylin SB: Hedgehog signalling within airway epithelial progenitors and in small-cell lung cancer. Nature 2003, 422:313–317
10. Kubo M, Nakamura M, Tasaki A, Yamanaka N, Nakashima H, Nomura M, Kuroki S, Katano M: Hedgehog signaling pathway is a new therapeutic target for patients with breast cancer. Cancer Res 2004, 64:6071–6074
11. Thayer SP, di Magliano MP, Heiser PW, Nielsen CM, Roberts DJ, Lauwers GY, Qi YP, Gysin S, Fernandez-del Castillo C, Yajnik V, Antoniu B, McMahon M, Warshaw AL, Hebrok M: Hedgehog is an early and late mediator of pancreatic cancer tumorigenesis. Nature 2003, 425:851–856
12. Berman DM, Karhadkar SS, Maitra A, Montes De Oca R, Gerstenblith MR, Briggs K, Parker AR, Shimada Y, Eshleman JR, Watkins DN, Beachy PA: Widespread requirement for Hedgehog ligand stimulation in growth of digestive tract tumours. Nature 2003, 425:846–851
13. Nusse R: Wnts and Hedgehogs: lipid-modified proteins and similarities in signaling mechanisms at the cell surface. Development 2003, 130:5297–5305
14. Taipale J, Beachy PA: The Hedgehog and Wnt signalling pathways in cancer. Nature 2001, 411:349–354
15. Wu R, Zhai Y, Fearon ER, Cho KR: Diverse mechanisms of beta-catenin deregulation in ovarian endometrioid adenocarcinomas. Cancer Res 2001, 61:8247–8255
16. Rask K, Nilsson A, Brannstrom M, Carlsson P, Hellberg P, Janson PO, Hedin L, Sundfeldt K: Wnt-signalling pathway in ovarian epithelial tumours: increased expression of beta-catenin and GSK3beta. Br J Cancer 2003, 89:1298–1304
17. Jackson DP, Quirke P, Lewis F, Boylston AW, Sloan JM, Robertson D, Taylor GR: Detection of measles virus RNA in paraffin-embedded tissue. Lancet 1989, 1:1391
18. Jackson DP, Lewis FA, Taylor GR, Boylston AW, Quirke P: Tissue extraction of DNA and RNA and analysis by the polymerase chain reaction. J Clin Pathol 1990, 43:499–504
19. Stanta G, Schneider C: RNA extracted from paraffin-embedded human tissues is amenable to analysis by PCR amplification. Biotechniques 1991, 11:304–308
20. Finke J, Fritzen R, Ternes P, Lange W, Dolken G: An improved strategy and a useful housekeeping gene for RNA analysis from formalin-fixed, paraffin-embedded tissues by PCR. Biotechniques 1993, 14:448–453
21. Stanta G, Bonin S, Perin R: RNA extraction from formalin-fixed and paraffin-embedded tissues. Methods Mol Biol 1998, 86:23–26
22. Goldsworthy SM, Stockton PS, Trempus CS, Foley JF, Maronpot RR: Effects of fixation on RNA extraction and amplification from laser capture microdissected tissue. Mol Carcinog 1999, 25:86–91
23. Blanquicett C, Johnson MR, Heslin M, Diasio RB: Housekeeping gene variability in normal and carcinomatous colorectal and liver tissues: applications in pharmacogenomic gene expression studies. Anal Biochem 2002, 303:209–214
24. Johnson MR, Wang K, Smith JB, Heslin MJ, Diasio RB: Quantitation of dihydropyrimidine dehydrogenase expression by real-time reverse transcription polymerase chain reaction. Anal Biochem 2000, 278:175–184
25. Roy S, Ingham PW: Hedgehogs tryst with the cell cycle. J Cell Sci 2002, 115:4393–4397
26. Incardona JP, Gaffield W, Kapur RP, Roelink H: The teratogenic Veratrum alkaloid cyclopamine inhibits sonic hedgehog signal transduction, Development 1998, 125:3553–3562
27. Taipale J, Chen JK, Cooper MK, Wang B, Mann RK, Milenkovic L, Scott MP, Beachy PA: Effects of oncogenic mutations in Smoothened and Patched can be reversed by cyclopamine. Nature 2000, 406:1005–1009
28. Ricken A, Lochhead P, Kontogiannea M, Farookhi R: Wnt signaling in the ovary: identification and compartmentalized expression of wnt-2, wnt-2b, and frizzled-4 mRNAs. Endocrinology 2002, 143:2741–2749
29. Boon EM, Keller JJ, Wormhoudt TA, Giardiello FM, Offerhaus GJ, van der Neut R, Pals ST: Sulindac targets nuclear beta-catenin accumulation and Wnt signalling in adenomas of patients with familial adenomatous polyposis and in human colorectal cancer cell lines. Br J Cancer 2004, 90:224–229
30. Dobbie Z, Muller PY, Heinimann K, Albrecht C, D'Orazio D, Bendik I, Muller H, Bauerfeind P: Expression of COX-2 and Wnt pathway genes in adenomas of familial adenomatous polyposis patients treated with meloxicam. Anticancer Res 2002, 22:2215–2220
31. Zhang Z, Bast Jr RC, Yu Y, Li J, Sokoll LJ, Rai AJ, Rosenzweig JM, Cameron B, Wang YY, Meng XY, Berchuck A, Van Haaften-Day C, Hacker NF, de Bruijn HW, van der Zee AG, Jacobs IJ, Fung ET, Chan DW: Three biomarkers identified from serum proteomic analysis for the detection of early stage ovarian cancer. Cancer Res 2004, 64:5882–5890
32. Chen Y, Zheng H, Yang X, Sun L, Xin Y: Effects of mutation and expression of PTEN gene mRNA on tumorigenesis and progression of epithelial ovarian cancer. Chin Med Sci J 2004, 19:25–30
33. Torng PL, Mao TL, Chan WY, Huang SC, Lin CT: Prognostic significance of stromal metalloproteinase-2 in ovarian adenocarcinoma and its relation to carcinoma progression. Gynecol Oncol 2004, 92:559–567
34. Barbieri F, Lorenzi P, Ragni N, Schettini G, Bruzzo C, Pedulla F, Alama A: Overexpression of cyclin D1 is associated with poor survival in epithelial ovarian cancer. Oncology 2004, 66:310–315

Dominant-Stable β-Catenin Expression Causes Cell Fate Alterations and Wnt Signaling Antagonist Expression in a Murine Granulosa Cell Tumor Model

Derek Boerboom,[1] Lisa D. White,[2] Sophie Dalle,[3] José Courty,[3] and JoAnne S. Richards[1]

Departments of [1]Molecular and Cellular Biology and [2]Molecular and Human Genetics, Baylor College of Medicine, Houston, Texas and [3]Laboratoire de Recherche sur la Croissance, la Regénération et la Réparation Tissulaires, Universite Paris XII-Val de Marne, UMR Centre National de la Recherche Scientifique 7149, Creteil, France

Abstract

Wnt/β-catenin signaling is normally involved in embryonic development and tissue homeostasis, and its misregulation leads to several forms of cancer. We have reported that misregulated Wnt/β-catenin signaling occurs in ovarian granulosa cell tumors (GCT) and have created the *Catnb*$^{flox(ex3)/+}$; *Amhr2*$^{cre/+}$ mouse model, which expresses a dominant-stable mutant of β-catenin in granulosa cells and develops late-onset GCT. To study the mechanisms leading to GCT development, gene expression analysis was done using microarrays comparing *Catnb*$^{flox(ex3)/+}$;*Amhr2*$^{cre/+}$ ovaries bearing pretumoral lesions with control ovaries. Overexpressed genes identified in *Catnb*$^{flox(ex3)/+}$;*Amhr2*$^{cre/+}$ ovaries included the Wnt/β-catenin signaling antagonists *Wif1, Nkd1, Dkk4*, and *Axin2*, consistent with the induction of negative feedback loops that counteract uncontrolled Wnt/β-catenin signaling. Expression of the antagonists was localized to cells forming the pretumoral lesions but not to normal granulosa cells. Microarray analyses also revealed the ectopic expression of bone markers, including *Ibsp, Cdkn1c, Bmp4*, and *Tnfrsf11b*, as well as neuronal/neurosecretory cell markers, such as *Cck, Amph, Pitx1*, and *Sp5*. Increased expression of the gene encoding the cytokine pleiotrophin was also found in *Catnb*$^{flox(ex3)/+}$;*Amhr2*$^{cre/+}$ ovaries and GCT but was not associated with increased serum pleiotrophin levels. *In situ* hybridization analyses using GCT from *Catnb*$^{flox(ex3)/+}$;*Amhr2*$^{cre/+}$ mice revealed that Wnt/β-catenin antagonists and neuronal markers localized to a particular cell population, whereas the bone markers localized to a distinct cell type associated with areas of osseous metaplasia. Together, these results suggest that misregulated Wnt/β-catenin signaling alters the fate of granulosa cells and that the GCT that arise in *Catnb*$^{flox(ex3)/+}$;*Amhr2*$^{cre/+}$ mice result from the clonal expansion of metaplastic cells. (Cancer Res 2006; 66(4): 1964-73)

Introduction

Wnts comprise a large family of secreted, local-acting signaling glycoproteins known mostly for the critical roles they play in embryonic development (1, 2). Following embryogenesis, Wnts and Wnt signaling pathway components continue to be expressed in many tissues, leading to the widely held view that Wnts play additional roles in adult tissue homeostasis (3, 4), although the precise nature of these homeostatic roles remains poorly defined. Recently, several lines of evidence have converged to suggest that Wnt signaling is required for the maintenance or proliferation of stem/progenitor cell types in several tissues (5). For instance, deletion of the Wnt signaling-activated transcription factor *Tcf4* (6) or overexpression of the Wnt signaling antagonist *Dkk1* (7, 8) resulted in the loss of intestinal crypts, which are the progenitor cell compartments that give rise to the differentiated cells of the villi. Similarly, whereas Wnt3A and Wnt5A can promote self-renewal of hematopoietic stem cells (9–12), the opposite has been observed on addition of the Wnt signaling antagonist *Axin* (9).

In addition to affecting stem/progenitor cell proliferation, a growing body of evidence suggests that Wnt signaling plays a role in cell fate determination as well as in differentiation. In neural crest stem cells, Wnt1 or chronic activation of the Wnt/β-catenin pathway has been shown to direct a sensory neuron fate, whereas Wnt3A can promote differentiation into several lineages (13, 14). Likewise, Wnt11 and Wnt5A treatment of hematopoietic progenitor cells favored RBC and monocyte cell fates at the expense of macrophage formation (15). Even more dramatic results have been derived from genetically modified mouse models in which Wnt signaling has been altered in particular tissues, resulting in radical changes in cell fates. For example, constitutive activation of the Wnt pathway in the developing lung in *Sftpc-CAtCLef1* transgenic mice impaired the terminal differentiation of the pulmonary epithelium and resulted in the appearance of cells expressing markers of intestinal Paneth and goblet cells (16). Likewise, stabilization of the Wnt signaling effector β-catenin in the secretory cells of the prostate or mammary gland resulted in squamous metaplasia (17, 18). In skin, interference with Wnt signaling has been shown to adversely affect hair follicle formation by causing cell lineage changes and leads to the development of tumors exhibiting sebaceous differentiation (19, 20). Wnt/β-catenin signaling is therefore a key mediator of both proliferative and differentiation processes in stem/precursor cell biology, and its misregulation can dramatically alter differentiation and cell fate decisions.

Considering the nature of the aforementioned processes, it is perhaps not surprising that misregulation of Wnt signaling is a hallmark of many forms of cancer, notably including >90% of cases of familial and sporadic colorectal cancers (21). As Wnt signaling pathway components are normally expressed in ovarian granulosa cells (22–24), we have recently investigated the potential involvement of misregulation of this pathway in granulosa cell tumorigenesis (25). We showed that a subset of human and equine granulosa cell tumors (GCT) showed nuclear localization of β-catenin (the product of the *Catnb* gene), indicative of inappropriate activation of the Wnt/β-catenin pathway. To further

Requests for reprints: JoAnne Richards, Department of Molecular and Cellular Biology, Baylor College of Medicine, One Baylor Plaza, Houston, TX 77030. Phone: 713-798-6259; E-mail: joanner@bcm.tmc.edu.

doi:10.1158/0008-5472.CAN-05-3493

support the notion that the Wnt/β-catenin pathway plays a role in the etiology of GCT, mice were genetically engineered to express a dominant stable β-catenin mutant in granulosa cells. This was accomplished by mating *Catnb*$^{flox(ex3)}$ mice (which feature a *Catnb* allele whose third exon is flanked by *loxP* sites) to the *Amhr2*^{cre} strain, in which the anti-Mullerian hormone receptor type II coding sequences have been replaced by those encoding Cre recombinase. In the resulting female *Catnb*$^{flox(ex3)/+}$;*Amhr2*$^{cre/+}$ mice, the *Amhr2*$^{cre/+}$ locus drives the expression of Cre in granulosa cells, resulting in the excision of the third exon of *Catnb* from the floxed allele. The recombined *Catnb*$^{flox(ex3)}$ allele encodes a β-catenin protein that, although still functional, lacks a series of phosphorylation sites that are required for its degradation, resulting in its inappropriate accumulation and translocation to the nucleus. Interestingly, *Catnb*$^{flox(ex3)/+}$;*Amhr2*$^{cre/+}$ mice developed pretumoral lesions by 6 weeks of age, which consisted of follicle-like nests of disorganized, pleiomorphic granulosa cells (termed solid lesions) as well as ovarian cysts. These pretumoral lesions grew no larger than the size of antral follicles and contained very few proliferating cells but often evolved into GCT in older mice. These data showed a causal link between misregulated Wnt/β-catenin signaling and GCT development and provided a novel model system for the study of GCT biology.

In this study, we have employed the *Catnb*$^{flox(ex3)/+}$;*Amhr2*$^{cre/+}$ mouse model in an attempt to elucidate the molecular mechanisms by which misregulated Wnt/β-catenin signaling results in pretumoral lesion and GCT development. Misregulated Wnt/β-catenin presumably induces tumor formation by altering the expression of specific target genes, the induction and/or repression of which results in abnormal cellular proliferation. We hypothesized that these genes could be identified by profiling gene expression in ovaries from *Catnb*$^{flox(ex3)/+}$;*Amhr2*$^{cre/+}$ mice bearing pretumoral lesions and comparing these profiles with those of control *Catnb*$^{flox(ex3)/+}$ ovaries. Unexpectedly, our results indicated that dominant-stable β-catenin expression altered the fates of granulosa cells and resulted in multiple metaplasias, suggesting a potentially critical mechanism for GCT development.

Materials and Methods

Animals and serum pleiotrophin measurements. *Catnb*$^{flox(ex3)/+}$;*Amhr2*$^{Cre/+}$ mice were derived from previously described *Amhr2*^{Cre} and *Catnb*$^{flox(ex3)}$ parental strains, and genotyping analyses were done by PCR as described (26, 27). Blood samples were collected by cardiac puncture under anesthesia before euthanasia. Pleiotrophin immunoassays were done on serum as described previously (28). All procedures were approved by the Institutional Animal Care and Use Committee and conformed to the USPHS Policy on Humane Care and Use of Laboratory Animals.

Microarray analysis. Total ovarian RNA was isolated from 12-week-old *Catnb*$^{flox(ex3)/+}$;*Amhr2*$^{Cre/+}$ and control *Catnb*$^{flox(ex3)/+}$ ovaries using the RNeasy Mini kit (Qiagen Sciences, Germantown, MD). At this age, 100% of *Catnb*$^{flox(ex3)/+}$;*Amhr2*$^{Cre/+}$ ovaries bear pretumoral lesions, but GCT are never observed (25). To avoid ovarian cycle-related differences in gene expression that could arise by comparing single ovaries, RNA samples from six animals per genotype were pooled before microarray probe synthesis. *Catnb*$^{flox(ex3)/+}$;*Amhr2*$^{Cre/+}$ and *Catnb*$^{flox(ex3)/+}$;*Amhr2*$^{Cre/+}$ riboprobes were then hybridized to mouse expression set 430 microarrays (Affymetrix, Santa Clara, CA). All steps of RNA quality control, probe synthesis, hybridization, washing, array scanning, and statistical analyses were done by the Microarray Core Facility of the Baylor College of Medicine (Houston, TX).

Semiquantitative reverse transcription-PCR. Reverse transcription-PCR (RT-PCR) was done using the SuperScript One-Step RT-PCR System with Platinum Taq kit (Invitrogen, Carlsbad, CA), and ≈100 ng samples of ovarian and GCT total RNA that had been isolated as described above. Reactions were formulated as directed by the manufacturer, except that 0.625 μCi [α-^{32}P]dCTP (specific activity, 3,000 Ci/mmol; MP Biomedicals, Irvine, CA) was added to each reaction to generate quantifiable radioactive signal and to increase assay sensitivity. Oligonucleotides used are detailed in Table 1, except those for ribosomal protein L19 (*Rpl19*), which were as described previously (ref. 29; Sigma-Genosys, The Woodlands, TX). Cycling conditions were 50°C for 30 minutes and 94°C for 2 minutes followed by a variable number of cycles (as detailed in Table 1; 18 cycles were used for *Rpl19*) of 94°C for 15 seconds, 55°C for 30 seconds, and 72°C for 1 minute. A final extension step of 72°C for 7 minutes was also done. Preliminary experiments were done for all genes assayed to ensure that the cycle numbers selected fell within the linear range of PCR amplification (data not shown). Samples were separated by electrophoresis on 2% TAE-agarose gels, dried, and exposed to Biomax XAR film (Eastman Kodak Co., Rochester, NY) for 1 to 6 hours at −70°C to generate the presented images. The relative radioactive signal strengths from the RT-PCR products were subsequently quantified using a Storm 860 PhosphorImager (Molecular Dynamics, Inc., Sunnyvale, CA).

***In situ* hybridization.** *In situ* hybridization was done on paraformaldehyde-fixed, paraffin-embedded sections of ovaries from 12-week-old *Catnb*$^{flox(ex3)/+}$ and *Catnb*$^{flox(ex3)/+}$;*Amhr2*$^{Cre/+}$ mice as well as GCT isolated from *Catnb*$^{flox(ex3)/+}$;*Amhr2*$^{Cre/+}$ animals ages 7 to 11 months. Riboprobes were synthesized from cDNA fragments that had been generated by RT-PCR as described above and subsequently cloned into the pCR4-TOPO plasmid vector using the TOPO TA cloning kit (Invitrogen). Probe preparation, slide preparation, hybridization, washing, and exposure/developing steps were done as described previously (30, 31). Exposure times to NTB-2 emulsion (Eastman Kodak) of 2 to 7 days were required to generate the images shown. Control sense riboprobes for each gene failed to generate any specific signal when hybridized under the same conditions (data not shown).

Statistical methods. For the data presented in Fig. 1, unpaired *t* tests were used to test for differences between groups, with $P < 0.05$ considered statistically significant. In Fig. 3, one-way ANOVA was employed to test for differences between groups. When differences were identified ($P < 0.05$), Tukey's test was then used to compare *Catnb*$^{flox(ex3)/+}$;*Amhr2*$^{cre/+}$ data sets with *Catnb*$^{flox(ex3)/+}$ controls at each age examined. Dunnett's test was also employed to test the effects of age on mRNA levels in *Catnb*$^{flox(ex3)/+}$;*Amhr2*$^{cre/+}$ mice using the 3-week time point data set as a control for comparison with other data sets. One-way ANOVA and Tukey's test were also applied to the pleiotrophin data (Table 2). All tests were done using Prism software version 4.0a (GraphPad Software, Inc., San Diego, CA).

Results

Ovarian gene expression is altered in *Catnb*$^{flox(ex3)/+}$;*Amhr2*$^{Cre/+}$ mice. To elucidate putative changes in ovarian gene expression associated with the development of pretumoral lesions in *Catnb*$^{flox(ex3)/+}$;*Amhr2*$^{Cre/+}$ mice, microarray analyses were done comparing gene expression in *Catnb*$^{flox(ex3)/+}$;*Amhr2*$^{Cre/+}$ versus *Catnb*$^{flox(ex3)/+}$ ovaries from 12-week-old animals. Consistent with the prediction that stabilization of the β-catenin protein would result in the transcriptional activation of a set of target genes, >40 genes were found to be overexpressed by >2.5-fold in *Catnb*$^{flox(ex3)/+}$;*Amhr2*$^{Cre/+}$ ovaries (data not shown). Overexpressed genes notably included several known Wnt signaling pathway antagonists, among which *Wif1* was the single most highly overexpressed gene identified (Fig. 1*A*). Unexpectedly, no genes specifically associated with granulosa cell proliferation or biological functions were identified. Rather, most genes that were overexpressed in *Catnb*$^{flox(ex3)/+}$;*Amhr2*$^{Cre/+}$ ovaries were typically representative of nonovarian tissues and included multiple genes associated with neuronal and neurosecretory-type cells (Fig. 1*B*) and bone (Fig. 1*C*). These microarray data were confirmed by

Table 1. Sequences of the oligonucleotide primers employed in the RT-PCR described in the text along with the number of PCR cycles used in the semiquantitative analyses

Gene	Orientation	Sequence (5′→3′)	Cycles	Size (bp)
Amph	Forward	ATCCCTTCTGTTGTCATTGAGCCA	26	341
	Reverse	GAAGGCACCACGAGTACCACGT		
Axin2	Forward	CCACTTCAAGGAGCAGCTCAGCA	20	379
	Reverse	TACCCAGGCTCCTGGAGACTGA		
Bmp4	Forward	GGCGCGAGCCATGCTAGTTTGA	26	340
	Reverse	TCCCTGGGATGTTCTCCAGATGT		
Cck	Forward	CTAGCGCGATACATCCAGCAGGT	26	389
	Reverse	CTTTAATAGCATAGCAACATTAGGTCT		
Cdkn1c	Forward	GCCTCTCTCGGGGATTCCAGGA	26	385
	Reverse	TGCACATGGTACAGAGTGTTCTCA		
Dkk4	Forward	CAGTACGAAGAAATCACAAAGCAGT	24	264
	Reverse	ACTCTTAGCCTTGAATGTTGTCTGT		
Ibsp	Forward	CTACTACAAGGGGCATGGCTATGA	26	529
	Reverse	GGTTACATAAAATACATGAGGATGCA		
Nkd1	Forward	GAGAACTACACGTCTCAGTTTGGA	20	314
	Reverse	GGAGGCTTGCTTCTTGCACCTCT		
Peg3	Forward	AGCTACCTAGCCTGGTACTCTGA	24	330
	Reverse	GGGTTGATTTGGGTCACAGAGACA		
Pitx1	Forward	AGGAGAAGGGCTCAGCTCTGAGT	27	315
	Reverse	GCTTAGCACGCTCCGACTATGGT		
Ptn	Forward	GTCTGACTGTGGAGAATGGCAGT	20	366
	Reverse	ATCTTCTCCTGTTTCTTGCCTTCCT		
Sp5	Forward	CCATCGAGGTAGCTGACAAAGAGT	24	393
	Reverse	TGTAGCTCTGCGTGGAGCTGAGA		
Tnfrsf11b	Forward	TCAGGTTTGCTGTTCCTACCAAGA	32	284
	Reverse	GCTCTCCATCAAGGCAAGAAGCT		
Wif1	Forward	GCTGGCACGGCAGACACTGCA	20	400
	Reverse	ATCAACTGACACAATATAAGATCTGT		

NOTE: The amplicon sizes are listed and correspond to the cDNA fragments used for *in situ* hybridization riboprobe synthesis.

semiquantitative PCR, which yielded results comparable with the microarray data (Fig. 1). Microarray analyses also identified a limited number of genes whose expression was modestly decreased in $Catnb^{flox(ex3)/+}$;$Amhr2^{Cre/+}$ ovaries relative to $Catnb^{flox(ex3)/+}$ controls (data not shown), but no genes were found to be underexpressed by more than ~3-fold.

Ectopic gene expression localizes to pretumoral lesions in the ovaries of $Catnb^{flox(ex3)/+}$;$Amhr2^{Cre/+}$ mice. *In situ* hybridization analyses were done to localize the expression of the genes detailed in Fig. 1 in ovaries of normal and $Catnb^{flox(ex3)/+}$;$Amhr2^{Cre/+}$ mice. The Wnt signaling antagonists listed in Fig. 1*A* were undetectable in $Catnb^{flox(ex3)/+}$ ovaries, with the exception of *Axin2* and *Nkd1*, which localized exclusively to oocytes (Fig. 2*A*). In $Catnb^{flox(ex3)/+}$;$Amhr2^{Cre/+}$ ovaries, all antagonists localized to the pretumoral lesions, with the exception of *Dkk4*, which was expressed at levels below the detection threshold (Fig. 2*A*; data not shown). Whereas *Axin2* and *Nkd1* were detected in all lesions, *Wif1* expression was apparently confined to solid pretumoral lesions and could not be detected in cystic-type lesions (Fig. 2*A*, *arrowhead*), suggesting a functional difference between the cells that compose cystic and solid lesions. Together, these results indicate that *Axin2*, *Nkd1*, and *Wif1* are not normally expressed in ovarian granulosa cells and that their expression in $Catnb^{flox(ex3)/+}$;$Amhr2^{Cre/+}$ pretumoral granulosa cells likely represents the induction of multiple negative feedback loops to counteract the constitutive activation of the Wnt/β-catenin pathway.

Of the neuronal/neurosecretory and bone genes listed in Fig. 1*B* and *C*, only *Ptn* and *Cdkn1c* were detectable by *in situ*

Table 2. Serum pleiotrophin measurements, comparing animals of the indicated genotypes and age groups

Genotype	Age (wk)	*n*	Serum pleiotrophin (ng/mL), mean ± SE	Range, mean ± SE
$Catnb^{flox(ex3)/+}$	6-12	12	3.57 ± 0.42	2.01-7.34
$Catnb^{flox(ex3)/+}$	>24	10	3.15 ± 0.50	2.17-7.40
$Catnb^{flox(ex3)/+}$; $Amhr2^{cre/+}$	6-12	10	3.51 ± 0.53	0.67-5.72
$Catnb^{flox(ex3)/+}$; $Amhr2^{cre/+}$	>24	18	5.06 ± 1.21	0.15-22.88

NOTE: About 88.9% of $Catnb^{flox(ex3)/+}$;$Amhr2^{cre/+}$ animals ages >24 weeks bore unilateral or bilateral GCT.

hybridization in *Catnb*$^{flox(ex3)/+}$;*Amhr2*$^{Cre/+}$ ovaries, and none were detectable in *Catnb*$^{flox(ex3)/+}$ controls (Fig. 2*B*; data not shown). As for *Axin2* and *Nkd1*, *Ptn* was found to be expressed in all *Catnb*$^{flox(ex3)/+}$;*Amhr2*$^{Cre/+}$ pretumoral lesions. Although *Cdkn1c* was also found in pretumoral lesions, it showed a more mottled, patchy expression pattern and great variability in expression levels between lesions, suggesting that only a small subset of cells within the lesions expressed *Cdkn1c* (Fig. 2*B*).

Time-dependent effects of pretumoral lesion and GCT formation on Wnt antagonist expression in *Catnb*$^{flox(ex3)/+}$;*Amhr2*$^{Cre/+}$ ovaries. To study the temporal changes in expression of the Wnt signaling antagonists *Axin2*, *Nkd1*, and *Wif1* in ovaries of *Catnb*$^{flox(ex3)/+}$;*Amhr2*$^{Cre/+}$ mice, ovaries were harvested from 3-day and 3-week-old mice (i.e., before pretumoral lesion development), from 6-week-old, 3-month-old, and 7.5-month-old mice (i.e., with pretumoral lesions but before GCT development), and from mice with GCT. Semiquantitative RT-PCR analyses showed similar patterns of expression for *Axin2* and *Nkd1*. They were found to be expressed at high and comparable levels in both *Catnb*$^{flox(ex3)/+}$;*Amhr2*$^{Cre/+}$ and control *Catnb*$^{flox(ex3)/+}$ ovaries in 3-day-old mice (Fig. 3). As both genes are expressed in oocytes (Fig. 2*A*), this was likely reflective of the oocyte-rich composition of the developing ovary in neonatal mice. In *Catnb*$^{flox(ex3)/+}$ controls, ovarian *Axin2* and *Nkd1* mRNA levels then dropped by 3 weeks as ovarian development progressed and the oocyte/ovarian stroma ratio decreased and then remained relatively constant throughout adulthood. However, in *Catnb*$^{flox(ex3)/+}$;*Amhr2*$^{Cre/+}$ ovaries, *Axin2* and *Nkd1* transcripts were found to be significantly

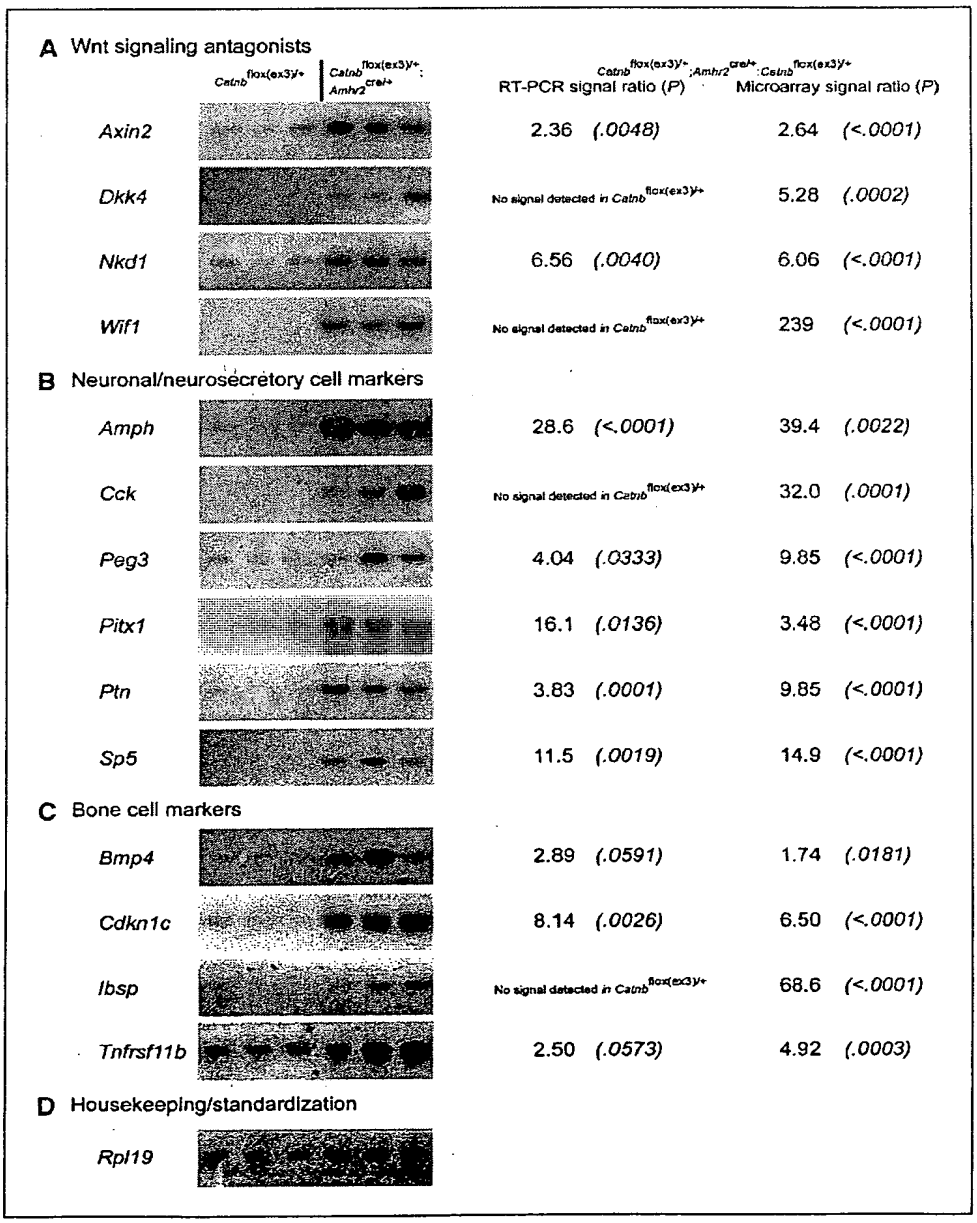

Figure 1. Altered gene expression in the ovaries of *Catnb*$^{flox(ex3)/+}$;*Amhr2*$^{cre/+}$ mice. Ovarian gene expression analyses comparing *Catnb*$^{flox(ex3)/+}$;*Amhr2*$^{cre/+}$ ovaries with *Catnb*$^{flox(ex3)/+}$ control animals were done using Affymetrix microarrays, and selected genes overexpressed in *Catnb*$^{flox(ex3)/+}$;*Amhr2*$^{cre/+}$ ovaries (except *Rpl19*, which was used for standardization) were categorized. Ovarian overexpression of all genes was verified by semiquantitative RT-PCR analyses using six animals per genotype, and results were expressed as the ratios of the means of *Rpl19*-standardized signal strengths from *Catnb*$^{flox(ex3)/+}$;*Amhr2*$^{cre/+}$ ovaries to *Catnb*$^{flox(ex3)/+}$ controls along with *P*s derived from statistical comparison tests between groups. Note that some ratios could not be calculated due to absence of detectable signal in control ovaries. Signal strength ratios and *P*s from the original microarray analysis are also shown for comparison. Autoradiographic images illustrate RT-PCR results from three randomly selected animals per genotype.

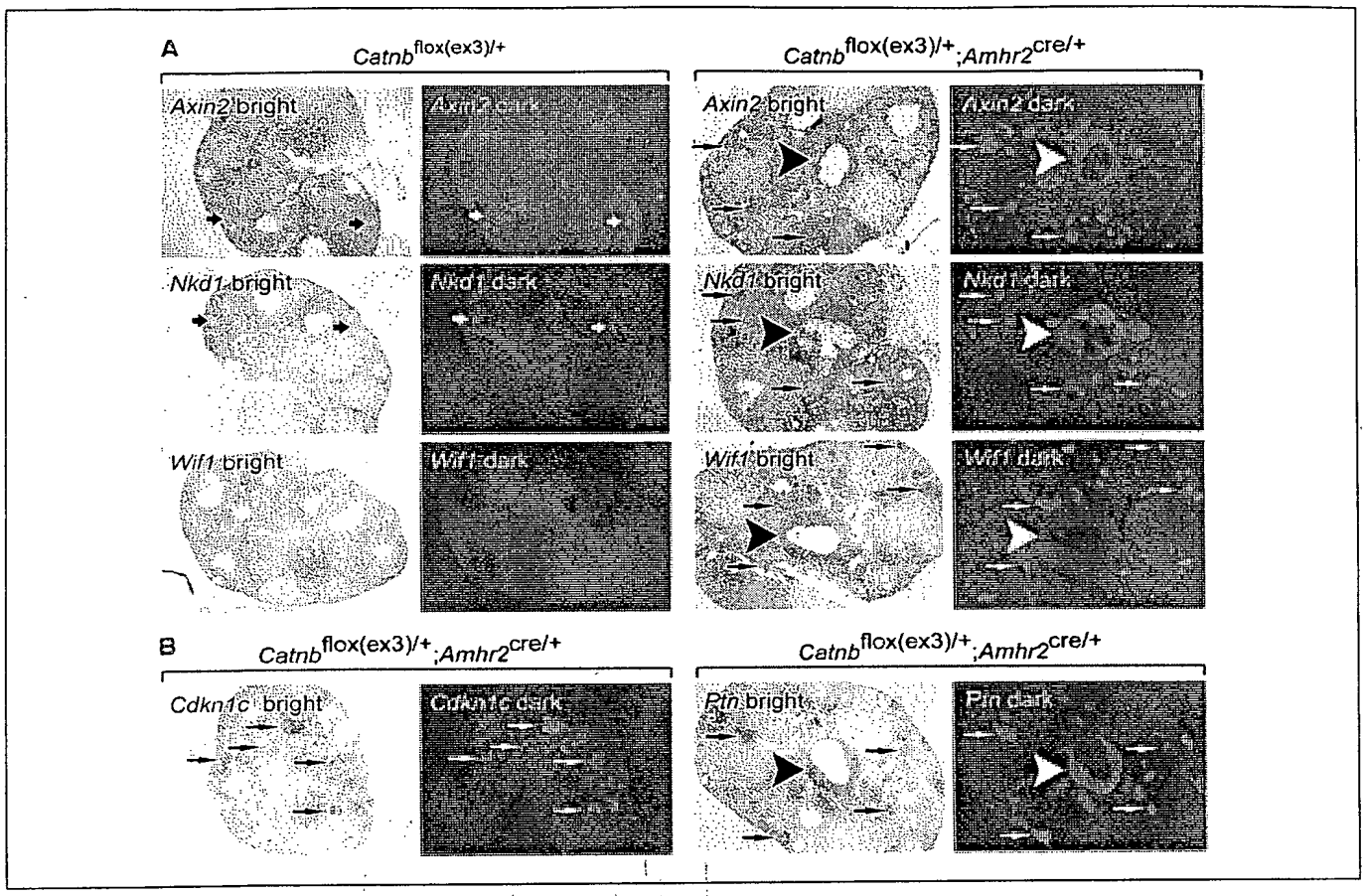

Figure 2. *In situ* hybridization analyses of genes of interest in ovaries of 12-week-old *Catnb*$^{flox(ex3)/+}$;*Amhr2*$^{cre/+}$ and *Catnb*$^{flox(ex3)/+}$ mice localize their expression to pretumoral lesions. Sections in bright-field views are counterstained with hematoxylin; radioactive signal appears as light-colored grains in dark-field views. *Short arrows*, oocytes; *long arrows*, examples of solid pretumoral lesions; *arrowheads*, cystic lesions. Original magnifications, ×50. *A*, analysis of Wnt signaling inhibitor expression. Ovarian sections from animals of the indicated genotypes were hybridized with the indicated riboprobes. Note that the dark-field view for *Axin2* in the *Catnb*$^{flox(ex3)/+}$ section was overexposed to enhance the weak, oocyte-specific signal. No signal was detected for *Wif1* in *Catnb*$^{flox(ex3)/+}$ ovaries. *B*, analysis of *Cdkn1c* and *Ptn* expression in *Catnb*$^{flox(ex3)/+}$;*Amhr2*$^{cre/+}$ ovaries. No signal was detected for either gene in *Catnb*$^{flox(ex3)/+}$ controls (data not shown).

more abundant (≈4- to 12-fold) than in age-matched controls as early as 3 weeks of age and continuing through adulthood. *Axin2* and *Nkd1* expression increased further in GCT, and mRNA levels were found to be significantly (albeit modestly, ≈2-fold) higher than at 3 weeks, which was more likely reflective of the loss of normal ovarian tissue than a tumorigenesis-associated increase in expression in the granulosa cells. A different pattern of expression was observed for *Wif1*, as its expression was not detected at any time in *Catnb*$^{flox(ex3)/+}$ controls (Fig. 3). It was, however, detectable in *Catnb*$^{flox(ex3)/+}$;*Amhr2*$^{Cre/+}$ ovaries at 3 days and its expression increased rapidly by 3 weeks and attained highest levels in the oldest mice with pretumoral lesions and mice with GCT. This pattern of expression closely mirrored that of Δex3 *Catnb* mRNA (i.e., the transcript derived from the Cre-recombined *Catnb* allele) in *Catnb*$^{flox(ex3)/+}$;*Amhr2*$^{Cre/+}$ ovaries (25). Together, these data indicate that Wnt signaling antagonist expression in *Catnb*$^{flox(ex3)/+}$;*Amhr2*$^{Cre/+}$ ovaries is initiated in parallel with Cre-mediated recombination well before the appearance of the pretumoral lesions and that pretumoral lesion and GCT formation occurs despite the uninterrupted presence of their Wnt signaling antagonist activities. This suggests that these genes are incapable of completely repressing misregulated Wnt/β-catenin signaling in *Catnb*$^{flox(ex3)/+}$;*Amhr2*$^{Cre/+}$ ovaries and that their silencing is not required for later development of GCT.

Expression of bone and neurosecretory cell markers in distinct cell populations in *Catnb*$^{flox(ex3)/+}$;*Amhr2*$^{Cre/+}$ GCT reveals the presence of distinct metaplastic cell types. To study the expression of the genes described in Fig. 1 in GCT from *Catnb*$^{flox(ex3)/+}$;*Amhr2*$^{Cre/+}$ ovaries, *in situ* hybridization analyses were done for each gene using a panel of tumors. Results showed the presence of nests of neoplastic granulosa cells within many GCT that expressed all Wnt signaling antagonists detected in the pretumoral lesions (Fig. 4*A*). These cells also expressed the neuronal marker *Ptn* as well as *Cck*, which encodes the neuropeptide cholecystokinin. A distinct, less common cell population was found to express the bone marker *Ibsp* (Fig. 4*B*). Areas of *Ibsp* expression failed to show expression of the Wnt antagonist or neurosecretory cell markers described in Fig. 4*A* and were invariably associated with foci of ossification. Together with the data showing bone marker expression in pretumoral lesions before GCT development and before obvious bone formation (Figs. 1*C* and 2*B*), these results show that stabilization of β-catenin

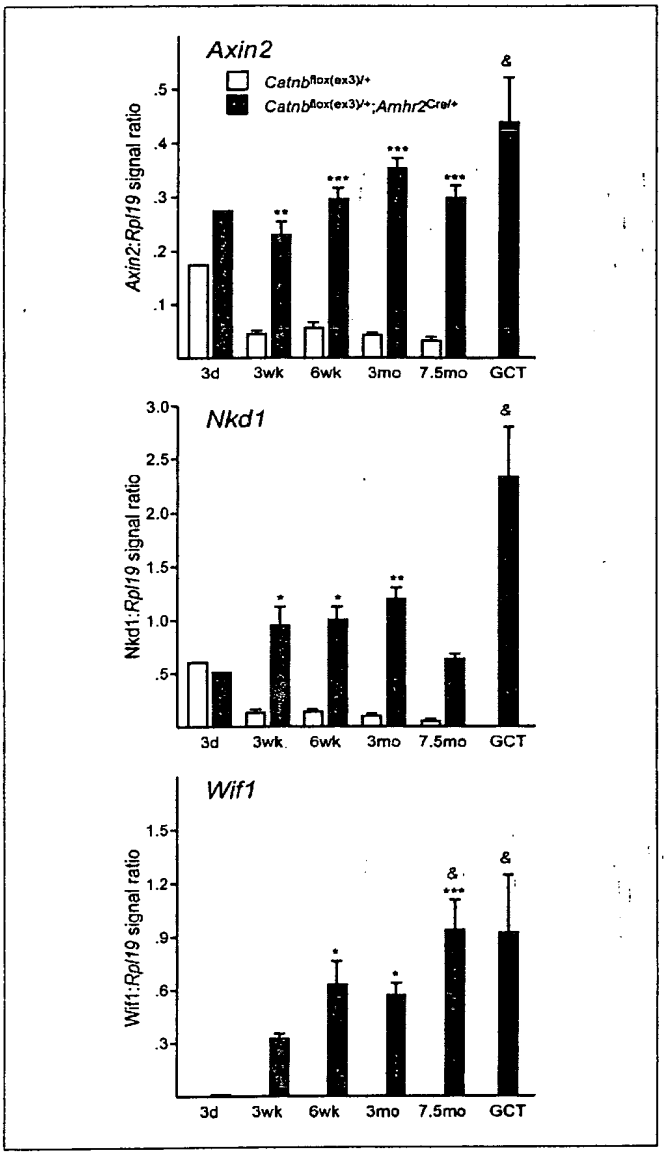

Figure 3. Age-dependent ovarian expression of Wnt signaling inhibitors in $Catnb^{flox(ex3)/+};Amhr2^{cre/+}$ and $Catnb^{flox(ex3)/+}$ mice. Total ovarian RNA was isolated from mice at the indicated ages as well as from GCT obtained from $Catnb^{flox(ex3)/+};Amhr2^{cre/+}$ mice. RT-PCR analyses were done to quantify Wnt signaling inhibitor mRNA levels relative to the housekeeping gene *Rpl19*. *Columns*, averages of the normalized values; *bars*, SE. Only single values were obtained at $t = 3$ days, as RNA samples from five animals per genotype had to be pooled to obtain samples of sufficient size. For other time points, $n = 2$ ($Catnb^{flox(ex3)/+}$, $t = 3$ months), $n = 4$ ($Catnb^{flox(ex3)/+}$, $t = 3$ weeks and 7.5 months; $Catnb^{flox(ex3)/+};Amhr2^{cre/+}$, $t = 3$ months), or $n = 3$ (all other time points). *, $P < 0.05$; **, $P < 0.01$; ***, $P < 0.001$, statistically significant differences between $Catnb^{flox(ex3)/+};Amhr2^{cre/+}$ and $Catnb^{flox(ex3)/+}$ groups at a given time point. &, $P < 0.05$, statistically significant time-dependent (or tumorigenesis-dependent) increases in gene expression in $Catnb^{flox(ex3)/+};Amhr2^{cre/+}$ animals (using the 3-week time point as a reference). Note that *Wif1* mRNA could not be detected at any time point in $Catnb^{flox(ex3)/+}$ ovaries.

induces osseous metaplasia in ovarian granulosa cells. Likewise, the presence of *Cck*-positive populations in the GCT, in addition to the expression of neuronal/neurosecretory markers in the pretumoral stages (Figs. 1*B* and 2*A*), is suggestive of neuronal metaplasia. Although the presence of cholecystokinin-positive nerve fibers has been reported in the interstitium of the normal ovary (32, 33), these are thought to originate from neurons situated in the dorsal root ganglia rather than an endogenous ovarian neurosecretory cell population, which is supported by our inability to detect *Cck* mRNA in normal ovaries (Fig. 1*B*). It is therefore unlikely that the tumoral *Cck*-positive cells represent a neoplastic proliferation of ovarian neurosecretory cells. Indeed, the tumoral *Cck*-positive cells morphologically resemble granulosa cells, supporting the concept that they are of granulosa cell origin and are undergoing metaplastic transformation.

A third, spindle-shaped cell population was typically found immediately adjacent to foci of ossification (Fig. 4*C*, *arrows*). Unlike the other cell types, these were found to be strongly positive for *Cdkn1c* (which encodes the cell cycle inhibitor $p57^{Kip2}$) and no other markers were examined. As *Cdkn1c* expression is induced in osteoblast precursors, as these cease proliferating and undergo differentiation (34), the *Cdkn1c*-positive cells may represent a differentiating precursor subpopulation of the metaplastic bone cells. This is supported by the presence of *Cdkn1c*-positive cells in pretumoral lesions (Fig. 2*B*) before bone formation and before *Ibsp* can be detected by *in situ* hybridization. Although circumstantial, the localization of the *Cdkn1c*-positive population between the *Cck*-positive cell population and the foci of osseous metaplasia could indicate that the former may give rise to the latter or vice versa.

Serum pleiotrophin levels in $Catnb^{flox(ex3)/+};Amhr2^{cre/+}$ mice. The cytokine pleiotrophin, the product of the *Ptn* gene, has recently been found at increased levels in serum from patients with several tumor types, suggesting its potential use as a diagnostic or prognostic marker (refs. 35–37). Our observation that *Ptn* was highly expressed in both the pretumoral lesions and GCT in $Catnb^{flox(ex3)/+};Amhr2^{cre/+}$ mice (Figs. 1*B*, 2*B*, and 4) raised the possibility that serum pleiotrophin levels could also be increased in this model and by extension perhaps in human GCT. To test this, serum pleiotrophin levels were measured in both young (6-12 weeks) $Catnb^{flox(ex3)/+};Amhr2^{cre/+}$ mice bearing pretumoral lesions and older (>24 weeks) mice susceptible to developing GCT as well as in age-matched $Catnb^{flox(ex3)/+}$ controls. The highest levels of pleiotrophin were identified in two >24-week-old $Catnb^{flox(ex3)/+};Amhr2^{cre/+}$ mice bearing large GCT (12.42 and 22.88 ng/mL, respectively). However, serum pleiotrophin levels comparable with controls were detected in the vast majority of $Catnb^{flox(ex3)/+};Amhr2^{cre/+}$ mice, and no statistically significant differences could be detected between experimental groups (Table 2).

Discussion

Metaplasia, defined simply as the transformation of one tissue type to another, is a poorly understood process that has been observed in a wide range of tumor types (38–40). Although the relevance of metaplasia to the disease process remains unclear in most tumors, in some cases, it is thought to represent an essential premalignant step in the series of events that give rise to cancer. Perhaps the best-known example of this is Barrett's esophagus, a condition in which the squamous epithelium of the lower esophagus is replaced by intestinal epithelium, which predisposes the patient to develop esophageal adenocarcinoma (40). In this study, we report that changes in gene expression indicative of both osseous and neuronal metaplasia occur in the ovarian pretumoral lesions in the $Catnb^{flox(ex3)/+};Amhr2^{cre/+}$ model and that the GCT

that develop later in life consist (at least in part) of clonal expansions of these metaplastic cell types. To our knowledge, this is therefore the first report to show a metaplastic intermediate step in the etiology of GCT. Furthermore, although osseous metaplasia has long been known to occur in a variety of tumor types (38, 39), the molecular mechanisms underlying its development are completely unknown. Our results indicate that constitutive activation of the Wnt/β-catenin pathway results in metaplastic ossification in the ovary, and the *Catnb*$^{flox(ex3)/+}$;*Amhr2*$^{cre/+}$ mouse could serve as a model for the study of this poorly understood phenomenon. Whether Wnt/β-catenin signaling defects are involved in the etiology of metaplastic ossification in other tissue and tumor types is an important question that remains to be resolved.

The exact origin of the metaplastic cells that form the pretumoral lesions in *Catnb*$^{flox(ex3)/+}$;*Amhr2*$^{cre/+}$ ovaries remains unclear. Some extent of Cre-mediated genetic recombination is thought to occur prenatally/perinatally in the ovaries of *Catnb*$^{flox(ex3)/+}$;*Amhr2*$^{cre/+}$ mice (25), which is supported by our observation of ectopic *Wif1* expression in the ovaries of animals as young as 3 days. Recombination leads to the appearance of visibly discernable pretumoral lesions by the 5th or 6th week of life, and these do not

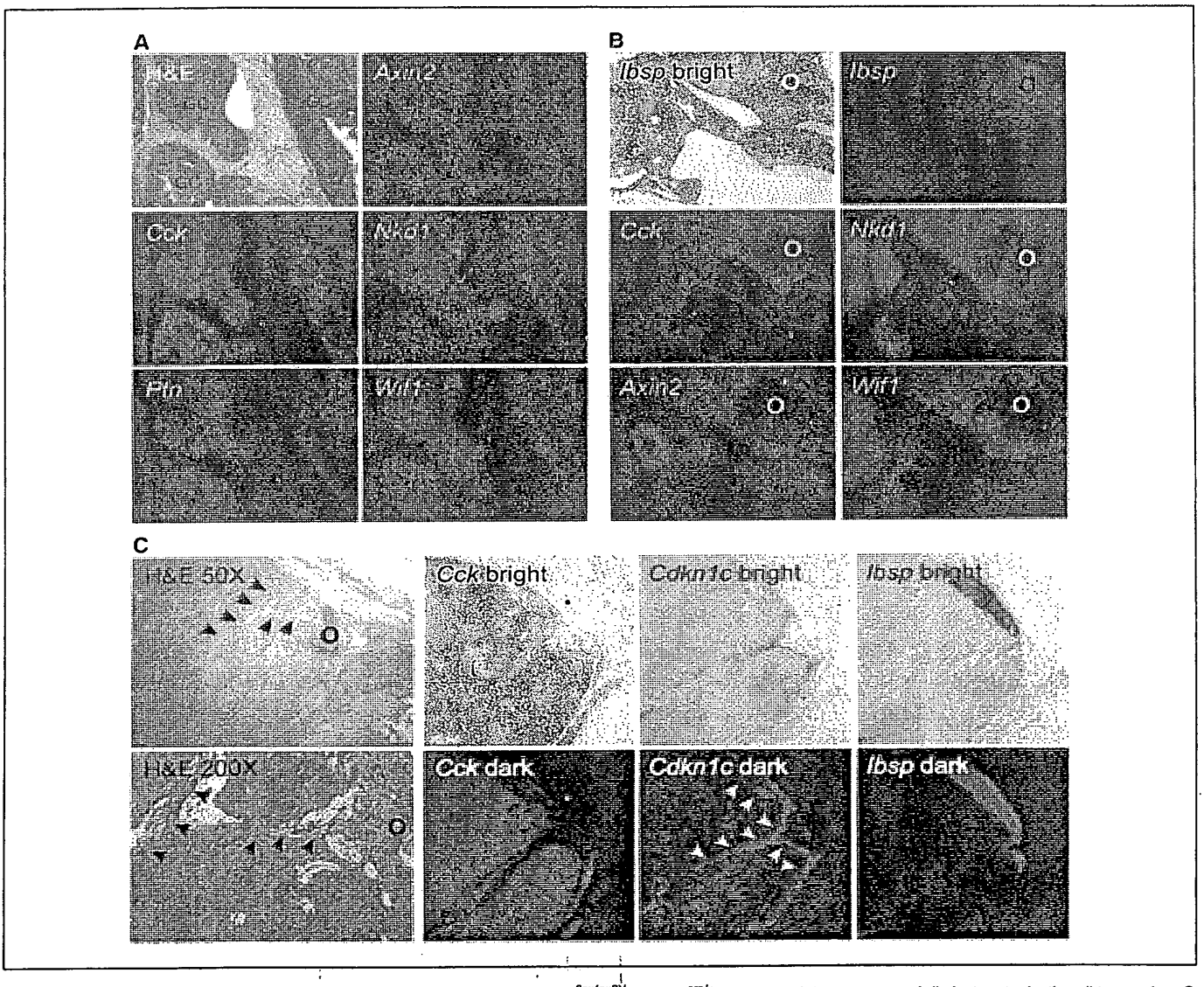

Figure 4. *In situ* hybridization analyses of genes of interest in GCT from *Catnb*$^{flox(ex3)/+}$;*Amhr2*$^{cre/+}$ mice reveal the presence of distinct metaplastic cell types. *A* to *C*, results from the hybridization of the riboprobes described in Table 1 to three different tumors, respectively. Although the same field is shown in all images of each panel, slight differences in tissue morphology occur from one image to the next due to the use of nonconsecutive histologic sections. Original magnifications, ×50, except as indicated (H&E stain). *A*, dark-field views of sections hybridized to the indicated riboprobes. In all cases, signals corresponded to nests of tumorous granulosa cells as shown in the bright-field image (*top left*). *GC*, granulosa cells. *B*, a region of metaplastic ossification (O) hybridized to the *Ibsp* riboprobe but not to the markers characteristic the cell type defined in (*A*), which are also seen surrounding the ossified region. The bright-field view of the hematoxylin-stained section hybridized to *Ibsp* is shown to illustrate tissue morphology. *C*, a third, spindle-shaped cell type that was typically found at the boundaries of ossified regions (O) is shown at low and high magnification (*arrows*). These cells hybridized specifically to the *Cdkn1c* riboprobe but not to the other markers shown in (*A* and *B*).

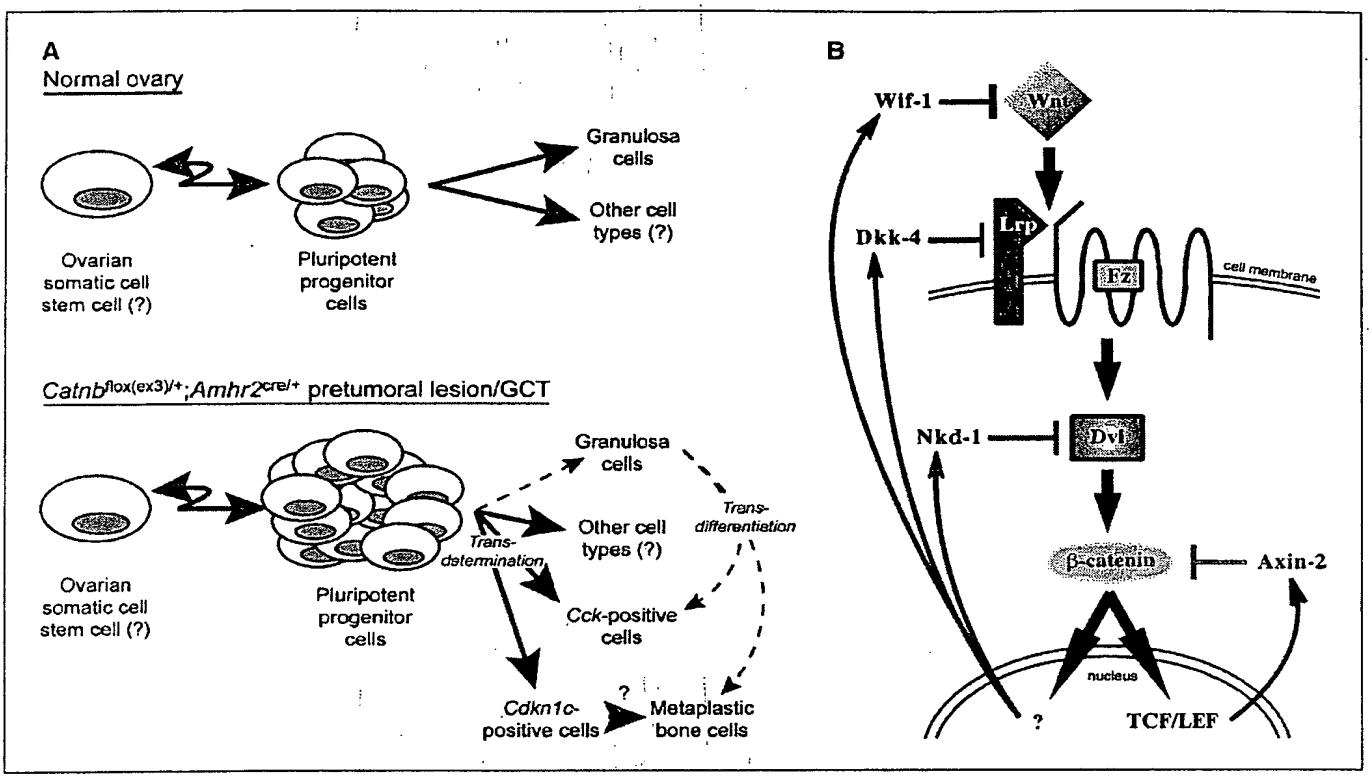

Figure 5. Cellular and molecular processes in *Catnb*$^{flox(ex3)/+}$;*Amhr2*$^{cre/+}$ granulosa cells. *A*, theoretical model illustrating the proliferation and differentiation dynamics of ovarian granulosa cells and their precursors in normal ovaries versus *Catnb*$^{flox(ex3)/+}$;*Amhr2*$^{cre/+}$ pretumoral and tumoral lesions. Metaplastic cell types may arise either by transdetermination (i.e., commitment of a multipotent stem/precursor cell type to an inappropriate lineage) or by transdifferentiation (i.e., alteration of the fate of a cell already committed to a particular lineage). *B*, misregulated Wnt/β-catenin signaling induces multiple, complementary negative feedback loops. The level at which each signaling antagonist described in Fig. 1 affects the canonical Wnt signaling pathway is illustrated. *Axin2* transcription is activated by TCF/LEF family transcription factors (44) and is a direct target of the canonical Wnt/β-catenin signaling pathway; whether this is true for the other antagonists has not been reported.

seem to grow in number thereafter despite the presence of abundant normal-looking follicles whose granulosa cells predictably express *Cre* (25, 27). The prenatal/perinatal phase therefore seems to represent the critical time period for the formation of the pretumoral cells, after which these proliferate to form pretumoral lesions, but few, if any, additional "founder" pretumoral cells are created. The earliest events of follicular development also occur during this time in the normal mouse ovary, as ovarian somatic cells proliferate, differentiate into granulosa cell precursors, and become organized with oocytes to form primordial follicles (41). Given this and the known effect of misregulated Wnt signaling on cell fate decisions in other cell types (16–20), it would seem reasonable to propose that the pretumoral cells could arise from a multipotent ovarian somatic stem/progenitor cell type that undergoes genetic recombination early during ovarian development (Fig. 5*A*). Metaplasia then results, as misregulated Wnt/β-catenin signaling causes these progenitor cells to commit to inappropriate lineages, a process that Okubo and Hogan have recently called transdetermination (16). Alternatively, cells that are committed to become granulosa cells may have their fates altered on genetic recombination and Wnt/β-catenin signaling activation, a mechanism that many authors now call transdifferentiation (16, 42). Although our experimental design could not permit us to distinguish between these two scenarios, we believe transdifferentiation to be less likely than transdetermination, as the granulosa cells present in normal-looking follicles found in adult *Catnb*$^{flox(ex3)/+}$;*Amhr2*$^{cre/+}$ ovaries seem incapable of undergoing metaplastic changes following commitment to the granulosa cell fate.

Our results indicate that *Axin2* and *Nkd1* are expressed in oocytes, and the expression of these two genes was also observed in pretumoral lesions and the GCT *Cck*-positive cell population in *Catnb*$^{flox(ex3)/+}$;*Amhr2*$^{cre/+}$ mice. Considering the pluripotency of tumoral germ cells (as observed in teratomas in particular) and the pluripotent characteristics of the GCT in the *Catnb*$^{flox(ex3)/+}$;*Amhr2*$^{cre/+}$ model, this would suggest that one or more cell types observed in *Catnb*$^{flox(ex3)/+}$;*Amhr2*$^{cre/+}$ GCT may be oocyte derived. However, the *Cck*-positive cell population morphologically resembles granulosa cells, and extensive histopathologic analyses showed that all ovarian tumors observed in *Catnb*$^{flox(ex3)/+}$;*Amhr2*$^{cre/+}$ mice to be GCT, without bearing any resemblance to teratomas or any other type of germ cell tumor (25). Furthermore, direct targeting of β-catenin stabilization to oocytes using *Catnb*$^{flox(ex3)}$ and Tg(Zp3-cre) mice failed to generate germ cell tumors.[4] Therefore, although an oocyte contribution to the GCT observed in *Catnb*$^{flox(ex3)/+}$;*Amhr2*$^{cre/+}$ mice cannot be ruled out, we believe that the vast majority of the cells in these tumors arise from a somatic stem/progenitor cell type as stated above.

[4] D. Boerboom and J.S. Richards, unpublished observations.

Another important finding reported herein is the induction of the expression of multiple antagonists of Wnt/β-catenin signaling in *Catnb*$^{flox(ex3)/+}$;*Amhr2*$^{cre/+}$ ovarian pretumoral and tumoral cells. *Axin2, Dkk4, Nkd1*, and *Wif1* each interact with a different component of the Wnt/β-catenin signaling cascade, indicating the existence of multiple, nonredundant feedback loops that could act in a coordinate manner to shutdown the Wnt/β-catenin pathway at many levels simultaneously (Fig. 5*B*). Although the involvement of each of these Wnt antagonists in negative feedback loops has been suggested in previous reports (43–48), the concept that multiple loops could act coordinately within a given cell is unusual. As the activation of the Wnt/β-catenin pathway in *Catnb*$^{flox(ex3)/+}$;*Amhr2*$^{Cre/+}$ mice occurs at the level of β-catenin itself and all of the negative feedback loops act upon or upstream of β-catenin, all of these mechanisms predictably fail to inhibit pathway activity in this model. Indeed, as Wnts can signal via at least two additional pathways (the Wnt/Ca^{2+} and planar cell polarity pathways; ref. 2), many of the negative feedback loops could conceivably be harmful, contributing to the pathogenesis by shutting down potentially beneficial Wnt signals that are transduced via β-catenin-independent mechanisms.

Of the genes that are induced in *Catnb*$^{flox(ex3)/+}$;*Amhr2*$^{cre/+}$ ovaries, *Ptn* may be of particular pathophysiologic relevance to both metaplasia and tumorigenesis phenotypes. We have listed *Ptn* as a neuronal marker as it is expressed in specific areas of the developing and adult nervous system (49), *Ptn*-deficient mice exhibit neurophysiologic and behavioral phenotypes (50, 51), and it is thought to affect the proliferation and differentiation of particular neuronal cell types (52, 53). However, *Ptn* has also been proposed to play important roles in bone physiology, specifically as a positive regulator of both osteoblast differentiation and function (54, 55). The induction of *Ptn* could thus conceivably influence the lineages to which pretumoral cells are diverted in *Catnb*$^{flox(ex3)/+}$;*Amhr2*$^{cre/+}$ ovaries, leading to the observed osseous and neuronal metaplasias. Furthermore, pleiotrophin is thought to be a positive regulator of both physiologic and tumoral angiogenesis (56, 57). This may relate to the highly vascularized organization of the pretumoral lesions in *Catnb*$^{flox(ex3)/+}$;*Amhr2*$^{cre/+}$ ovaries and of GCT in all species (25, 58), which contrasts sharply with the normally avascular granulosa cell layer of ovarian follicles. Beyond angiogenesis, *Ptn* is believed to contribute to carcinogenesis in a variety of additional ways in many types of cancer, affecting processes as diverse as apoptosis, mitosis, transformation, and chemotaxis (57). Expression of *Ptn* in certain tumors correlates with increased levels of circulating pleiotrophin, leading several authors to suggest that serum pleiotrophin measurements may be of diagnostic or prognostic value in a clinical setting (35–37). Our serum pleiotrophin results in the *Catnb*$^{flox(ex3)/+}$;*Amhr2*$^{cre/+}$ mouse show that increased circulating pleiotrophin levels are occasionally found with advanced age following GCT development. However, the infrequency of this observation suggests that pleiotrophin measurement may not be a useful tool for GCT diagnosis. Whether this will be the case for human GCT patients will be grounds for further research.

In summary, we have used microarray analyses to elucidate the molecular processes underlying pretumoral lesion and GCT development in *Catnb*$^{flox(ex3)/+}$;*Amhr2*$^{cre/+}$ mice. Our results show that constitutive activation of the Wnt/β-catenin pathway during ovarian development leads to the appearance of distinct metaplastic cell types, suggesting that metaplasia is a key intermediate step in the development of GCT in this model. This study further illustrates the effect of the Wnt/β-catenin pathway on cell fate decision-making processes and provides insight into how its misregulation can lead to tumor development.

Acknowledgments

Received 9/28/2005; revised 11/5/2005; accepted 12/13/2005.

Grant support: NIH grants HD16272 and HD07495 (J.S. Richards), Association pour la Recherche sur le Cancer, France grant 3242 (J. Courty), and Canadian Institutes of Health Research fellowship (D. Boerboom).

The costs of publication of this article were defrayed in part by the payment of page charges. This article must therefore be hereby marked *advertisement* in accordance with 18 U.S.C. Section 1734 solely to indicate this fact.

We thank Yuet K. Lo and Laura Liles for important technical contributions to the work and Drs. Marilene Paquet and Hubert Burden for helpful discussions.

References

1. Lustig B, Behrens J. The Wnt signaling pathway and its role in tumor development. J Cancer Res Clin Oncol 2003;129:199–221.
2. Huelsken J, Birchmeier W. New aspects of Wnt signaling pathways in higher vertebrates. Curr Opin Genet Dev 2001;11:547–53.
3. Miller JR. The Wnts. Genome Biol 2002;3:REVIEWS3001.
4. Pinto D, Clevers H. Wnt, stem cells and cancer in the intestine. Biol Cell 2005;97:185–96.
5. Reya T, Clevers H. Wnt signalling in stem cells and cancer. Nature 2005;434:843–50.
6. Korinek V, Barker N, Moerer P, et al. Depletion of epithelial stem-cell compartments in the small intestine of mice lacking Tcf-4. Nat Genet 1998;19:379–83.
7. Pinto D, Gregorieff A, Begthel H, Clevers H. Canonical Wnt signals are essential for homeostasis of the intestinal epithelium. Genes Dev 2003;17:1709–13.
8. Kuhnert F, Davis CR, Wang HT, et al. Essential requirement for Wnt signaling in proliferation of adult small intestine and colon revealed by adenoviral expression of Dickkopf-1. Proc Natl Acad Sci U S A 2004;101:266–71.
9. Reya T, Duncan AW, Ailles L, et al. A role for Wnt signalling in self-renewal of haematopoietic stem cells. Nature 2003;423:409–14.
10. Willert K, Brown JD, Danenberg E, et al. Wnt proteins are lipid-modified and can act as stem cell growth factors. Nature 2003;423:448–52.
11. Van Den Berg DJ, Sharma AK, Bruno E, Hoffman R. Role of members of the Wnt gene family in human hematopoiesis. Blood 1998;92:3189–202.
12. Murdoch B, Chadwick K, Martin M, et al. Wnt-5A augments repopulating capacity and primitive hematopoietic development of human blood stem cells *in vivo*. Proc Natl Acad Sci U S A 2003;100:3422–7.
13. Lee HY, Kleber M, Hari L, et al. Instructive role of Wnt/β-catenin in sensory fate specification in neural crest stem cells. Science 2004;303:1020–3.
14. Muroyama Y, Kondoh H, Takada S. Wnt proteins promote neuronal differentiation in neural stem cell culture. Biochem Biophys Res Commun 2004;313:915–21.
15. Brandon C, Eisenberg LM, Eisenberg CA.WNT signaling modulates the diversification of hematopoietic cells. Blood 2000;96:4132–41.
16. Okubo T, Hogan BL. Hyperactive Wnt signaling changes the developmental potential of embryonic lung endoderm. J Biol 2004;3:11.
17. Miyoshi K, Shillingford JM, Le Provost F, et al. Activation of β-catenin signaling in differentiated mammary secretory cells induces transdifferentiation into epidermis and squamous metaplasias. Proc Natl Acad Sci U S A 2002;99:219–24.
18. Bierie B, Nozawa M, Renou JP, et al. Activation of β-catenin in prostate epithelium induces hyperplasias and squamous transdifferentiation. Oncogene 2003;22:3875–87.
19. Niemann C, Owens DM, Hulsken J, Birchmeier W, Watt FM. Expression of ΔNLef1 in mouse epidermis results in differentiation of hair follicles into squamous epidermal cysts and formation of skin tumours. Development 2002;129:95–109.
20. Merrill BJ, Gat U, DasGupta R, Fuchs E. Tcf3 and Lef1 regulate lineage differentiation of multipotent stem cells in skin. Genes Dev 2001;15:1688–705.
21. Giles RH, van Es JH, Clevers H. Caught up in a Wnt storm: Wnt signaling in cancer. Biochim Biophys Acta 2003;1653:1–24.
22. Hsieh M, Johnson MA, Greenberg NM, Richards JS. Regulated expression of Wnts and Frizzleds at specific stages of follicular development in the rodent ovary. Endocrinology 2002;143:898–908.
23. Hsieh M, Mulders SM, Friis RR, Dharmarajan A, Richards JS. Expression and localization of secreted frizzled-related protein-4 in the rodent ovary: evidence for selective up-regulation in luteinized granulosa cells. Endocrinology 2003;144:4597–606.
24. Ricken A, Lochhead P, Kontogiannea M, Farookhi R. Wnt signaling in the ovary: identification and compartmentalized expression of wnt-2, wnt-2b, and frizzled-4 mRNAs. Endocrinology 2002;143:2741–9.
25. Boerboom D, Paquet M, Hsieh M, et al. Misregulated Wnt/β-catenin signaling leads to ovarian

granulosa cell tumor development. Cancer Res 2005; 65:9206–15.
26. Harada N, Tamai Y, Ishikawa T, et al. Intestinal polyposis in mice with a dominant stable mutation of the β-catenin gene. EMBO J 1999;18:5931–42.
27. Jorgez CJ, Klysik M, Jamin SP, Behringer RR, Matzuk MM. Granulosa cell-specific inactivation of follistatin causes female fertility defects. Mol Endocrinol 2004;18: 953–67.
28. Soulie P, Heroult M, Bernard I, et al. Immunoassay for measuring the heparin-binding growth factors HARP and MK in biological fluids. J Immunoassay Immunochem 2002;23:33–48.
29. Robker RL, Russell DL, Espey LL, Lydon JP, O'Malley BW, Richards JS. Progesterone-regulated genes in the ovulation process: ADAMTS-1 and cathepsin L proteases. Proc Natl Acad Sci U S A 2000;97:4689–94.
30. Wilkensen DG. *In situ* hybridization. In: Stern CD, Holland PWH, editors. Essential developmental biology, a practical approach. New York: Oxford University Press; 1993. p. 258–63.
31. Robker RL, Richards JS. Hormone-induced proliferation and differentiation of granulosa cells: a coordinated balance of the cell cycle regulators cyclin D2 and $p27^{Kip1}$. Mol Endocrinol 1998;12:924–40.
32. McNeill DL, Burden HW. Neuropeptides in sensory perikarya projecting to the rat ovary. Am J Anat 1987; 179:269–76.
33. Doss DN, Mekhail NA, Ekladdios EY. The localization of cholecystokinin immunoreactivity in the rat ovary and uterine tube. Neuropeptides 1991;18:87–91.
34. Urano T, Hosoi T, Shiraki M, Toyoshima H, Ouchi Y, Inoue S. Possible involvement of the p57(Kip2) gene in bone metabolism. Biochem Biophys Res Commun 2000; 269:422–6.
35. Jager R, List B, Knabbe C, et al. Serum levels of the angiogenic factor pleiotrophin in relation to disease stage in lung cancer patients. Br J Cancer 2002;86:858–63.
36. Souttou B, Juhl H, Hackenbruck J, et al. Relationship between serum concentrations of the growth factor pleiotrophin and pleiotrophin-positive tumors. J Natl Cancer Inst 1998;90:1468–73.
37. Aigner A, Brachmann P, Beyer J, et al. Marked increase of the growth factors pleiotrophin and fibroblast growth factor-2 in serum of testicular cancer patients. Ann Oncol 2003;14:1525–9.
38. Byard RW, Thomas MJ. Osseous metaplasia within tumours. A review of 11 cases. Ann Pathol 1988;8:64–6.
39. Haque S, Eisen RN, West AB. Heterotopic bone formation in the gastrointestinal tract. Arch Pathol Lab Med 1996;120:666–70.
40. Flejou JF. Barrett's oesophagus: from metaplasia to dysplasia and cancer. Gut 2005;54 Suppl 1:i6–12.
41. Pepling ME, Spradling AC. Mouse ovarian germ cell cysts undergo programmed breakdown to form primordial follicles. Dev Biol 2001;234:339–51.
42. Okada TS. Cellular metaplasia or transdifferentiation as a model for retinal cell differentiation. Curr Top Dev Biol 1980;16:349–80.
43. Yan D, Wiesmann M, Rohan M, et al. Elevated expression of axin2 and hnkd mRNA provides evidence that Wnt/β-catenin signaling is activated in human colon tumors. Proc Natl Acad Sci U S A 2001;98:14973–8.
44. Jho EH, Zhang T, Domon C, Joo CK, Freund JN, Costantini F. Wnt/β-catenin/Tcf signaling induces the transcription of Axin2, a negative regulator of the signaling pathway. Mol Cell Biol 2002;22:1172–83.
45. Vaes BL, Dechering KJ, van Someren EP, et al. Microarray analysis reveals expression regulation of Wnt antagonists in differentiating osteoblasts. Bone 2005;36:803–11.
46. Reguart N, He B, Xu Z, et al. Cloning and characterization of the promoter of human Wnt inhibitory factor-1. Biochem Biophys Res Commun 2004;323:229–34.
47. Ishikawa A, Kitajima S, Takahashi Y, et al. Mouse Nkd1, a Wnt antagonist, exhibits oscillatory gene expression in the PSM under the control of Notch signaling. Mech Dev 2004;121:1443–53.
48. Diep DB, Hoen N, Backman M, Machon O, Krauss S. Characterisation of the Wnt antagonists and their response to conditionally activated Wnt signalling in the developing mouse forebrain. Brain Res Dev Brain Res 2004;153:261–70.
49. Vanderwinden JM, Mailleux P, Schiffmann SN, Vanderhaeghen JJ. Cellular distribution of the new growth factor pleiotrophin (HB-GAM) mRNA in developing and adult rat tissues. Anat Embryol (Berl) 1992; 186:387–406.
50. Pavlov I, Voikar V, Kaksonen M, et al. Role of heparin-binding growth-associated molecule (HB-GAM) in hippocampal LTP and spatial learning revealed by studies on overexpressing and knockout mice. Mol Cell Neurosci 2002;20:330–42.
51. Amet LE, Lauri SE, Hienola A, et al. Enhanced hippocampal long-term potentiation in mice lacking heparin-binding growth-associated molecule. Mol Cell Neurosci 2001;17:1014–24.
52. Hienola A, Pekkanen M, Raulo E, Vanttola P, Rauvala H. HB-GAM inhibits proliferation and enhances differentiation of neural stem cells. Mol Cell Neurosci 2004;26: 75–88.
53. Szabat E, Rauvala H. Role of HB-GAM (heparin-binding growth-associated molecule) in proliferation arrest in cells of the developing rat limb and its expression in the differentiating neuromuscular system. Dev Biol 1996;178:77–89.
54. Tare RS, Oreffo RO, Clarke NM, Roach HI. Pleiotrophin/osteoblast-stimulating factor 1: dissecting its diverse functions in bone formation. J Bone Miner Res 2002;17:2009–20.
55. Imai S, Kaksonen M, Raulo E, et al. Osteoblast recruitment and bone formation enhanced by cell matrix-associated heparin-binding growth-associated molecule (HB-GAM). J Cell Biol 1998;143:1113–28.
56. Christman KL, Fang Q, Kim AJ, et al. Pleiotrophin induces formation of functional neovasculature *in vivo*. Biochem Biophys Res Commun 2005;332: 1146–52.
57. Kadomatsu K, Muramatsu T. Midkine and pleiotrophin in neural development and cancer. Cancer Lett 2004;204:127–43.
58. Schumer ST, Cannistra SA. Granulosa cell tumor of the ovary. J Clin Oncol 2003;21:1180–9.

Available online at www.sciencedirect.com
SCIENCE DIRECT®
Cancer Letters 206 (2004) 107–113
CANCER Letters
www.elsevier.com/locate/canlet

Wnt inhibitory factor-1: a candidate for a new player in tumorigenesis of intestinal epithelial cells

Malgorzata Cebrat, Leon Strzadala, Pawel Kisielow*

Institute of Immunology and Experimental Therapy, Polish Academy of Sciences, Rudolf Weigl St. 12, 53-114 Wroclaw, Poland

Received 15 July 2003; received in revised form 15 October 2003; accepted 22 October 2003

Abstract

Using cDNA-Representational Difference Analysis it was found that expression of *Opg, Ctse, Krt2-4, Fut-2, 24p3 and Wif-1* genes was elevated in intestinal adenomas as compared to normal epithelial cells of $Apc^{Min/+}$ mutant mice. Expression of *Wif-1*, which encodes Wnt inhibitory factor-1 was also detected in a number of tumor cell lines of epithelial cell origin including two human colon adenocarcinoma cell lines. The possible role of *Wif-1* over-expression in the etiology of colorectal cancer is discussed.

Keywords: *Wif-1*; $Apc^{Min/+}$ mice; Intestinal adenomas; cDNA-representational difference analysis

1. Introduction

The Wnt signaling pathway plays a central role in regulation of proliferation and differentiation of epithelial cells and its deregulation, due to mutations of adenomatous polyposis coli (*APC*) gene, leads to the development of colorectal cancer. The key function of APC protein in normal cells lies in its ability to destabilize β-catenin. Signaling by extracellular Wnt proteins blocks the destabilizing activity of the APC containing protein complex and allows translocation of β-catenin to the nucleus. In the nucleus β-catenin interacts with T-cell factors (Tcf) and stimulates the transcription of target genes [1]. Little is known about the nature and cellular origin of factors regulating the activity of Wnt proteins in the microenvironment of epithelial cells. Secreted molecules, which have been shown to bind to Wnt proteins and inhibit their activity, were described in several species. They include the secreted Frizzled-related [2,3] and Dickkopf [4] protein families and Wnt inhibitory factor-1 (Wif-1) [5]. The oncogenic transformation of normal intestinal epithelial cells into adenomas is believed to result from constitutive transcriptional activity of the β-catenin/Tcf4 complex in the nucleus, which is the consequence of inefficient degradation of β-catenin due to defective APC protein [6]. Transformation of an intestinal epithelial cells into metastatic cancer is accompanied by mutations in multiple genes some of which have been identified [7] but other probably still remain to be discovered.

To date, following genes have been identified as targets of β-catenin/Tcf4 complex activity in adenomas: c-*MYC*[8], *CCND*[9], *u-PAR*, c-*JUN* and *FRA-1*,

* Corresponding author. Tel.: +48-71-337-1172; fax: +1-48-71-337-1382.
E-mail address: kisielow@iitd.pan.wroc.pl (P. Kisielow).

0304-3835/$ - see front matter © 2003 Elsevier Ireland Ltd. All rights reserved.
doi:10.1016/j.canlet.2003.10.024

ZO-1[10], gastrin [11], *WISP-1*[12], *ITF-2*[13], *Id2*[14], *MDR1* [15], *Cox2*[16], matrilysin [17], laminin γ2 [18], VEGF [19]. Over-expression of c-*MYC* was found to play the central role in maintaining epithelial progenitor cells in proliferative state and in repressing genetic program responsible for their differentiation [20].

To search for new genes, which may be activated during malignant transformation of intestinal epithelium as a result of APC loss and disruption of Wnt pathway, we used $Apc^{Min/+}$ mutant mice model of human familial adenomatous polyposis (FAP) disease [21]. With the aid of cDNA-representation difference analysis (cDNA-RDA) [22] we identified genes overexpressed in adenoma cells as compared to normal intestinal epithelial cells obtained from these mice. Interestingly, one of the genes was found to encode Wnt inhibitory factor-1 (Wif-1). To explain this unexpected finding we hypothesize that Wif-1 could facilitate tumorigenesis by inhibiting Wnt dependent stages of normally developing epithelial cells in the vicinity of emerging adenomas.

2. Materials and methods

2.1. Mice

$Apc^{Min/+}$ mice were a gift from Dr Ursula Gunthert (Basel Institute of Immunology, Basel, Switzerland) and Dr Khashayarsha Khazaie (Institut Necker, INSERM U373, Paris, France). C57BL/6 BoyIiw (B6) mice were from the animal colony of the Institute of Immunology and Experimental Therapy.

2.2. Tissues

The small intestine from 3 months old $Apc^{Min/+}$ and B6 mice was dissected and perfused several times with PBS Macroscopically distinguishable intestinal adenomas which developed in $Apc^{Min/+}$ mice and morphologically normal fragments of small intestine were separated and cut out with scissors.

2.3. Cell lines

LL-2 (murine lung adenocarcinoma), Mac16/c (murine mammary gland adenocarcinoma), WEHI164 (murine fibrosarcoma), B16 (murine melanoma), T47D (human mammary gland adenocarcinoma), SW707 (human colon adenocarcinoma), LS180 (human colon adenocarcinoma), HCV29 (human bladder adenocarcinoma), A-549 (human lung adenocarcinoma) cell lines were grown in Optimem medium (Gibco) supplemented with 5% of FCS (Boehringer Mannheim). MC38 (mouse colon adenocarcinoma), VIII/d [23] (mouse thymic lymphoma) cell lines were grown in Iscove's Modified Dulbecco Medium (Gibco) supplemented with 10% of FCS.

2.4. cDNA- representation difference analysis

The cDNA-RDA was performed exactly as described by Hubank and Schatz [22] except that hybridisation step was performed in the total volume of 2 μl containing 20 μg of the DNA. The hybridisation between tester (neoplastic tissue) and driver (normal tissue), between first difference product and driver and between second difference product and driver was performed in the following ratios: 1/100,1/800 and 1/10000, respectively.

2.5. Cloning and sequencing of the difference product

The third difference product was cloned into *Bam*HI site of pUC18 plasmid Sequencing of the inserts was performed with the Big Dye Terminator Cycle Sequencing Kit (PE Applied Biosystems) and pUC18 (−40) forward primer. The reaction products were separated on ABI PRISM 377 DNA sequencer (PE Applied Biosystems). The sequence homology searches were performed using the BLASTN program at NCBI non-redundant and mouse EST databases (http://www.ncbi.nlm.nih.gov/BLAST).

2.6. RT-PCR analysis of mRNA expression levels

Total RNA was isolated using Trizol Reagent (Gibco) according to the manufacturer's protocol. 3 μg of total RNA was digested with DNase I (Promega) and reverse transcribed with M-MLV reverse transcriptase (Gibco) and oligo(dT12–18) primer. cDNA prepared from 100–150 ng of total RNA was amplified in the PCR reaction with the presence of indicated primers for 35 cycles of 30 s at

94 °C, 30 s of annealing step at indicated temperature and 1 min at 72 °C. To exclude the possibility of the presence of contaminating genomic DNA, equal amount of total RNA was amplified without previous reverse transcription step (RT-control). PCR products were analysed in agarose (2%) gel electrophoresis and visualized with ethidum bromide staining. The following primer pairs for murine and human genes were used

Hprt: (murine) sense, 5′GCTGGTGAAAAGGACCTCT3′; antisense, 5′CACAGGACTAGAACACCTGC3′; annealing temperature: 55 °C, product size: 240 bp;

GAPDH: (human) sense, TCATCTCTGCCCCCTCTGCT; antisense, CGACGCCTGCTTCACCACCT; annealing temperature: 58 °C, product size: 439 bp;

Wif-1: (murine): sense, 5′AACCTGCCACGAACCCAA3′; antisense, 5′GCTGCTATTGGCTTTATCCGA3′; annealing temperature: 54 °C, product size: 598 bp; (human): sense, GTTGGCATGGAAGACACTGCA; antisense, TGACTTACGCATTTTTGCCCA; annealing temperature: 55 °C, product size: 510 bp;

Opg: (murine): sense, 5′TCCTGGCACCTACCTAAAACAGCA3′; antisense, 5′CTACACTCTCGGCATTCACTTTGG3′; annealing temperature: 59 °C, product size: 578 bp

(murine) sense, 5′CTGGGCCTTGCCCTGCTTGGGGTC3′; antisense, 5′GTTGTCAATGCATTGGTCGGTGGG3′; annealing temperature: 60 °C, product size: 580 bp;

Fut-2: (murine) sense, 5′TCGTGGTTACAAGCAACGGT3′; antisense, 5′AGTGCTTAAGGAGTGGGGACA3′; annealing temperature: 57 °C, product size: 314 bp

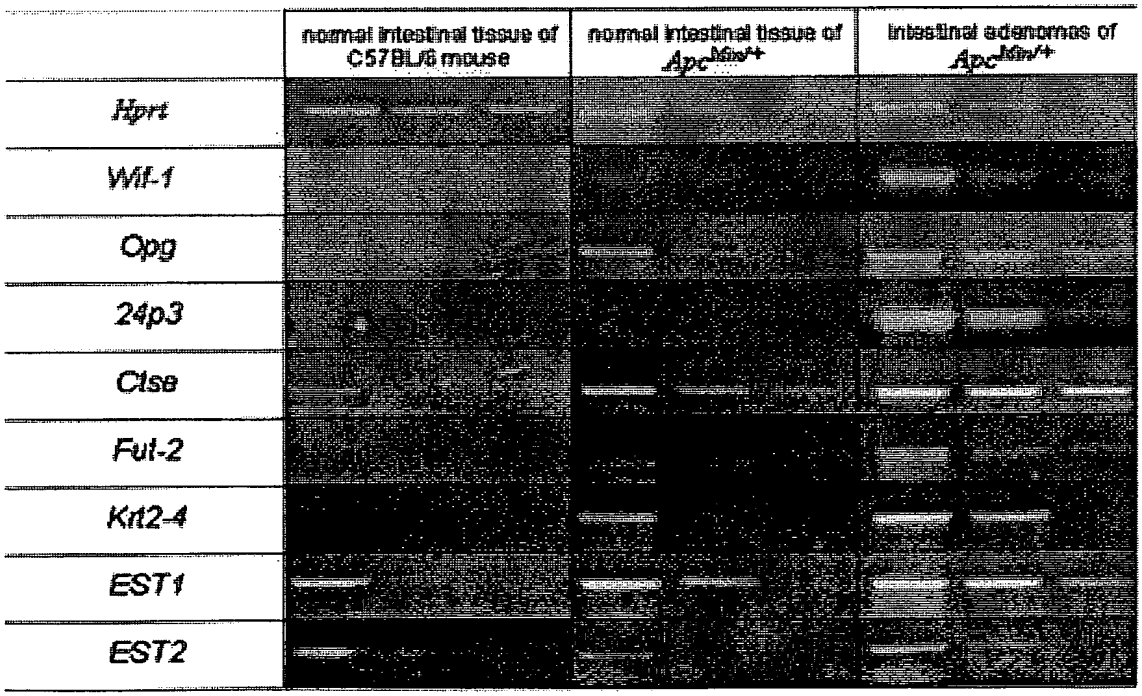

Fig. 1. Expression levels of the indicated genes, identified by the cDNA-RDA, in intestinal adenomas of $Apc^{Min/+}$ mice and in normal intestine tissue of $Apc^{Min/+}$ and C57BL/6 mice. The PCR amplification products of 1×, 10× and 100× diluted cDNA from indicated tissues are shown. Expression level of *Hprt* gene was used as internal control. The results shown are representative of at least three experiments.

Ctse: (murine) sense, 5′CACTGTGATGTT-CTGCTC3′; antisense, 5′TCTGAATACTCTGGG-GTGGCTA3′; annealing temperature: 57 °C, product size: 504 bp

Krt2–4: (murine) sense, 5′-GAATGCAA-GAGTGCTGTGAG-3′; antisense, 5′GGAGTTTCT-GCTCTTCATCC-3′; annealing temperature:55 °C, product size: 479 bp

EST1: (murine) sense, 5′-ATGAGACCTCC-TACGCTACA-3′; antisense, 5′-ACGTGGAAAG-CATGCCACTT-3′; annealing temperature:55 °C, product size: 477 bp

EST2: (murine) sense, 5′-AATGTGGAGCTTGG-GATCAG-3′; antisense, 5′-GGCTGCCTTGTGTT-AGTACA3′; annealing temperature:55 °C, product size: 472 bp

3. Results and discussion

3.1. cDNA-RDA

The difference products of the third round of subtractive hybridisation between the tester and the driver (representations of tumor and morphologically normal intestine of $Apc^{Min/+}$ mouse, respectively) were amplified by PCR and cloned. Thirty eight sequenced inserts were found to represent 15 different sequences. Three sequences corresponded to the known expressed sequence tags (EST) found in NCBI database, and twelve sequences turned out to be highly (over 94%) homologous to fragments of the genes encoding: Wif-1, 24p3 glycoprotein, osteoprotegerin, cathepsin E, α1,2-fucosyltransferase, ADP ribosylation factor-like, annexin A1, gastrotropin, keratin 4, 28s RNA and neuritin.

3.2. Identification of genes over-expressed in intestinal adenomas of $Apc^{Min/+}$ mice

In order to determine which of the genes identified by the cDNA-RDA were in fact over-expressed in intestinal adenomas as compared to normal intestinal epithelium, we analysed their expression in these tissues by RT-PCR. It was found that the two ESTs and the following genes had elevated level of expression in adenomas: *Wif-1*, *Opg*, *24p3*, *Ctse*, *Fut-2*and *Krt2-4*. Their expression levels in adenomatous and normal intestinal tissue of $Apc^{Min/+}$ mouse and in normal intestine of healthy B6 mouse are shown in Fig. 1. In morphologically normal intestine fragments of $Apc^{Min/+}$ mice, most of the transcripts, except *24p3* and EST-2, displayed intermediate levels of expression between adenomas and normal B6 intestine. This observation could reflect the early events occurring in epithelial cells undergoing malignant transformation or could be due to the contamination of normal intestinal tissue by tumor cells from neighbouring adenomas. Considering the fact that not all genes over-expressed in adenomas showed intermediate

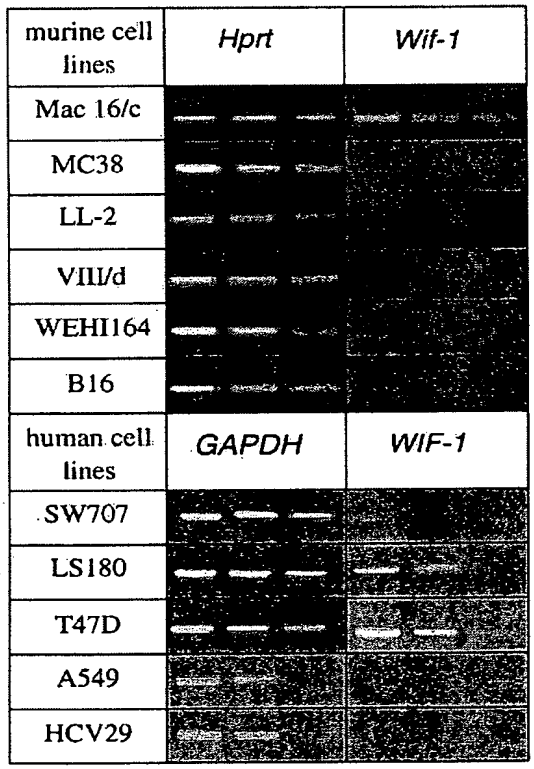

Fig. 2. Expression of *Wif-1* in murine and human tumour cell lines.The PCR amplification products of 1×, 10× and 100× diluted cDNA from indicated cell lines are shown. Expression of *Hprt* or *GAPDH* genes was used as internal controls for murine and human cell lines, respectively. The results shown are representative of at least three experiments.

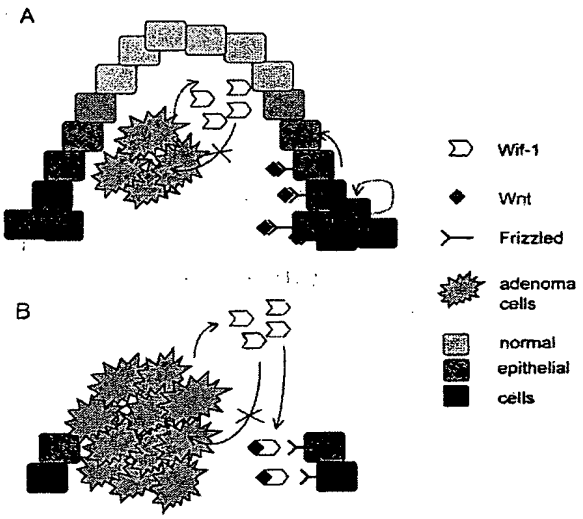

Fig. 3. Hypothetical role of Wif-1 in facilitating the growth of intestinal adenomas. Two possible scenarios are illustrated: (A) Wif-1 is a byproduct of oncogenic transformation and has no influence on the growth of adenoma (B) Production of Wif-1 by adenoma cells inhibits generation and/or maintenance of normal epithelial stem cell compartment and thereby facilitates tumor growth.

expression in morphologically normal $Apc^{Min/+}$ intestine and the fact that the great care has been taken to avoid the contamination by adenomatous tissue during dissection of the normal intestine from $Apc^{Min/+}$ mice, we favour the former possibility.

3.3. Expression of Wif-1 in tumor cell lines

To our knowledge, in contrast to *Ctse*, *24p3*, *Fut-2* and *Krt2-4*, over-expression of *Wif-1* and *Opg* genes in intestinal adenomas or colon carcinomas has not been described before. High levels of osteoprotegerin production by prostate cancer was recently reported [24] but no information has been so far published with regard to *Wif-1* expression in tumor cells. We have therefore examined a number of murine and human tumor cell lines for expression of *Wif-1*. As shown in Fig. 2, *Wif-1* was detected in murine (Mac16/c) and human (T47D) mammary gland adenocarcinoma cell line and in human colon adenocarcinoma cell lines (LS180-strong expression; SW707-weak expression) but not in murine intestinal adenocarcinoma cell line (MC38), murine lung adenocarcinoma cell line (LL-2), human lung adenocarcinoma cell line (A-549), human bladder adenocarcinoma cell line (HCV29), murine thymic lymphoma cell line (VIII/d), murine fibrosarcoma cell line (WEHI164) and murine melanoma cell line (B16). These results indicate that expression of *Wif-1*, which so far has been detected in heart, lung, brain and eye of the mouse and in the human retina [5] is also found in several tumors of epithelial cell origin. This observation, together with our finding of Wif-1 overexpression in intestinal adenomas developing in $Apc^{Min/+}$ mice, raises the question of its possible role in tumorogenesis.

3.4. Possible role of Wif-1 in the development of epithelial cell tumors

During normal development of epithelial cells, Wnt signaling is essential for the establishment and maintenance of the epithelial stem cell compartment [25] but little is known about mechanisms regulating activity of Wnt proteins. Wif-1 is a recently described secreted protein that binds to Wnt proteins and inhibits their interaction with the receptor [5], which may lead to the termination of transcription of genes activated by Tcf4/β-catenin complex. Thus, although there is as yet no evidence that *Wif-1* is a downstream target gene of Wnt pathway it is tempting to speculate

that in normal cells Wif-1 could be a part of the feedback inhibition loop negatively regulating the Wnt signaling.

In adenoma cells, in which constitutive activity of Tcf4/β-catenin complex is critically involved in acquisition of the malignant phenotype, Wif-1 would not be able to inhibit the Wnt signaling pathway due to the defect in APC protein.

In view of the above considerations over-expression of *Wif-1* could be regarded as a side effect of the constitutive activity of Tcf4/β-catenin complex without any significance for the growth of adenomas. Alternatively, and more interestingly overproduction of Wif-1 could facilitate the growth of adenomas by inhibiting the maintenance and proliferation of normal epithelial stem cells as illustrated in Fig. 3. We believe that in view of the fact that the mechanisms by which tumour cells influence their microenvironment and thereby facilitate their growth are poorly understood, the above hypothesis would be worth testing by generation of *Wif-1* deficient $Apc^{Min/+}$ mice.

Acknowledgements

We thank Dr Khashayarsha Khazaie and Dr Ursula Gunthert for $Apc^{Min/+}$ mice, Ewa Ziolo and Lidia Damska for technical assistance. This work was supported by the European Scientific Award to Pawel Kisielow from Koerber Foundation and by grant PAN No. 3/2002.

References

[1] M. Bienz, H. Clevers, Linking colorectal cancer to Wnt signaling, Cell 103 (2000) 311–320.
[2] A. Wodarz, R. Nusse, Mechanisms of Wnt signaling in development, Annu. Rev. Cell. Dev. Biol. 14 (1998) 59–88.
[3] R.T. Moon, J.L. Christian, R.M. Campbell, L.L. McGrew, A.A. DeMarais, M. Torres, et al., Dissecting Wnt signalling pathways and Wnt-sensitive developmental processes through transient misexpression analyses in embryos of *Xenopus laevis*, Dev. Suppl. (1993) 85–94.
[4] A. Glinka, W. Wu, H. Delius, A.P. Monaghan, C. Blumenstock, C. Niehrs, Dickkopf-1 is a member of a new family of secreted proteins and functions in head induction, Nature 391 (1998) 357–362.
[5] J.C. Hsieh, L. Kodjabachian, M.L. Rebbert, A. Rattner, P.M. Smallwood, C.H. Samos, et al., A new secreted protein that binds to Wnt proteins and inhibits their activities, Nature 398 (1999) 431–436.
[6] S. Munemitsu, I. Albert, B. Souza, B. Rubinfeld, P. Polakis, Regulation of intracellular beta-catenin levels by the adenomatous polyposis coli (APC) tumor-suppressor protein, Proc. Natl Acad. Sci. USA 92 (1995) 3046–3050.
[7] K.W. Kinzler, B. Vogelstein, Lessons from hereditary colorectal cancer, Cell 87 (1996) 159–170.
[8] T.C. He, A.B. Sparks, C. Rago, H. Hermeking, L. Zawel, L.T. da Costa, et al., Identification of c-MYC as a target of the APC pathway, Science 281 (1998) 1509–1512.
[9] O. Tetsu, F. McCormick, β-catenin regulates expression of cyclin D1 in colon carcinoma cells, Nature 398 (1999) 422–426.
[10] B. Mann, M. Gelos, A. Siedow, M.L. Hanski, A. Gratchev, M. Ilyas, et al., Target genes of β-catenin-T cell-factor/lymphoid-enhancer-factor signaling in human colorectal carcinomas, Proc. Natl Acad. Sci. USA 96 (1999) 1603–1608.
[11] T.J. Koh, C.J. Bulitta, J.V. Fleming, G.J. Dockray, A. Varro, T.C. Wang, Gastrin is a target of the beta-catenin/TCF-4 growth-signaling pathway in a model of intestinal polyposis, J. Clin. Invest. 106 (2000) 533–539.
[12] D. Pennica, T.A. Swanson, J.W. Welsh, M.A. Roy, D.A. Lawrence, J. Lee, et al., WISP genes are members of the connective tissue growth factor family that are up-regulated in wnt-1-transformed cells and aberrantly expressed in human colon tumors, Proc. Natl Acad. Sci. USA 95 (1998) 14717–14722.
[13] F.T. Kolligs, M.T. Nieman, I. Winer, G. Hu, D. Van Mater, Y. Feng, et al., ITF-2, a downstream target of the Wnt/TCF pathway, is activated in human cancers with beta-catenin defects and promotes neoplastic transformation, Cancer Cell 1 (2002) 145–155.
[14] S.P. Rockman, S.A. Currie, M. Ciavarella, E. Vincan, C. Dow, R.J. Thomas, W.A. Phillips, Id2 is a target of the beta-catenin/T cell factor pathway in colon carcinoma, J. Biol. Chem. 276 (2001) 45113–45119.
[15] T. Yamada, A.S. Takaoka, Y. Naishiro, R. Hayashi, K. Maruyama, C. Maesawa, et al., Transactivation of the multidrug resistance 1 gene by T-cell factor 4/beta-catenin complex in early colorectal carcinogenesis, Cancer Res. 60 (2000) 4761–4766.
[16] Y. Araki, S. Okamura, S.P. Hussain, M. Nagashima, P. He, M. Shiseki, et al., Regulation of cyclooxygenase-2 expression by the Wnt and ras pathways, Cancer Res. 63 (2003) 728–734.
[17] H.C. Crawford, B.M. Fingleton, L.A. Rudolph-Owen, K.J. Goss, B. Rubinfeld, P. Polakis, L.M. Matrisian, The metalloproteinase matrilysin is a target of beta-catenin transactivation in intestinal tumors, Oncogene 18 (1999) 2883–2891.
[18] F. Hlubek, A. Jung, N. Kotzor, T. Kirchner, T. Brabletz, Expression of the invasion factor laminin gamma2 in colorectal carcinomas is regulated by beta-catenin, Cancer Res. 61 (2001) 8089–8093.
[19] X. Zhang, J.P. Gaspard, D.C. Chung, Regulation of vascular endothelial growth factor by the Wnt and K-ras pathways in colonic neoplasia, Cancer Res. 61 (2001) 6050–6054.

[20] M. van de Wetering, E. Sancho, C. Verweij, W. de Lau, I. Oving, A. Hurlstone, et al., The beta-catenin/TCF-4 complex imposes a crypt progenitor phenotype on colorectal cancer cells, Cell 111 (2002) 241–250.
[21] L.K. Su, K.W. Kinzler, B. Vogelstein, A.C. Preisinger, A.R. Moser, C. Luongo, et al., Multiple intestinal neoplasia caused by a mutation in the murine homolog of the APC gene, Science 256 (1992) 668–670.
[22] M. Hubank, D.G. Schatz, cDNA representational difference analysis: a sensitive and flexible method for identification of differentially expressed genes, Method Enzymol. 303 (1999) 325–349.
[23] M. Kobzdej, J. Matuszyk, L. Strzadala, Overexpression of Ras, Raf and L-myc but not Bcl-2 family proteins is linked with resistance to TCR-mediated apoptosis and tumorigenesis in thymic lymphomas from TCR transgenic mice, Leukemia Res. 24 (2000) 33–38.
[24] I. Holen, P.I. Croucher, F.C. Hamdy, C.L. Eaton, Osteoprotegerin (OPG) is a survival factor for human prostate cancer cells, Cancer Res. 62 (2002) 1619–1623.
[25] V. Korinek, N. Barker, P. Moerer, E. Donselaar, G. Huls, P.J. Peters, H. Clevers, Depletion of epithelial stem-cell compartments in the small intestine of mice lacking Tcf-4, Nat. Genet. 19 (1998) 379–383.

Available online at www.sciencedirect.com
SCIENCE DIRECT®
Biochemical and Biophysical Research Communications 323 (2004) 229–234
BBRC
www.elsevier.com/locate/ybbrc

Cloning and characterization of the promoter of human Wnt inhibitory factor-1

Noemi Reguart[a,b], Biao He[a], Zhidong Xu[a], Liang You[a], Amie Y. Lee[a], Julien Mazieres[a,c], Iwao Mikami[a], Sonny Batra[a], Rafael Rosell[b], Frank McCormick[a], David M. Jablons[a,*]

[a] *Thoracic Oncology Laboratory, Department of Surgery, Comprehensive Cancer Center University of California, San Francisco, CA 94115, USA*
[b] *Medical Oncology Service, Institut Català d'Oncologia, Hospital Germans Trias i Pujol, 08916 Barcelona, Spain*
[c] *Department Innovation Therapeutique et Oncologie Moleculaire, INSERM U563, Institut Claudius Regaud, 31052 Toulouse Cedex, France*

Received 4 August 2004

Abstract

Wnt inhibitory factor-1 (WIF-1) is a secreted antagonist of Wnt signaling and functions by directly binding to Wnt ligands in the extracellular space. Here we report the identification of the 5′ promoter region (~1.5 kb) of the human WIF-1 gene. Functional analysis of this region shows that a whole fragment displays high basal promoter activity in different cell lines, while the truncated forms do not, indicating that integrity of the WIF-1 promoter region may be important for WIF-1 activity. Moreover, we found that the expression level of β-catenin in cancer cell lines correlates with the WIF-1 promoter activity, suggesting that the WIF-1 promoter may be regulated by the Wnt/β-catenin pathway and may function in a negative feedback manner. Our results also suggest that a methylated CpG island, which we observed recently in human lung cancer, lies within the functional WIF-1 promoter region and therefore bears the importance of the methylation-status of this CpG island as an important key in Wnt activation in human cancer.

Keywords: WIF-1; Promoter; Luciferase reporter; Wnt/β-catenin signaling; Cancer

The Wnt protein family consists of at least 19 members [1,2]. These secreted glycoproteins are signaling molecules widely involved in developmental processes and oncogenesis [3,4]. Aberrant activation of the Wnt signaling pathway has been demonstrated in a variety of human cancers such as colorectal cancer [5], head and neck carcinoma [6], melanoma [7], and leukemia [8]. We recently reported that Wnt activation is associated with overexpression of Disheveled (Dvl) proteins in mesothelioma and non-small-cell lung cancer (NSCLC) [9,10] and that blocking Wnt-1 signaling induces apoptosis and suppresses growth in NSCLC and mesothelioma cells [11,12].

Two groups of Wnt antagonists with different mechanisms of action have been identified so far [1]. The first group, which includes the secreted frizzled-related protein (sFRP) family, Wnt inhibitory factor (WIF)-1, and Cerberus, inhibits Wnt signaling by directly binding to Wnt molecules. The second group consists of the Dickkopf (Dkk) family, which inhibits Wnt signaling by binding to the LRP5/LRP6 component of the Wnt receptor complex [1]. Involvement of the sFRP family in oncogenesis has recently been reported. Loss of expression of sFRP family proteins has been found in cervical carcinomas [13], breast cancer [14], and gastric cancer [15]. The sFRP promoter has been found methylated in colorectal cancer and restoration of sFRPs in colon cancer cells results in apoptosis and suppression of Wnt-dependent transcription [16–18].

The role of WIF-1 in Wnt signaling was first identified in the human retina with highly conserved orthologues in

* Corresponding author. Fax: +1 415 502 3179.
E-mail address: jablonsd@surgery.ucsf.edu (D.M. Jablons).

0006-291X/S - see front matter © 2004 Elsevier Inc. All rights reserved.
doi:10.1016/j.bbrc.2004.08.075

Xenopus and zebrafish [19]. WIF-1 is an evolutionarily conserved protein located at chromosome 12q14 which contains an N-terminal signal sequence, a unique WIF domain, and five-epidermal growth factor (EGF)-like repeats. It does not share any similarities with the cysteine-rich domain (CRD) of frizzled (Fz) or sFRP [20]. It has been shown that WIF-1 can bind to XWnt-8 and *Drosophila* wingless (Wg) in the extracellular space and inhibit Xwnt-8–Dfz2 interactions and Armadillo stabilization in Xwnt-8-treated *Drosophila* clone-8 cells [19]. Wissman et al. [21] reported the downregulation of WIF-1 in several cancer types including lung cancer, however the role that WIF-1 plays in human cancers still remains unclear. We recently investigated the expression and the epigenetic regulation of WIF-1 in lung cancer. We found WIF-1 underexpression in NSCLC cell lines and tissue samples and this silencing correlates with the methylation of the CpG island located in the 5′ flanking region of the WIF-1 gene [22].

To further understand the involvement of WIF-1 in Wnt signaling, we report in this study the cloning and characterization of the human WIF-1 promoter. We found different activities of the WIF-1 promoter in different human cancer cell lines and the level of promoter activity is correlated with the expression level of cytosolic β-catenin. Moreover, we demonstrate that the CpG island is within the functional promoter of the WIF-1 gene. Therefore, methylation in this regulatory region may be an important mechanism of aberrant Wnt signaling activation in cancer.

Materials and methods

Cell cultures. Human kidney transfected epithelial cell line (293T), human non-small-cell lung cancer cell line (NCI-A549), human colorectal cancer cell lines (HCT116 and SW480), which harbor mutations in CTNNB1 and APC, respectively [23,5], and human mesothelioma cancer cell lines (H28, MS1) that lack β-catenin expression [12] were obtained from American Type Culture Collections (ATCC, Manassas, Virginia). These cells, except human kidney transfected epithelial cell line (293T), were cultured in RPMI 1640. Human kidney epithelial cell line (293T) was cultured in Dulbecco's modified Eagle's medium (DME H-21). All cells were supplemented with 10% fetal bovine serum, penicillin (100 IU/ml), and streptomycin (100 μg/ml). Cells were cultured at 37 °C in a humid incubator with 5% CO_2.

Cloning and sequence analysis. We used a PCR-based technique to clone the human WIF-1 promoter region. Sense and anti-sense primers were chosen from the genomic sequence of the human WIF-1 gene (Accession No. NM007191), corresponding to the sequence −1512 to +6 (the start codon ATG of human WIF-1 gene is defined as +1). FailSafe PCR (Epicentre, Madison, Wisconsin) (38 cycles) was performed using human genomic DNA isolated from cultured cells and normal tissue as template. To amplify the different fragments we used the following primers: construct 1, forward—5′-GCCAGCTTTGCCA GTCTTAC-3′, reverse—5′-TGCTCAGGACCTCCTCGCTG-3′ (from −292 to +6); construct 2, forward—5′-GAGTGATGTCCCAGGGG TCT-3′, reverse—5′-GTAAGACTGGCAAAGCTGGC-3′ (from −557 to −272); construct 3, forward—5′-GGAGGGTCAGGTACAGCT AT-3′, reverse—5′-AGACCCCTGGGACATCACTC-3′ (from −1012 to −535); construct 4, forward—5′-GCTGGGCCAGGTGGA TAGGT-3′, reverse—5′-AGACCCCTGGGACATCACTC-3′ (from −1512 to −535); and construct 5, forward—5′-GCTGGGCCAGG TGGATAGGT-3′, reverse—5′-TGCTCAGGACCTCCTCGCTG-3′ (from −1512 to +6). The position of all the primers is also marked in Fig. 1. The PCR products were extracted from agarose gel using an extraction kit (QUIAquick Gel Extraction kit, Qiagen, Valencia, CA) and were subsequently sequenced at the DNA-sequencing Core Facility of the University of California, San Francisco Comprehensive Cancer Center.

Construction of the human WIF-1 promoter region. We used PCR to generate truncated forms of the human WIF-1 promoter region (−1512 to+6) and subcloned them into the *Nhe*I (5′) and *Hin*dIII (3′) sites of pGL3Basic vector purchased from Promega (Madison, WI). Sense primers for generating truncated forms described above contain an adaptor with an *Nhe*I restriction site (5′-CCAATTGCTAGC-3′) at the 5′ end. Anti-sense primers contain an adaptor with a *Hin*dIII restriction site (5′-CCTTGGAAGCTT-3′) at the 5′ end. Then pGL3Basic vector and all PCR products that have *Nhe*I site at 5′ and

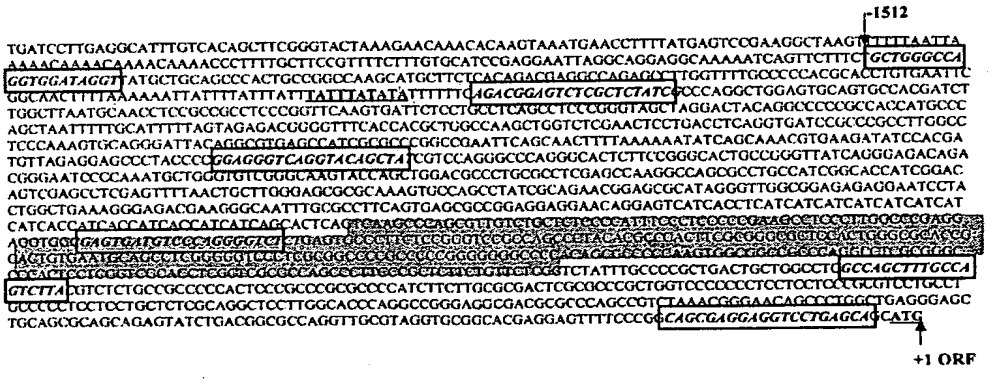

Fig. 1. The 5′ flanking region of human WIF-1 gene. A ~1.5 kb fragment was amplified using genomic DNA as a template. A standard PCR was used to amplify the different fragments. Sequences corresponding to the primers used for the amplification are in bold and boxed. Putative ATG open reading frame codon side (defined as +1) as well as the TATA box-containing region is in bold and underlined. The gray box indicates a rich CpG island region found within the upstream promoter region. The 5′ end of the region cloned is indicated as −1512. The sequence cloned includes the whole sequence from +1 to −1512. The sequence was obtained from the human genome sequence database at the UCSF web server (http://genome.ucsf.edu/) and the promoter search program (http://www.genomatix.de/).

*Hin*dIII site at 3′ were doubly digested with *Nhe*I and *Hin*dIII enzymes (New England Biolabs, Beverly, MA). The digested inserts were gel-purified by electrophoresis and ligated (Quick Ligation Kit, New England Biolabs, Beverly, MA) to generate the deletion constructs. The constructs were then transformed into competent *Escherichia coli* (One Shot Competent E.Coli, Invitrogen, Carlsbad, CA) for amplification. The created plasmids were purified by using QIAprep Spin Miniprep Kit (Qiagen, Valencia, CA) and afterwards confirmed by restriction enzyme digestion. All constructs were sequenced using GLprimer2 (counter clockwise) and RVprimer3 (clockwise) to check the correct orientation of the insert inside the vector (primers purchased from Promega, Madison, WI).

Transfection and promoter activity analysis. One day before transfection, cells (2×10^5) were plated in six-well plates with growth medium without antibiotics. When cells reached 80–90% confluence they were co-transfected using 2.0 μg of each DNA construct in pGL3Basic vector and 0.05 μg pRL-TK Vector (Promega, Madison, WI) containing *Renilla* luciferase as an internal control for the transfection efficiency. Lipofectamine 2000 (Invitrogen, Carlsbad, CA) was used to mediate transfection. The resulting cells were cultured in the medium for an additional day and subjected to luciferase assay. One day after the transfection, cells were lysed in a lysis buffer and firefly and *Renilla* luciferase activities in cells of each well were measured using Dual-Luciferase Assay System (Promega, Madison, WI) and a luminometer. All the measured luciferase activities were normalized to pRL-TK Vector activity and were given relative to the basal activity of empty pGL3Basic vector, which was set to unity. The data shown represent mean values (±SD). All measurements were performed in triplicate and repeated in at least three independent experiments.

Western blotting. Standard protocol was used. Whole cell lysates (A549, SW480, HCT116, H28, and MS-1) were obtained with M-PER mammalian protein extraction reagent (Pierce, Rockford, IL). Cytosolic fraction was prepared according to a protocol described previously [24]. Anti-β-catenin mouse monoclonal antibody was purchased from Transduction Laboratories (Lexington, KY). Anti-β-actin mouse monoclonal antibody was obtained from Sigma (St. Louis, MO).

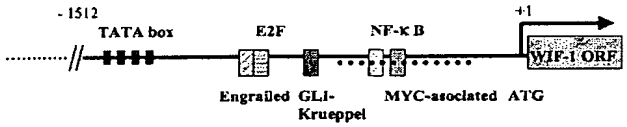

Fig. 2. Schematic representation of human WIF promoter region. A ~1.5 kb segment is shown. Binding sites of transcription factors such as Engrailed, E2F, GLI-Krueppel, NF-κB, and MYC are indicated as well as the rich CpG island region (dot lines) and TATA box.

Statistical analysis. Unpaired *t* test was used for comparing activities of different constructs.

Results

Identification of the WIF-1 promoter region

To identify the WIF-1 promoter, we conducted a BLAST search with the 1140-bp coding sequence of WIF-1 as a virtual probe against the human genomic database at the UCSC web server (http://genome.ucsc.edu/). We used a promoter search program (http://www.genomatix.de/) to confirm that the 5′ flanking region of the gene presents classical features of a promoter region (Fig. 1). Several important transcription sites were observed in this fragment such as Homobox Protein Engrailed (−826 to −830 from ATG), E2F (−807 to −811), GLI-Krueppel (−548 to −552), MYC-associated (−419 to −423), and NF-κB (−421 to −425) (Fig. 2). We observed that the G/C content of the human WIF-1 promoter region is high (approximately 63.5%). We then used a CpG island search program (http://www.uscnorris.com/cpgislands/cpg.cgi) to map the CpG dinucleotides within the WIF-1 promoter and found a CpG island (105 CpGs) in this promoter (Figs. 1 and 2). In addition, we found that this promoter region contained one putative TATA box (−1368 to −1378 ahead of the ATG) (Figs. 1 and 2). We also found that the human WIF-1 promoter region is largely conserved compared to the chimp promoter (99% identity), but less conserved in mouse and rat promoters (approximately 5.9% and 5.7%, respectively) (Fig. 3).

Functional analysis of the human WIF-1 promoter constructs

We cloned the complete 1506-bp fragment (from the TATA box to the ATG), as well as five truncated fragments into a promoterless luciferase (LUC) expression vector pGL3Basic (Fig. 4A). These constructs were transfected into 293T cells and LUC activities were then

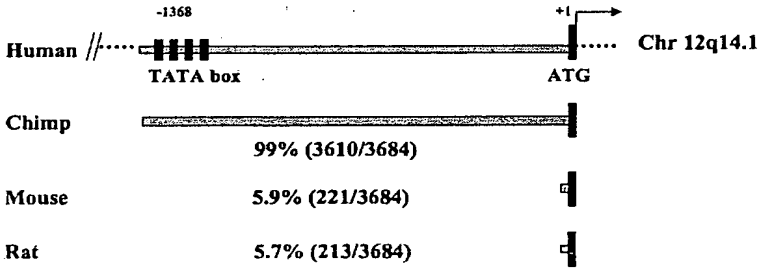

Fig. 3. Comparison of WIF-1 promoter regions of human, chimp, mouse, and rat. The identical region corresponds to the 5′ site before the ATG of open reading frame. In parentheses, the number of identical amino acids in those regions is shown.

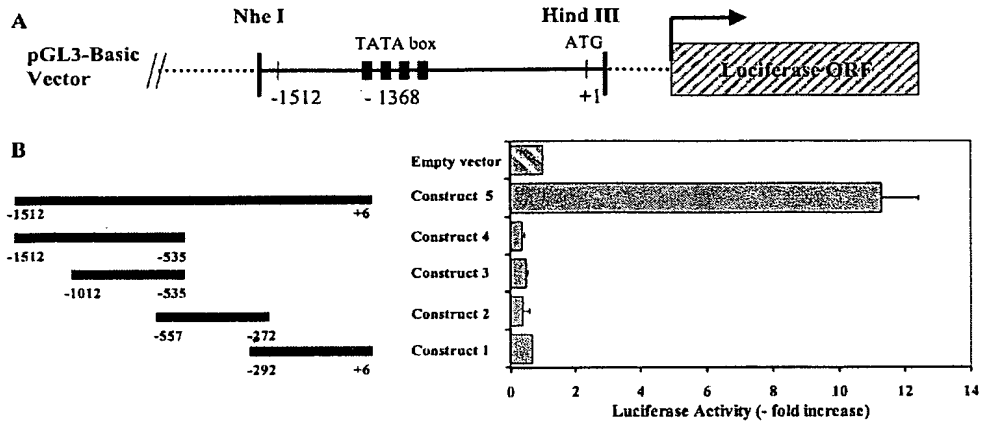

Fig. 4. (A) Schematic representation of the ~1.5 kb construct used in this experiment inserted in a pGL3Basic vector (pGL3B) upstream of the firefly luciferase gene. The restriction sites used to clone the different constructs (*NheI*/*Hin*dIII) are shown. (B) Luciferase activity of different constructs of the genomic human WIF-1 promoter. The constructs correspond to 5 different segments of a ~1.5 kb region of the 5′ promoter region. They were inserted into pGL3Basic vector upstream of firefly luciferase gene (described in Materials and methods). Each promoter construct was verified by sequencing. 293T cells were transiently transfected with each construct. All relative luciferase activities were normalized to the activity of an empty pGL3Basic vector (pGL3B) and pRL-K was used as an internal control. Cells were harvested 24–36 h after transfection, and cell lysates were assayed for luciferase activity in a luminometer using Dual-Luciferase Assay Reporter System. Results are expressed as the ratio of activity of firefly to *Renilla* luciferase. Results are means ± SD (error bars) of at least three individual experiments.

measured (Fig. 4B). The four truncate constructs with deletion of some part of the whole region (construct 1; −292/+6 construct 2; −557/−272, construct 3; −1012/−535, and construct 4; −1512/−535) did not display any basal activity. Basal activity of the construct that contained all the elements (construct 5: 1512/+6) was significantly higher (approximately 11.3-fold increase of LUC activity) than those described above (construct 1, 2, 3, and 4) ($p < 0.02$). Taken together, these results indicate that the integrity of the WIF-1 promoter is likely necessary for its activity. Therefore, our results confirm that the whole fragment that we amplified (−1512/+6) could function as a promoter element.

Analysis of the WIF-1 promoter activity in human cancer cell lines

Next, we transfected the complete wild type WIF-1 promoter construct (construct 5) into different human cancer cell lines, including a non-small-cell lung cancer cell line (A549), mesothelioma cell lines (H28, MS-1), and colon cancer cell lines (HCT116, SW480) and examined the LUC activity after 24–48 h (Fig. 5A). We found that this construct (construct 5) displayed significantly high LUC activity in A549, SW480, and HCT116 cell lines (7- to 8-fold increase compared to that of empty vector) ($p < 0.04$), but only moderate LUC activity in the two mesothelioma cell lines MS-1 and H28. Interestingly, we found that the WIF-1 promoter activity correlates with the level of cytosolic β-catenin expression in these cell lines (Fig. 5B). These results suggest that the WIF-1 promoter may be under the regulation of the Wnt/β-catenin pathway.

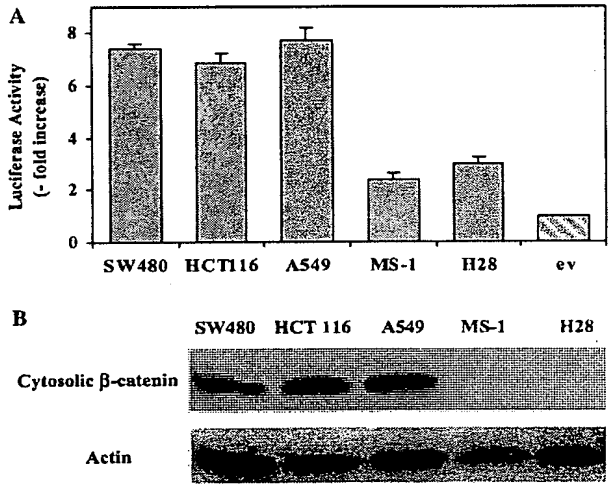

Fig. 5. (A) Luciferase activity of the complete human ~1.5 kb WIF-1 promoter construct in a pGL3Basic vector transfected in NSCLC cell line (A549), mesothelioma cell lines (H28, MS-1), and colorectal carcinoma cell lines (HCT 116, SW480) The average means ± SD (errors bars) are shown of at least three individual experiments. (B) Western blot analysis of cytosolic β-catenin in the different cell lines (A549, H28, MS-1, HCT 116, and SW480). β-Actin was used as loading control.

Discussion

The Wnt pathway plays a significant role in carcinogenesis. It is well known that mutations in the adenomatous polyposis coli gene (APC), axin, or β-catenin lead to β-catenin accumulation in the nucleus which is often observed in human cancers [25]. Moreover, β-cate-

nin does not bind to DNA itself, but needs to bind to TCF/LEF transcription factors for transactivation in the nucleus of a specific subset of genes [26,27]. Although the intracytoplasmic Wnt pathway has been widely studied, little is known about the relation between the antagonists of Wnt ligands and their role in carcinogenesis. Recently, however, information about the role of these secreted proteins in carcinogenesis has been elucidated. For instance, secreted frizzled-related proteins (sFRPs), one of the secreted Wnt protein inhibitors, are transcriptionally downregulated in mesothelioma [28] and in colorectal carcinoma [17]. In both tumors sFRPs promoter hypermethylation was identified. Furthermore, we recently found that WIF-1 transcription is silenced in human lung cancer and that this silencing is due to frequent hypermethylation [22].

In this study, we cloned and characterized approximately ~1.5 kb of the 5′ genomic region of the human WIF-1 gene. This 5′ region shows baseline promoter activity and contains one putative TATA sequence and multiple potential transcription factor binding sites. The whole human construct 5 (−1512 to +6) that we cloned showed significantly high luciferase activity (~11.3-fold increase). Taken together, these results suggest that we have found a functional human WIF-1 promoter. Next, we examined promoter activity of the different truncated 5′ constructs (construct 4, −1512 to −535; construct 3, −1012 to −535; construct 2, −557 to −272; and construct 1, −292 to +6). When we used these truncated constructs we found that promoter activity dramatically decreased ($p < 0.02$). These results indicate that the entire WIF-1 promoter region may be needed for its activity.

These results are consistent with our recent data [22]. The functional WIF-1 promoter region that we analyzed contains the CpG island that we previously described as an important issue in Wnt signaling activation. It is well known that aberrant methylation of CpG islands is one of the major modes of inactivation of tumor suppressor genes in cancer and a growing list of genes is being identified as having abnormal methylation of promoters having CpG islands [29]. Taken together, our results demonstrate that the CpG island lies inside a functional WIF-1 promoter, thus holding this methylated region as an important mechanism of the WIF-1 gene silencing and therefore constitutive activation of Wnt/β-catenin pathway.

The human WIF-1 promoter construct that we cloned allowed us to examine the transcriptional activity of WIF-1 in different human cancer cell lines. We found that WIF-1 promoter activity of the whole fragment was different in the cell lines that we tested. Cell lines that lack cytosolic β-catenin expression (MS-1, H28) revealed lower LUC activity than those with high expression level of cytosolic β-catenin (SW480, HCT116, and A549), suggesting a correlation between expression levels of cytosolic β-catenin and WIF-1 promoter activity. It is known that Wnt pathway antagonists such as sFRP [30–32], Cerberus [33], and WIF-1 [19] prevent Wnt ligands from binding to their receptors and thereby inhibit the Wnt/β-catenin pathway. Little was known, however, about the regulation mechanisms of these Wnt pathway inhibitors. Our findings argue that WIF-1 could be a downstream target gene of Wnt/β-catenin pathway and may function as a feedback inhibitor of Wnt signaling. The two cell lines lacking cytosolic β-catenin (MS-1 and H28), however, still have some activity when compared with the empty vector. These data could be explained by the fact that Wnt/β-catenin pathway may not be the only pathway that controls WIF-1 expression although Wnt/β-catenin could be the major pathway of WIF-1 activation.

In summary, our study provides more insight into the regulation of WIF-1 expression and opens a way to future investigations on the role of WIF-1 in Wnt/β-catenin activation during carcinogenesis.

Acknowledgments

This work was supported by the Larry Hall memorial trust and the Kazan, McClain, Edises, Abrams, Fernandez, and Lyons & Farrise Foundation.

References

[1] Y. Kawano, R. Kypta, Secreted antagonists of the Wnt signalling pathway, J. Cell Sci. 116 (2003) 2627–2634.
[2] J.R. Miller, The Wnts, Genome Biol. 3 (2002), REVIEWS3001.
[3] P. Polakis, Wnt signaling and cancer, Genes Dev. 14 (2000) 1837–1851.
[4] B. Lustig, J. Behrens, The Wnt signaling pathway and its role in tumor development, J. Cancer Res. Clin. Oncol. 129 (2003) 199–221.
[5] P.J. Morin, A.B. Sparks, V. Korinek, N. Barker, H. Clevers, B. Vogelstein, K.W. Kinzler, Activation of beta-catenin-Tcf signaling in colon cancer by mutations in beta-catenin or APC, Science 275 (1997) 1787–1790.
[6] C.S. Rhee, M. Sen, D. Lu, C. Wu, L. Leoni, J. Rubin, M. Corr, D.A. Carson, Wnt and frizzled receptors as potential targets for immunotherapy in head and neck squamous cell carcinomas, Oncogene 21 (2002) 6598–6605.
[7] A.T. Weeraratna, Y. Jiang, G. Hostetter, K. Rosenblatt, P. Duray, M. Bittner, J.M. Trent, Wnt5a signaling directly affects cell motility and invasion of metastatic melanoma, Cancer Cell 1 (2002) 279–288.
[8] D. Lu, Y. Zhao, R. Tawatao, H.B. Cottam, M. Sen, L.M. Leoni, T.J. Kipps, M. Corr, D.A. Carson, Activation of the Wnt signaling pathway in chronic lymphocytic leukemia, Proc. Natl. Acad. Sci. USA 101 (2004) 3118–3123.
[9] K. Uematsu, B. He, L. You, Z. Xu, F. McCormick, D.M. Jablons, Activation of the Wnt pathway in non small cell lung cancer: evidence of dishevelled overexpression, Oncogene 22 (2003) 7218–7221.
[10] K. Uematsu, S. Kanazawa, L. You, B. He, Z. Xu, K. Li, B.M. Peterlin, F. McCormick, D.M. Jablons, Wnt pathway activation

in mesothelioma: evidence of Dishevelled overexpression and transcriptional activity of beta-catenin, Cancer Res. 63 (2003) 4547–4551.

[11] B. He, L. You, K. Uematsu, Z. Xu, A.Y. Lee, M. Matsangou, F. McCormick, D.M. Jablons, A monoclonal antibody against Wnt-1 induces apoptosis in human cancer cells, Neoplasia 6 (2004) 7–14.

[12] L. You, B. He, K. Uematsu, Z. Xu, J. Mazieres, A. Lee, F. McCormick, D.M. Jablons, Inhibition of Wnt-1 signaling induces apoptosis in beta-catenin-deficient mesothelioma cells, Cancer Res. 64 (2004) 3474–3478.

[13] J. Ko, K.S. Ryu, Y.H. Lee, D.S. Na, Y.S. Kim, Y.M. Oh, I.S. Kim, J.W. Kim, Human secreted frizzled-related protein is down-regulated and induces apoptosis in human cervical cancer, Exp. Cell Res. 280 (2002) 280–287.

[14] F. Ugolini, E. Charafe-Jauffret, V.J. Bardou, J. Geneix, J. Adelaide, F. Labat-Moleur, F. Penault-Llorca, M. Longy, J. Jacquemier, D. Birnbaum, M.J. Pebusque, WNT pathway and mammary carcinogenesis: loss of expression of candidate tumor suppressor gene SFRP1 in most invasive carcinomas except of the medullary type, Oncogene 20 (2001) 5810–5817.

[15] K.F. To, M.W. Chan, W.K. Leung, J. Yu, J.H. Tong, T.L. Lee, F.K. Chan, J.J. Sung, Alterations of frizzled (FzE3) and secreted frizzled related protein (hsFRP) expression in gastric cancer, Life Sci. 70 (2001) 483–489.

[16] H. Suzuki, D.N. Watkins, K.W. Jair, K.E. Schuebel, S.D. Markowitz, W. Dong Chen, T.P. Pretlow, B. Yang, Y. Akiyama, M. Van Engeland, M. Toyota, T. Tokino, Y. Hinoda, K. Imai, J.G. Herman, S.B. Baylin, Epigenetic inactivation of SFRP genes allows constitutive WNT signaling in colorectal cancer, Nat. Genet. 36 (2004) 417–422.

[17] H. Suzuki, E. Gabrielson, W. Chen, R. Anbazhagan, M. van Engeland, M.P. Weijenberg, J.G. Herman, S.B. Baylin, A genomic screen for genes upregulated by demethylation and histone deacetylase inhibition in human colorectal cancer, Nat. Genet. 31 (2002) 141–149.

[18] G.M. Caldwell, C. Jones, K. Gensberg, S. Jan, R.G. Hardy, P. Byrd, S. Chughtai, Y. Wallis, G.M. Matthews, D.G. Morton, The Wnt antagonist sFRP1 in colorectal tumorigenesis, Cancer Res. 64 (2004) 883–888.

[19] J.C. Hsieh, L. Kodjabachian, M.L. Rebbert, A. Rattner, P.M. Smallwood, C.H. Samos, R. Nusse, I.B. Dawid, J. Nathans, A new secreted protein that binds to Wnt proteins and inhibits their activities, Nature 398 (1999) 431–436.

[20] K. Lin, S. Wang, M.A. Julius, J. Kitajewski, M. Moos Jr., F.P. Luyten, The cysteine-rich frizzled domain of Frzb-1 is required and sufficient for modulation of Wnt signaling, Proc. Natl. Acad. Sci. USA 94 (1997) 11196–11200.

[21] C. Wissmann, P.J. Wild, S. Kaiser, S. Roepcke, R. Stoehr, M. Woenckhaus, G. Kristiansen, J.C. Hsieh, F. Hofstaedter, A. Hartmann, R. Knuechel, A. Rosenthal, C. Pilarsky, WIF1, a component of the Wnt pathway, is down-regulated in prostate, breast, lung, and bladder cancer, J. Pathol. 201 (2003) 204–212.

[22] J. Mazieres, B. He, L. You, Z. Xu, A.Y. Lee, I. Mikami, N. Reguart, R. Rosell, F. McCormick, D.M. Jablons, Wnt inhibitory factor-1 is silenced by promoter hypermethylation in human lung cancer, Cancer Res. 64 (2004) 4717–4720.

[23] V. Korinek, N. Barker, P.J. Morin, D. van Wichen, R. de Weger, K.W. Kinzler, B. Vogelstein, H. Clevers, Constitutive transcriptional activation by a beta-catenin-Tcf complex in APC−/− colon carcinoma, Science 275 (1997) 1784–1787.

[24] H. Shimizu, M.A. Julius, M. Giarre, Z. Zheng, A.M. Brown, J. Kitajewski, Transformation by Wnt family proteins correlates with regulation of beta-catenin, Cell Growth Differ. 8 (1997) 1349–1358.

[25] R.H. Giles, J.H. van Es, H. Clevers, Caught up in a Wnt storm: Wnt signaling in cancer, Biochim. Biophys. Acta 1653 (2003) 1–24.

[26] M. van de Wetering, R. Cavallo, D. Dooijes, M. van Beest, J. van Es, J. Loureiro, A. Ypma, D. Hursh, T. Jones, A. Bejsovec, M. Peifer, M. Mortin, H. Clevers, Armadillo coactivates transcription driven by the product of the Drosophila segment polarity gened TCF, Cell 88 (1997) 789–799.

[27] M. Molenaar, M. van de Wetering, M. Oosterwegel, J. Peterson-Maduro, S. Godsave, V. Korinek, J. Roose, O. Destree, H. Clevers, XTcf-3 transcription factor mediates beta-catenin-induced axis formation in *Xenopus* embryos, Cell 86 (1996) 391–399.

[28] A.Y. Lee, B. He, L. You, S. Dadfarmay, Z. Xu, J. Mazieres, I. Mikami, F. McCormick, and D.M. Jablons, Expression of the secreted frizzled-related protein gene family is downregulated in human mesothelioma, Oncogene (2004). *Oncogene* advance online publication 28 June, 2004, doi:10.1038/sj.onc.1207881.

[29] J.G. Herman, S.B. Baylin, Gene silencing in cancer in association with promoter hypermethylation, N. Engl. J. Med. 349 (2003) 2042–2054.

[30] P.W. Finch, X. He, M.J. Kelley, A. Uren, R.P. Schaudies, N.C. Popescu, S. Rudikoff, S.A. Aaronson, H.E. Varmus, J.S. Rubin, Purification and molecular cloning of a secreted, Frizzled-related antagonist of Wnt action, Proc. Natl. Acad. Sci. USA 94 (1997) 6770–6775.

[31] R.K. Ladher, V.L. Church, S. Allen, L. Robson, A. Abdelfattah, N.A. Brown, G. Hattersley, V. Rosen, F.P. Luyten, L. Dale, P.H. Francis-West, Cloning and expression of the Wnt antagonists Sfrp-2 and Frzb during chick development, Dev. Biol. 218 (2000) 183–198.

[32] L. Leyns, T. Bouwmeester, S.H. Kim, S. Piccolo, E.M. De Robertis, Frzb-1 is a secreted antagonist of Wnt signaling expressed in the Spemann organizer, Cell 88 (1997) 747–756.

[33] S. Piccolo, E. Agius, L. Leyns, S. Bhattacharyya, H. Grunz, T. Bouwmeester, E.M. De Robertis, The head inducer Cerberus is a multifunctional antagonist of Nodal, BMP and Wnt signals, Nature 397 (1999) 707–710.